National Observatory of Athens

Department of Informatics and Telecommunications

University of Peloponnese

Master of Science in Space Science, Technologies, and Applications

DEEP SPACE COMMUNICATION SYSTEMS AND TECHNOLOGY

MARGARITA BELALI

belalimargarita@gmail.com

space18007@uop.gr

Supervisor Dr.Nikos Sagias - Professor, University of Peloponnese

ACKNOWLEDGEMENTS

Despite completing SSTA master's program courses in 2020, like many other students, I faced significant challenges in fulfilling my obligations in delivering the thesis part due to the COVID-19 pandemic period and the lack of internal guidance in the special field of the deep space communications field.

Despite these challenges, I remained committed to space exploration and actively pursued remote work opportunities on space-related topics over two years.
These opportunities allowed me to interact with other master's students, accomplished aerospace scientists, and engineers from various parts of the world, further deepening my interest in space science and technology.

I would like to express my heartfelt gratitude to all the international space initiatives that generously provided remote participation opportunities during this challenging period. These initiatives not only allowed us to explore the fascinating field of space exploration but also significantly enhanced our knowledge and skills.

Special thanks go to Mr. George Salazar, a systems engineer and Human-Computer Interface Technical Discipline Lead at NASA, with 45 years of experience. His invaluable and unconditional assistance in reviewing my thesis, along with his kindness in advising new professionals in this field, has been greatly appreciated. His support and guidance were pivotal in helping me to feel confident that this thesis was adequate.

Ad Astra ✨

Abstract:

This thesis explores the critical role of deep space communication systems and technologies in enabling successful space exploration and scientific discovery. In addition, this work contributes to the understanding of deep-space communication systems and technologies and offers guidance for future research and development. The study provides a comprehensive overview of the principles, challenges, and technologies associated with deep-space communication, as well as the design and operation of ground stations and antennas. Through an analysis of current communication protocols and standards, the thesis offers insights into how data is transmitted across vast distances in space. Case studies of successful deep space missions showcase the practical application of various communication strategies and technologies. The study concludes by examining emerging trends, challenges, and potential solutions for the future of deep space communication.

Introduction

Deep space communication systems and technologies play an indispensable role in the success of space exploration missions as well as in the advancement of our understanding of the universe. As human knowledge and capabilities expand, the need to explore the far reaches of our solar system and beyond increases proportionally. This exploration requires robust and reliable communication systems that can transmit data across vast distances, often millions or billions of miles away from Earth. Some of the current challenges of communication in deep space are the extreme distances and limited bandwidth that present obstacles such as signal attenuation. The term "deep space" is commonly employed to denote significant distances from the Earth. According to NASA (2014), deep space is defined as any distance beyond the moon, which is approximately 384,000 km. Nevertheless, the European Space Agency (ESA) employs distances exceeding 2,000,000 km from Earth (ESA, 2012), as the International Telecommunication Union defines approximately 0.01 AU. To provide a perspective, the definitions provided by NASA and ESA consider the commencement of deep space to occur at distances approximately 9.6 and 50 times greater than the circumference of the Earth, respectively. These distances are notably larger than any terrestrial communication links.

For this reason, the use of powerful transmitters and sensitive receivers, as well as efficient data compression, modulation techniques, and error correction coding, are employed to maximize the utilization of the available bandwidth. Due to the vast distance between Earth and the spacecraft, significant signal propagation delays must also be taken into account when designing communication protocols and systems. Other challenges have to do with the interference and noise encountered in deep-space communication from a variety of sources, including background noise from space, solar radiation, and radio frequency interference from terrestrial sources. To mitigate the effects of noise and ensure reliable communication, advanced error correction techniques are necessary. Also, onboard spacecraft power, weight, and size are finite resources. Transmitters and other forms of communication equipment must be designed to operate under stringent power restrictions. Conversely, the construction and functionality of antennas and ground installations involve utilizing substantial dish antennas with diameters extending from 34 to 70 meters, as witnessed in terrestrial antenna structures like the Deep Space Network (DSN) and the Estrack network (by ESA) geographically distributed stations [89]. They are strategically positioned to provide global coverage and enable communication with spacecraft in deep space. Deep-space communication involves various technologies and methods. Traditional radio-frequency communication is commonly used due to its reliability and long-range capabilities (Williamson, 1998). However, there is also ongoing research and development in the field of deep-space optical communication, which utilizes lasers for high-speed data transmission (Hemmati et al., 2011). Optical communication has the potential to significantly increase data rates and enable more efficient communication in deep space. In addition to communication, deep space missions often require precise tracking and navigation. Tracking systems such as the DSN and Estrack provide data to determine the precise state vector of the spacecraft based on the signals received from the spacecraft (Bocanegra-Bahamón, 2017). This information is crucial for accurately navigating and controlling spacecraft in deep space.

These antennas exhibit significant gain, facilitating long-range transmissions. Advanced tracking and pointing instruments, such as motor-driven azimuth and elevation mounts, are necessary for maintaining an exact line-of-sight connection with the spacecraft. The spacecraft's motion across the heavens necessitates

constant tracking by the antennas. Ground installations utilize extremely sensitive receivers to intercept weak signals originating from distant space. To enhance receiver sensitivity, low-noise amplifiers are implemented, and the ground stations process received signals using demodulation and decoding methodologies. Ground stations leverage sophisticated modulation methods, like binary phase-shift keying (BPSK) and quadrature phase-shift keying (QPSK), to transmit data over radio waves effectively. The data received by ground stations is documented, processed, and forwarded to relevant mission control centers for further assessment and dissemination. [2]

The Consultative Committee for Space Data Systems (CCSDS) has developed a broad array of deep space communication standards addressing aspects such as telemetry, tracking, command protocols, and data interchange file formats. For instance, Space Link Extension (SLE), a protocol introduced by CCSDS, outlines the data flow mechanism between spacecraft and ground installations, emphasizing secure and dependable data transfers, data segmentation, retransmission, and acknowledgment protocols. Delay/Disruption Tolerant Networking (DTN) protocols have been crafted specifically to address communication in deep space, where communication delays and occasional disruptions are commonplace. The CCSDS Bundle Protocol (BP), a standard Data Transmission Network (DTN) protocol, ensures dependable store-and-forward communication in severe environments like deep space.

Telecommand and Telemetry Exchange (CCSDS) protocols are deployed to facilitate data transfer between spacecraft and ground installations, defining the command formats transmitted to spacecraft along with the telemetry data received. Due to limited bandwidth, reliable data transmission is ensured using various compression techniques and error correction codes. Standards like CCSDS Image Data Compression (IDC) and Reed-Solomon codes are often employed in deep space missions.

These core concepts, design aspects, and communication protocols form the foundation for successful deep-space communication, enabling a reliable and efficient exchange of data and commands between Earth and space vehicles exploring the extremities of our solar system and beyond.

This dissertation provides an in-depth examination of deep space communication systems and technologies, along with an understanding of their impact on contemporary and future space exploration efforts. The research seeks to explain the fundamental principles and challenges of deep space communication, delve into the operations of antennas and ground installations, and scrutinize the communication protocols and standards adopted in deep space missions.

At the conclusion of this thesis, have been analyzing several scenarios using MATLAB.

TABLE OF CONTENTS

Section 1

Role of Light and Electromagnetic Spectrum in Space Communications.

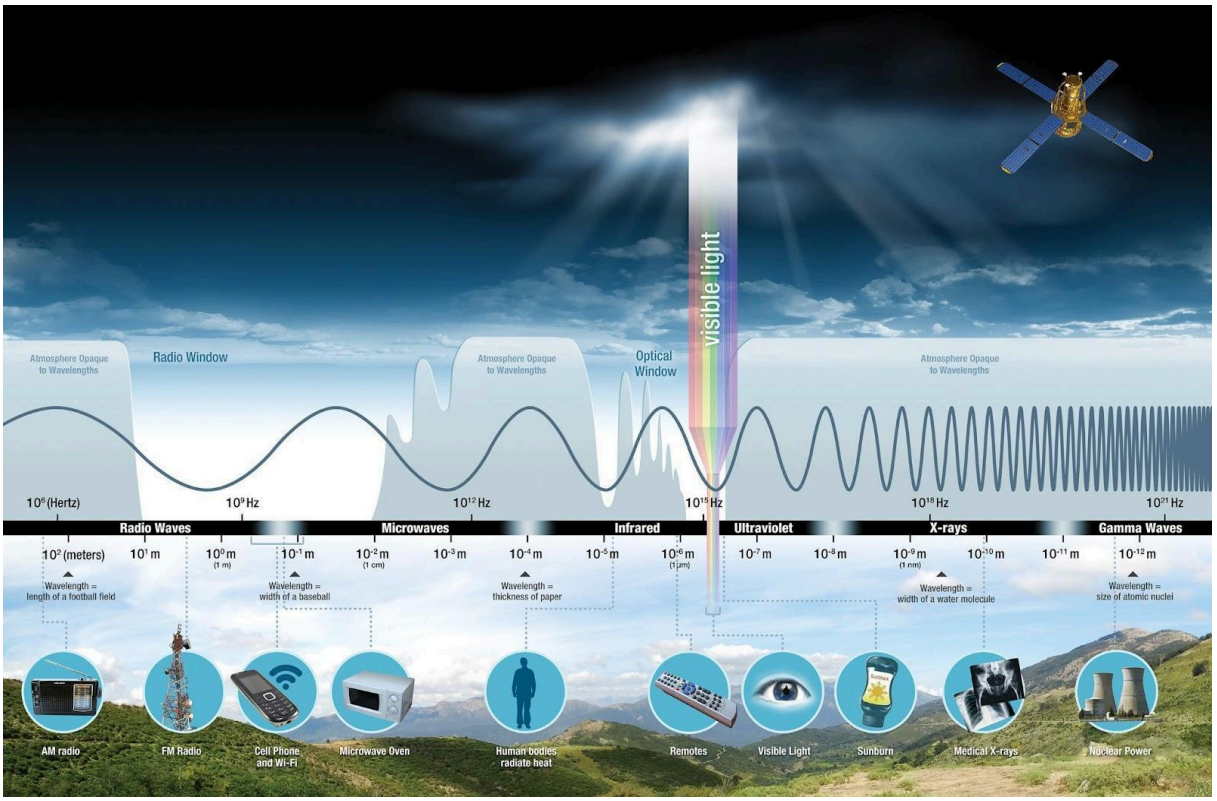

Figure 1 Electromagnetic Spectrum, Source: NASA Science

When we hear the word "light» most of us think of something about the sun, electric lights, and smartphone flashlights. The rainbow's spectrum of colors, from red to violet, may also spring to mind, although many additional wavelengths of light are not visible to the human eye. Thanks to technological advancements, people have understood the vast spectrum of light emitted, reflected, and refracted across the universe. This has taught us a great deal, such as what distant stars are made of and how the universe first came into existence. In a few lines, these advancements led to significant improvements in various fields, including communication, imaging, sensing, and material processing.

1.1 Electromagnetic spectrum and Light

To properly delve into the intricacies of deep space communication systems and technologies, it's paramount first to grasp the fundamentals of light and its behavior in the electromagnetic spectrum. Whenever the topic of space is broached, some of the inherent questions that arise include: "What is light?" and "How does it traverse space?".

During the initial productive science years, light was identified as a subset of electromagnetic radiation that travels through the vacuum of space in wave-like patterns. The behavior of light has historically been explained through two predominant theories: The particle theory, propounded by Sir Isaac Newton, asserts that light consists of discrete particles, referred to as photons, as well as the wave theory, championed by James Clerk Maxwell, and this concept suggests light behaves with wave-like properties.

The debate over the particle-versus-wave nature of light dates to the early days of scientific exploration. However, a transformative moment occurred in 1905 when Albert Einstein introduced evidence for the photoelectric effect, suggesting the existence of photons, or discrete particles that constitute light. This groundbreaking revelation played a pivotal role in the evolution of quantum mechanics [1].

Quantum entanglement in a section about light and the electromagnetic spectrum can highlight the dual wave-particle nature of light, bridge classical and quantum perspectives, and offer a holistic understanding of the subject.

In 1982, Aspect, Dalibard, and Roger [2] conducted a significant experiment to investigate Bell's inequalities—mathematical constructs introduced by John Bell in the 1960s to distinguish quantum mechanics from classical physics. Their research centered on "entanglement," a fundamental quantum phenomenon in which particles become so interconnected that the state of one instantly influences the state of the other, regardless of distance. This investigation sought to determine whether the behavior of entangled particles contradicted Bell's inequalities, thereby distinguishing quantum mechanics from classical physics. Their findings strongly supported the principles of quantum mechanics and highlighted the inability of classical physics

paradigms to explain entanglement. This experiment, which used photon pairs extracted from excited calcium ions, has significantly improved our understanding of quantum reality. Given that photons are light particles and light is an integral part of the electromagnetic spectrum, an in-depth comprehension of the quantum behaviors and nuances of light provides a thorough understanding of the topic at hand.

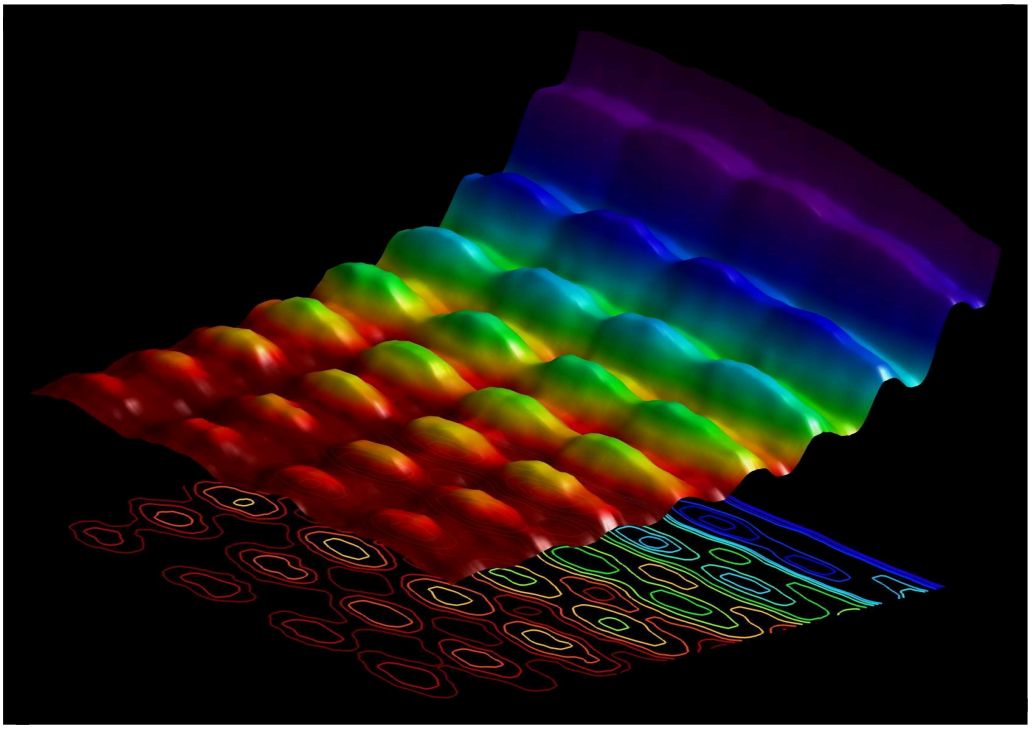

Figure 1.1.1 Visual of light (photon-wave state), Source: S. Tanzilli from CNRS

Despite numerous experiments, no one had concurrently captured the dual wave-particle nature of light behaviors until EPFL scientists, led by Fabrizio Carbone, achieved this feat in 2015. They innovatively used electrons to visualize light as it interacted with a metallic nanowire. When light waves met in opposition, they created a stationary wave, which the scientists imaged by observing the interaction between electrons and this light. The electrons' varying speeds, caused by their encounters with light particles or photons, confirmed light's dual character. Carbone referred to this groundbreaking experiment as a direct filming of quantum mechanics, suggesting its potential impact on future quantum computing technologies [3].

At the forefront of Figure 1.1.1, there are no discernible oscillations, signifying a particle-like demeanor. Between these endpoints, the behavior of individual photons gradually transitions from resembling waves to resembling particles. This showcases the coexistence of both states, highlighting that a straightforward wave or particle interpretation of light falls short. Kaiser and colleagues have connected this visual to their study. Image credit goes to S. Tanzilli from CNRS. A more comprehensive elucidation of the phenomenon of light propagation in the vacuum of space is that in a vacuum, such as the expanse of space, the velocity of light remains constant, approximately 299,792 kilometers per second (or roughly 186,282 miles per second). As we know it, it is recognized as the "speed of light" by the symbol c. In the absence of gravitational forces, light can travel in a linear trajectory through the vacuum of space. The phenomenon of light as a wave exhibits distinct properties such as wavelength, which represents the distance between successive peaks, and frequency, which indicates the number of waves passing through a given point in one second. The determination of the hue of light, e.g., within the visible spectrum, is reliant upon these characteristics.

The conceptualization of light's nature involves the recognition of discrete units of energy in photons. On the other hand, light appears to follow a curved trajectory when traversing regions of space characterized by strong gravitational fields, such as celestial bodies like stars or black holes, which is a noteworthy aspect of the interaction between light and gravity. The distortion of light by gravity, as predicted by Einstein's theory of general relativity, has been empirically validated through observational evidence [1], [4], [5], [6], [7], [8], and [9].

Even in some of the first space probes in history, like the Viking 1 (Figure 1.1.2) and Viking 2 Landers in the 1970s, during their voyages to the Red Planet, their radio signals provided some of the earliest confirmations of the effects predicted by general relativity. Gravity's effect on light is a key prediction of the general theory of relativity, and it has far-reaching implications for how we detect and interpret light in various contexts, especially astrophysics.

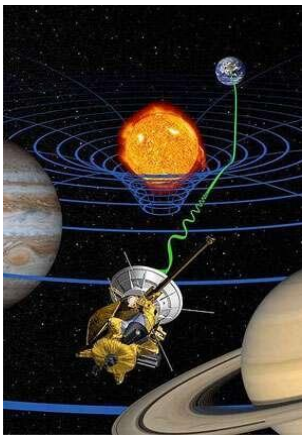

Figure 1.1.2 Viking 1 & 2, NASA

Simply, gravitational waves are perturbations in the fabric of space-time that propagate at the speed of light and are generated as a consequence of the acceleration of massive entities.

Also, various phenomena characterized by wavelengths give rise to ripples that span from a few miles to dimensions exceeding the observable universe. The gravitational waves serve a similar purpose as the water waves, sound waves, and electromagnetic waves possess the capability to transport energy, momentum, and angular momentum, thereby facilitating the transfer of these quantities away from their respective sources [8]. In deep space, combinations of stellar-mass objects encompass pairs consisting of black holes, neutron stars, and white dwarfs. To investigate these wavelengths, scientists require a variety of detectors, ranging from terrestrial and space-based facilities constructed by humans to pulsar timing arrays of galactic proportions. These arrays consist of rapidly rotating neutron stars that are meticulously observed for any alterations. The cosmic microwave background (CMB), which is the most ancient form of light in the universe, contains intricate information that can potentially unveil gravitational waves that were produced within an extremely minuscule timeframe of less than one trillionth of a second after the occurrence of the Big Bang [11].

A look at some of how gravity affects the detection of light using modern technology is given below:

- The Gravitational Lens: When a massive object, such as a galaxy cluster, rests between a distant light source and an observer, it can magnify the light from the source by acting as a lens. This is the result of the massive object distorting spacetime and, consequently, the light's path. Gravitational lensing can enable astronomers to detect faint or distant objects that would otherwise be impossible to observe directly. It is as if there were a natural telescope in orbit.

Figure 1.1.3 below depicts the concept of gravitational lensing, where clusters of elliptical galaxies possess immense gravitational strength, bending light from galaxies positioned behind them. This bending process can amplify light and make nearly imperceptible objects discernible, even though it might lead to distorted or duplicated images of the background galaxies. Utilizing the gravitational lens of Abell 383, astronomers observed a remote galaxy, revealing that it contained ancient stars. This discovery suggests that galaxies might have originated earlier in the universe's timeline than previously believed.

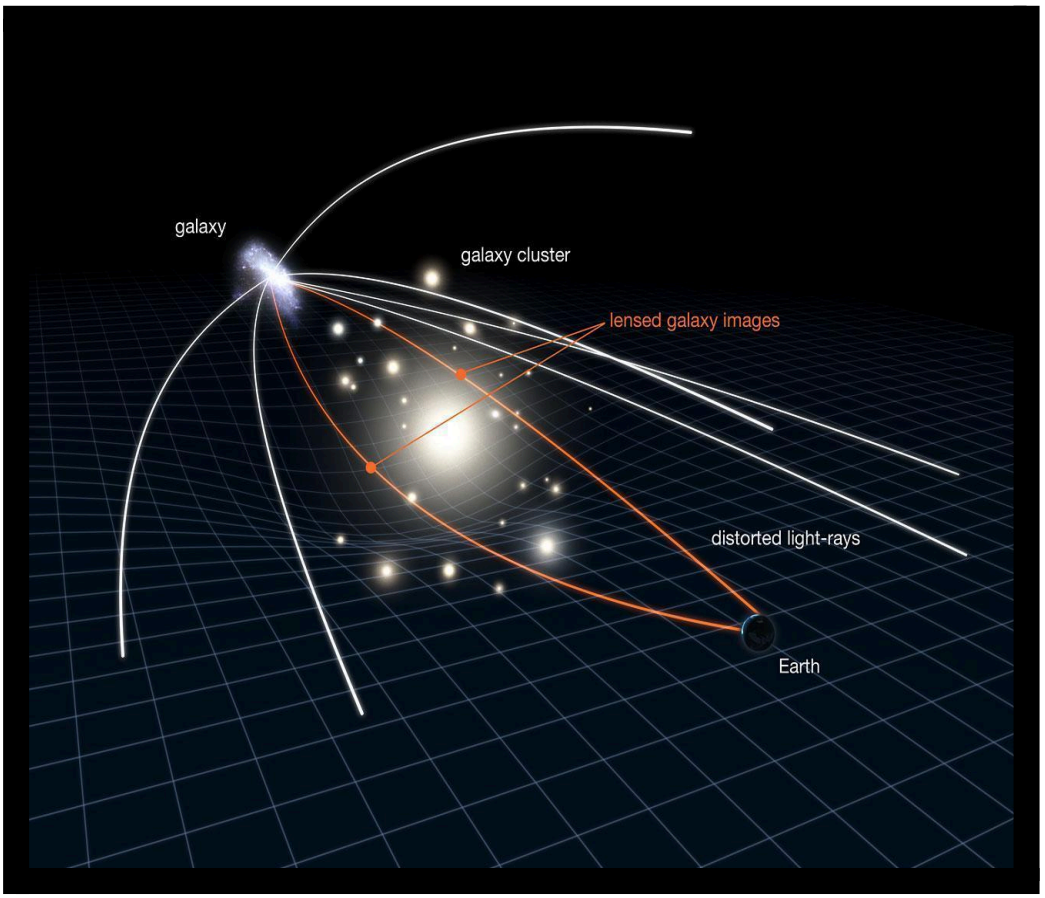

Figure 1.1.3 gravitational lensing Source: NASA, ESA & L. Calçada

- Black Holes and Event Horizons: As light nears a black hole, it can be significantly deflected. When light approaches a black hole too closely, it cannot escape its gravitational influence and is absorbed. This limit is referred to as the event horizon. Detecting the absence of light (and other signals) can be an indicator of a black hole's existence.

- Gravitational Redshift/Blueshift: When electromagnetic radiation or light climbs out of a gravitational well (such as a planet's gravitational field), it loses energy and its wavelength increases, resulting in a redshift. Light gains energy when it falls into a gravitational well, resulting in a blueshift. This phenomenon must be taken into account when performing precise astronomical measurements and interpreting data from sources with strong gravitational fields.

- Gravitational Waves and Light: Additionally, about this part in the above references, the detection of gravitational waves (via instruments such as LIGO and Virgo) is frequently accompanied by electromagnetic observations. For instance, the merger of two neutron stars can generate both gravitational waves and electromagnetic radiation (light) in the form of gamma-ray bursts. Detecting both signals can provide a more complete picture of such occurrences.The Effect of Time Dilation on Light: In a strong gravitational field, time appears to pass more slowly than in a weakened field. This can affect the frequency and phase of light and must be taken into account for certain precise measurements or observations. [12]

- Global Positioning System (GPS) satellites transmit signals (electromagnetic radiation) to the Earth. To obtain precise location data, both the satellites' motion and the gravitational field of the Earth must be taken into consideration. Without the corrections provided by general and special relativity, GPS readings would be significantly off [13].

In modern technology and observations, these effects are no longer merely theoretical. They are practical considerations in disciplines such as astronomy, astrophysics, and navigation. Scientists and engineers can make precise measurements and inferences about the universe and our location within it if they comprehend and account for gravity's effect on light. Therefore, the electromagnetic spectrum encompasses a broad range of energy wavelengths, spanning from thousands of kilometers to minute atomic fractions. Every wavelength, represented by λ when in a vacuum, corresponds to a specific frequency (f) and photon energy

(E). The relationship between these variables is dictated by the formulas involving the speed of light (c) and Planck's constant (h). Essentially, electromagnetic waves with high frequency display short wavelengths and high energy, while those with low frequency show longer wavelengths and decreased energy. When these waves pass through a medium, their wavelengths decrease. Yet, their radiation length is typically cited based on the vacuum context [14].

$$\lambda = \frac{c}{f} \quad , \quad E = h.f \quad \text{or} \quad E = \frac{h.c}{\lambda}$$

where:

wave speed (c) = frequency * wavelength

c is the speed of light, 299,792,458 m/s (exact).

h is Planck's constant, (SI), the constant value is $6.62607015 \times 10^{-34}$ joule * $hertz^{-1}$ (or joule*seconds). Known as the fundamental universal constant that characterizes the quantum nature of energy and relates the energy and frequency of a photon.

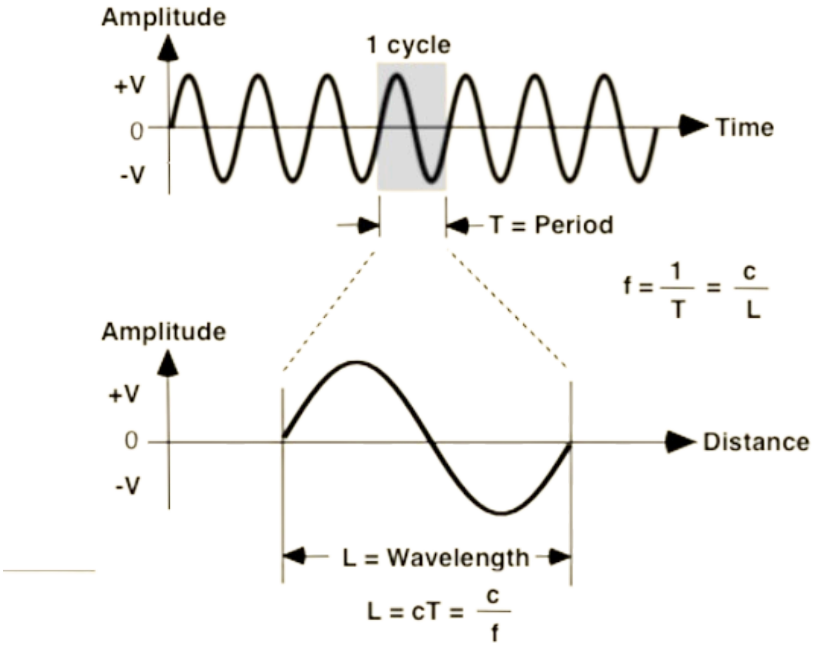

Figure 1.1.4 Electromagnetic Wave Parameters

The characteristics of electromagnetic radiation include amplitude, wavelength, frequency, and period. The relationship **E = h*f** demonstrates that the energy of a light wave is proportional to its frequency. These photons have distinct energy units, or quanta, which can be transferred to atoms and molecules upon absorption. Similarly, atoms and molecules can emit photons to discharge energy.

$$\lambda = \frac{c}{f} \qquad \rightleftarrows \lambda = \frac{300 \times 10^{-8} m/s}{1.5 \times 10^{14} \frac{1}{s}}$$

e.g. A particular wave of electromagnetic radiation has a frequency of 1.5 ×1014 Hz, and according to the equation that relates frequency, wavelength, and the speed of light, the λ is λ = 2.00×10^{-6} m. [15]

According to the electromagnetic spectrum (Figure 1), the result of λ corresponds to the visible spectrum.The visible light spectrum, which our eyes can perceive, is a tiny portion of the existing radiation types. On its right side are low-frequency energies like infrared rays, microwaves, and radio waves; these are non-harmful due to their low frequencies and energies. Conversely, on the left side are high-frequency radiations: ultraviolet (UV) rays, X-rays, and gamma rays. Their high frequencies and energies can be harmful. Fortunately, our atmosphere filters out the extremely damaging gamma rays from space, keeping us safe.

e.g. Calculating of a photon's energy if its frequency is 2.0×1024 Hz Planck's equation: E=hf , E= (6.626×10−34 J⋅ s) × (2.0×1024 s−1) = 1.3×10−9 J or 1.3252 nJ

The given frequency is extremely high, far exceedingly even gamma-ray frequencies. There isn't a commonly discussed region of the electromagnetic spectrum beyond gamma rays at such a high frequency.

The interaction of EM radiation with atoms and molecules is influenced by its energy per quantum. It can even be segmented similarly to sound waves, into octaves, totaling around eighty-one octaves. Spectroscopy, which can detect a broader spectrum range beyond the visible 400 nm to 700 nm, provides intricate data about objects' physical attributes and is a tool frequently used in astrophysics. For instance, hydrogen atoms often release radio waves with a 21.12 cm wavelength.

1.2 Electromagnetic spectrum, light and applications in the telecommunication field.

According to the 1.1 references about the electromagnetic spectrum and its range, is followed by Radio frequencies, Microwaves, Terahertz radiation, Infrared radiation, Visible radiation (light) Ultraviolet light, X-rays, and Gamma rays with their applications mainly in the communication field. [16]

1.2.1 Radio frequencies

Antennas, crafted on resonance principles, utilize radio waves, spanning from hundreds of meters to about a millimeter, for data transmission. These waves support technologies like TV, mobile phones, Wi-Fi, and amateur radio. Information transmission involves modifying wave characteristics, such as amplitude, frequency, and phase. When these waves encounter conductors, they induce an electric current on the surface, a phenomenon used in antennas. This property is also behind the working of microwave ovens, where molecules absorb the radiation and heat up. The radio spectrum, which spans from 3 Hz to 3,000 GHz (3 THz), has become indispensable in modern telecommunications. Its usage is tightly regulated by national and international entities like the ITU, which divides the spectrum for varied applications. As demand surges, parts of this spectrum are sometimes licensed to private entities. This increased demand and spectrum congestion is driving innovations in telecommunications, like spread spectrum and cognitive radio [17], [18],[19].

- Broadcast frequencies for AM radio span various ranges from longwave to shortwave.

- Television and FM radio frequencies differ globally, with parts of the TV broadcasting band in North America being repurposed for cellular use.
  The U.S. Apex band, a pre-WWII VHF (World War II Very High Frequency) audio broadcasting frequency, was supplanted by FM broadcasting. The Airband, crucial for aircraft communication, spans 108 to 137 MHz in the VHF spectrum, while marine bands facilitate communication for sea vessels, with the marine VHF radio aiding short-range coastal communication.

- Amateur radio frequencies vary worldwide, with specific bands available based on regional allocations. The Citizens' Band radio, common in many countries, supports personal and business communication. The ISM bands, initially for non-communication uses, now support devices like Wi-Fi and Bluetooth.

- Terrestrial bands cater to fixed stations and land-based mobile devices, with a growing portion allocated for cellular communication. Finally, dedicated bands ensure reliable radio control, with a trend towards 2.4 GHz systems, and specific frequencies cater to specialized uses like industrial controls.

- Radar applications utilize relatively potent pulse transmitters and sensitive receivers; therefore, radar operates on frequencies that are not used for other purposes. The vast majority of radar frequencies are located in the microwave region of the electromagnetic spectrum, but potent UHF transmitters are utilized for meteorologically significant applications.

The IEEE Standard 521-2002, titled "IEEE Standard Letter Designations for Radar-Frequency Bands," affirms letter band designations corresponding to specific radar frequency ranges. The 1984 edition introduced the usage of the V and W designations for a segment of the millimeter wave region, while maintaining prior frequency letter designations. [20]

Table 1. IEEE Standard Radar Bands

IEEE Standard Radar Band Nomenclature (*IEEE Std. 521-2002, IEEE Standard Letter Designations for Radar-Frequency Bands)		
Designation	**Frequency**	**Wavelength**
HF	3 - 30 MHz	100 m - 10 m
VHF	30 - 300 MHz	10 m - 1 m
UHF	300 - 1000 MHz	100 cm - 30 cm
L Band	1 - 2 GHz	30 cm - 15 cm
S Band	2 - 4 GHz	15 cm - 7.5 cm
C Band	4 - 8 GHz	7.5 cm - 3.75 cm
X Band	8 - 12 GHz	3.75 cm - 2.50 cm
Ku Band	12 - 18 GHz	2.50 cm - 1.67 cm
K Band	18 - 27 GHz	1.67 cm - 1.11 cm
Ka Band	27 - 40 GHz	1.11 cm - .75 cm
V Band	40 - 75 GHz	7.5 mm - 4.0 mm
W Band	75 - 110 GHz	4.0 mm - 2.7 mm
mm Band	110 - 300 GHz	2.7 mm - 1.0 mm

The 2002 update upholds these designations but modifies the millimeter wave frequencies definition to align with ITU naming conventions. While these letter designations are pertinent for radar purposes, they aren't intended to replace the precise frequency limits, which should be employed when needed.

These designations, while created for radar applications, are not designed for other radio or telecommunications contexts unless they relate to radar. Notably, the UHF (upper), SHF, and EHF segments of the electromagnetic spectrum are typically categorized as microwave frequencies. Despite originally being designated for radar, letter classifications like L, S, C, X, Ku, K, and Ka have gained popularity in other microwave frequency usages. [21]

Table **2.** *Radar Bands (ITU)*

International Telecommunications Union (ITU) Radar Band Nomenclature (ITU classifications are based on region-2 radiolocation service allocations)	
Band Designation	**Frequency**
VHF	138 - 144 MHz 216 - 225 MHz
UHF	420 - 450 MHz 890 - 942 MHz
L	1.215 - 1.400 GHz
S	2.3 - 2.5 GHz 2.7 - 3.7 GHz
C	5.250 - 5.925 GHz
X	8.500 - 10.680 GHz
Ku	13.4 - 14.0 GHz 15.7 - 17.7 GHz
K	24.05 - 24.25 GHz 24.65 - 24.75 GHz
Ka	33.4 - 36.0 GHz
V	59.0 - 64.0 GHz
W	76.0 - 81.0 GHz 92.0 - 100.0 GHz
mm	126.0 - 142.0 GHz

	144.0 - 149.0 GHz
	231.0 - 235 GHz
	238.0 - 248.0 GHz

The key differences are that the ITU nomenclature is broader and less granular, covering wider frequency ranges for general telecommunications and regulatory purposes, while the IEEE nomenclature is more granular with narrower frequency ranges, making it useful for detailed radar and high-frequency communications. Some bands have overlapping or nearly overlapping frequency ranges but are

labeled differently; for example, the ITU SHF band (3 GHz to 30 GHz) includes multiple IEEE bands such as S, C, X, Ku, and part of K. The ITU focuses on broad communication and regulatory applications, whereas the IEEE targets technical and engineering uses, particularly in radar.

1.2.2 Microwaves

Wavelength range: 1 mm - 1m
Frequency range: Ultra high frequency (UHF) (300 MHz-3 GHz)
Super high frequency (SHF) (3-30 GHz)
Extremely high frequency (EHF) (30-300 GHz).
Photon energy (eV): 1.24 meV – 1.24 μeV

Table 3. Microwaves frequency bands

Bands	Frequency range	Wavelength range	Typical uses
L band	1 to 2 GHz	15 cm to 30 cm	military telemetry, GPS, mobile phones (GSM), amateur radio
S - band	2 to 4 GHz	7.5 cm to 15 cm	weather radar, surface ship radar, some communications satellites, microwave ovens, microwave devices/communications, radio astronomy, mobile phones, wireless LAN, Bluetooth, ZigBee, GPS, amateur radio
C band	4 to 8 GHz	3.75 cm to 7.5 cm	long-distance radio telecommunications, wireless LAN, amateur radio
X band	8 to 12 GHz	25 mm to 37.5 mm	satellite communications, radar, terrestrial broadband, space communications, amateur radio, molecular rotational spectroscopy

Ku band	12 to 18 GHz	16.7 mm to 25 mm	satellite communications, molecular rotational spectroscopy
K band	18 to 26.5 GHz	11.3 mm to 16.7 mm	radar, satellite communications, astronomical observations, automotive radar, molecular rotational spectroscopy
Ka- band	26.5 to 40 GHz	5.0 mm to 11.3 mm	satellite communications, molecular rotational spectroscopy
Q band	33 to 50 GHz	6.0 mm to 9.0 mm	satellite communications, terrestrial microwave communications, radio astronomy, automotive radar, molecular rotational spectroscopy
U band	40 to 60 GHz	5.0 mm to 7.5 mm	
V band	50 to 75 GHz	4.0 mm to 6.0 mm	millimeter wave radar research, molecular rotational spectroscopy, and other kinds of scientific research
W band	75 to 110 GHz	2.7 mm to 4.0 mm	satellite communications, millimeter-wave radar research, military radar targeting and tracking applications, some non-military applications, automotive radar
F band	90 to 140 GHz	2.1 mm to 3.3 mm	SHF transmissions: Radio astronomy, microwave devices/communications, wireless LAN, most modern radars, communications satellites, satellite television broadcasting, DBS, amateur radio
D band	110 to 170 GHz	1.8 mm to 2.7 mm	EHF transmissions: Radio astronomy, high-frequency microwave radio relay, microwave remote sensing, amateur radio, directed-energy weapon, millimeter wave scanner

Microwaves, which are typically associated with television weather forecasts and kitchen ovens, operate distinctively. Microwaves of approximately 12 centimeters in length induce rotation in water and lipid molecules, which produces heat when cooking food. On a broader spectrum, microwaves are classified as high-frequency radio waves. Their application varies based on the wavelengths or "sub-bands" of their electromagnetic radiation. C-band microwaves, for instance, can penetrate through atmospheric obstructions to reveal the Earth's surface, whereas L-band microwaves, such as those in GPS systems, can detect the soil moisture of rainforests by penetrating forest canopies. The SeaWinds instrument on the QuikSCAT satellite uses Ku-band microwaves to measure oceanic wind velocities. Communication satellites typically use C-, X-, and Ku-bands. The ability of these microwaves to travel through clouds enables scientists to examine the conditions beneath hurricanes.

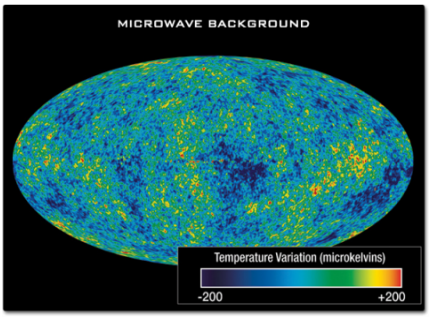

Figure 1.2.2.1

A comprehensive image of the young universe when it was just 380,000 years old is provided by the Wilkinson Microwave Anisotropy Probe (WMAP). The captured light, which was emitted around 13.7 billion years ago, now has a temperature of approximately 2.7 Kelvin. The variations in temperature, evident as color variations in the image, later formed the basis for the development of galaxy clusters. Source: NASA/WMAP Science Team

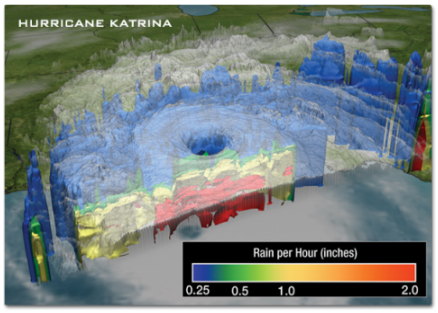

Figure 1.2.2.2 Passive remote sensing

A microwave imager from NASA's Tropical Rainfall Measuring Mission (TRMM) can collect data from beneath storm clouds, providing insight into the formation of rain. Source: NASA/Goddard Space Flight Center Scientific Visualization Studio

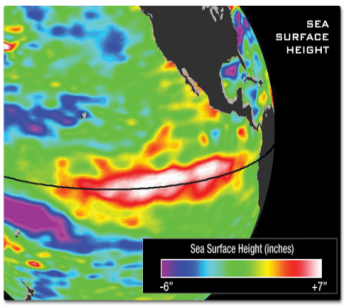

Figure 1.2.2.3 The radar altimeter on the Jason-2 satellite of the NASA/CNES Ocean Surface Topography Mission measures sea surface height. It emits microwaves at two distinct frequencies and measures the time required for these vibrations to return. By combining this information with data from other instruments that account for the effects of altitude and water vapor, the satellite can estimate the height of the sea surface to within a few centimeters.Source:NASA/JPL Ocean Surface Topography Team.

Radar is distinguished as an active remote sensing system. It emits a microwave discharge and detects the energy that is reflected. Based on this principle, devices such as Doppler Radar and Radar Altimeters operate. By timing microwave pulse returns, the radar altimeter aboard the NASA/CNES OSTM/Jason-2 satellite (Figure 1.2.2.3) can calculate the height of the sea surface with remarkable accuracy. Passive remote sensing, which solely detects electromagnetic waves, has revolutionized weather forecasting.

The NASA TRMM (figure 1.2.2.2) microwave imager is an example of a device that provides insight into rain structures beneath storm clouds. In a seminal discovery made in 1965, Arno Penzias and Robert Wilson of Bell Labs detected cosmic microwave background radiation, evidence of the Big Bang, also known as the beginning of the universe. The WMAP image provides a glimpse of the universe 380,000 years ago, emphasizing the fluctuations in temperature that led to the formation of galaxy clusters. [22],[23],[24],[25],[26],[27],[28]

1.2.3 Gamma Rays

Wavelength range: $< 1\times10^{-12}$ m
Frequency range: $3 *10^{18}$ Hz to $5*10^{22}$ Hz.
Speed of wave: 3×10^{8} ms^{-1}

Gamma rays the most energetic waves in the electromagnetic spectrum, are distinguished by their incredibly short wavelengths and intense energy levels, exceeding the energy of the visible spectrum by an astounding 10,000 times. Gamma-ray bursts are astoundingly powerful, even outshining the Sun's entire expected 10-billion-year energy output in just 10 seconds. Originating from cosmic events like neutron stars, supernovas, and black holes, as well as terrestrial processes including nuclear explosions and radioactive decay, they play a crucial role in both terrestrial and space research. As they move through substances, their potent energy ionizes the medium, giving them ionizing radiation. This capacity to ionize allows them to modify atomic configurations through interactions, leading to emissions of γ radiation. Such high energy is pivotal in various applications. NASA's

Swift satellite has recorded distant gamma-ray events, like a black hole birth 12.8 billion light years away. Moreover, gamma rays offer a unique method to discern planetary compositions; for instance, NASA's MESSENGER and Mars Odyssey Orbiter use gamma rays to identify elements on Mercury and Mars, respectively. NASA's Fermi telescope even mapped the Milky Way using gamma rays [29], revealing a dynamic gamma-ray perspective of the universe, unlike the static constellations we observe in visible light.

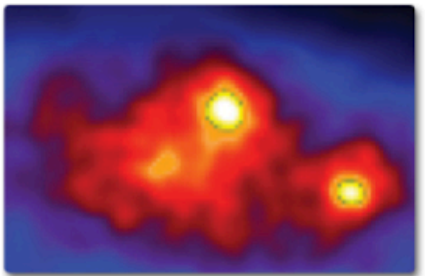

Figure 1.2.3.1 Cygnus gamma rays region detected by Fermi gamma-ray space telescope.
Source:NASA/DOE/International LAT Team NASA/JPL-Caltech/ASU

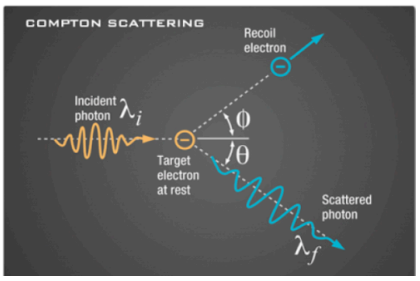

Figure1.2.3.2 Compton Scattering

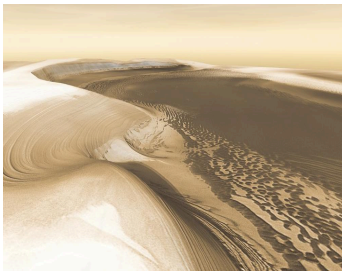

Figure 1.2.3.3 Chasma Boreale valley into Mars' north polar ice cap.

Moreover, due to their short wavelengths, capturing gamma rays is challenging as they can bypass spaces within detector atoms. However, using dense crystal blocks in detectors, scientists can track them when they collide with electrons, known also as the Compton scattering phenomenon. Some of its applications on the Earth are to disinfect medical instruments, enhance crystal value, preserve food, and detect oil pipeline breaks. In medical applications, while they're instrumental in targeting tumors, there's also potential harm to healthy cells, necessitating continuous advancements in radiation therapy for safety.

1.2.4 X-Rays

Wavelength range: 1×10^{-9} – 1×10^{-12} m

Frequency range: 1×10^{17} – 1×10^{20} Hz

Speed of wave: 3×10^{8} ms^{-1}

Photon energy (eV): 124 keV – 124 eV

X-rays have substantially greater energy and shorter wavelengths than ultraviolet light, with some having wavelengths as small as a single atom. Wilhelm Conrad Roentgen discovered these in 1895 and identified their ability to generate detailed images of bones within the body. The Sun's corona, which is hotter than its interior, emits predominantly x-rays. Instruments on satellites, such as Japan's Hinode spacecraft, capture these x-rays, casting light on energy dynamics within the corona. Extremely heated objects, such as pulsars and black holes, emitting X-rays can provide information about the characteristics of distant celestial entities. X-ray telescopes use grazing incidence mirrors to focus x-rays onto detectors. On Mars, the Spirit Rover utilized x-rays to detect the presence of metals such as zinc and nickel in boulders. Since the Earth's atmosphere blocks x-ray radiation, observations from space are vital. For example, the supernova remnant Cassiopeia A was analyzed using data from multiple NASA observatories, with x-rays emphasizing the formation of hot gases during explosive interactions. Such insights assist researchers in comprehending phenomena such as the coexistence of calm dust grains in gases emitting x-rays at extremely high temperatures. In addition, during solar cyclones, the Earth's magnetosphere can capture Sun-emitted energetic particles, resulting in auroras. Even though the resulting x-ray emissions are absorbed by the Earth's atmosphere and are therefore innocuous to us, the Polar satellite's PIXIE instrument reveals captivating images. [30]

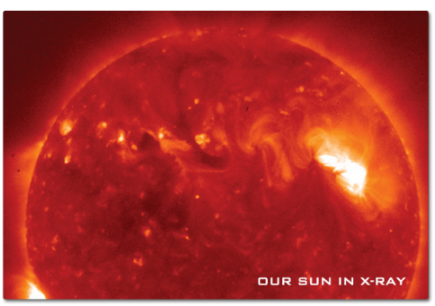

Figure 1.2.4.1 Our Sun in X-RAY

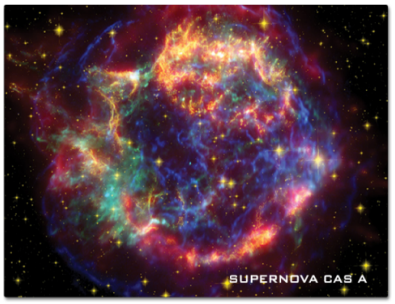

Figure 1.2.4.5 Supernova CAS A

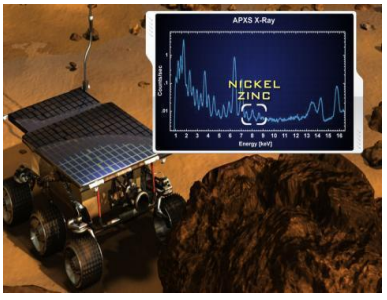

Figure 1.2.4.6 NASA's Mars Exploration Rover

Figure 1.2.4.1: Source: Hinode JAXA/NASA/PPARC

Figure 1.2.4.5 Source: X-ray: NASA/CXC/SAO; Optical: NASA/STScI; Infrared: NASA/JPL-Caltech/Steward/O.Krause et al.

Figure 1.2.4.6 : NASA's Mars Exploration Rover, detected the spectral signatures of zinc and nickel in Martian minerals using x-rays. The Alpha Proton X-Ray Spectrometer (APXS) instrument employs two techniques, one for determining structure and the other for determining composition,to determine structure and composition,respectively. These methods are most effective for metals.

1.2.5 Terahertz radiation

Frequency range: 0.3 THz to 3 ThZ
Wavelength range: 1mm to 100μm

Terahertz (THz) radiation, also called submillimeter waves or T-rays, has a frequency range of 0.3 to 3 terahertz, but some sources say it goes up to 30 THz. One terahertz is equal to 1,000 GHz, and its widths are between 1mm and 100m. This puts THz radiation between microwave and far-infrared radiation. It can be thought of as either one. At certain frequencies, it can be absorbed by gases in the air, but there are times when it can travel up to a kilometer or more. The 0.3 THz band is likely to be used for 6G communications. THz radiation can go through some materials but not others, which makes it useful for seeing inside solid things without the dangers of X-rays. Terahertz radiation fills the "terahertz gap" in the electromagnetic spectrum. This is a part of the spectrum where waves can't be made or changed by regular electronic devices, so new technology is needed. Terahertz energy is like a mix of microwaves and infrared light in terms of how it works. Like microwaves, it can pass through many things that don't carry electricity, but not as deeply. Also, like infrared, it has a hard time getting through air, clouds, liquid water, or metal. Even though it can go through body tissue like X-rays, it doesn't ionize, which makes it a better option for medical imaging. But because it has a longer wavelength than X-rays, it can't make pictures with as much detail. Atmospheric absorption and technical problems limit how terahertz radiation can be used right now, but study is being done to find ways around these problems. In May 2012, scientists from the Tokyo Institute of

Technology[36] reported in Electronics Letters that they had achieved a new milestone in wireless data transmission using T-rays[37]. They highlighted the potential of T-rays in future data transmission bandwidths. Their innovative device utilized terahertz band waves created by a resonant tunneling diode (RTD) negative resistance oscillator. This RTD enabled the transmission of a signal at 542 GHz, achieving a data transfer rate of 3 Gigabits per second[37]. This surpassed the previous data transmission speed record established just a few months earlier[38]. While the research indicated that the effective range for Wi-Fi using this technology would be around 10 meters (33 feet), it has the potential to achieve transmission speeds of up to 100 Gbit/s[39]. A year prior, the electronic components manufacturer, Rohm, in collaboration with researchers at Osaka University, developed a chip capable of transmitting 1.5 Gbit/s using terahertz energy[39]. Such technology could prove valuable in high-altitude communication scenarios where water vapor can disrupt signals, such as communication from aircraft to satellites or between satellites. [40]

NASA also remarked on the possibility of terahertz imaging in 2012. Terahertz imaging is on the electromagnetic spectrum between microwave and infrared. This imaging can make some materials see-through, which is useful at airports to find hidden things under clothes and at NASA's Kennedy Space Center to check the insulation foam on the space shuttle tanks. Robert Youngquist from Kennedy said that problems with this foam caused a flight disaster in the past. NASA used terahertz photography to find these problems, which made sure the material was safe. NASA asked for proposals in 2009 for 3D imaging tools for possible future space vehicles. LongWave Photonics and MIT in Boston got NASA's attention with their high-power terahertz radiation source, the quantum cascade laser (QCL). Alan Lee of LongWave Photonics said that the QCL, which was made for infrared frequencies at first, was changed to work with terahertz frequencies. With help from NASA, LongWave Photonics improved the QCL and made the "Easy QCL" widely available in 2011. When used with a certain camera, this tool allows for sensitive real-time imaging. At the moment, they are used in experimental biological microscopes, but they could also be used in the future in medicines, such as to look at the coatings on controlled-release tablets. This 3D imaging can find flaws below

the surface without hurting samples, making sure that tablet coatings are of high quality. As the partnership goes on, both sides expect to find many uses for it, such as in future NASA projects.

From the side we are interested, in the telecommunication part, the rapidly increasing demand for high-speed wireless communication has spurred interest in broader frequency bands, particularly the millimeter-wave and terahertz bands (0.1–3 THz) [41].

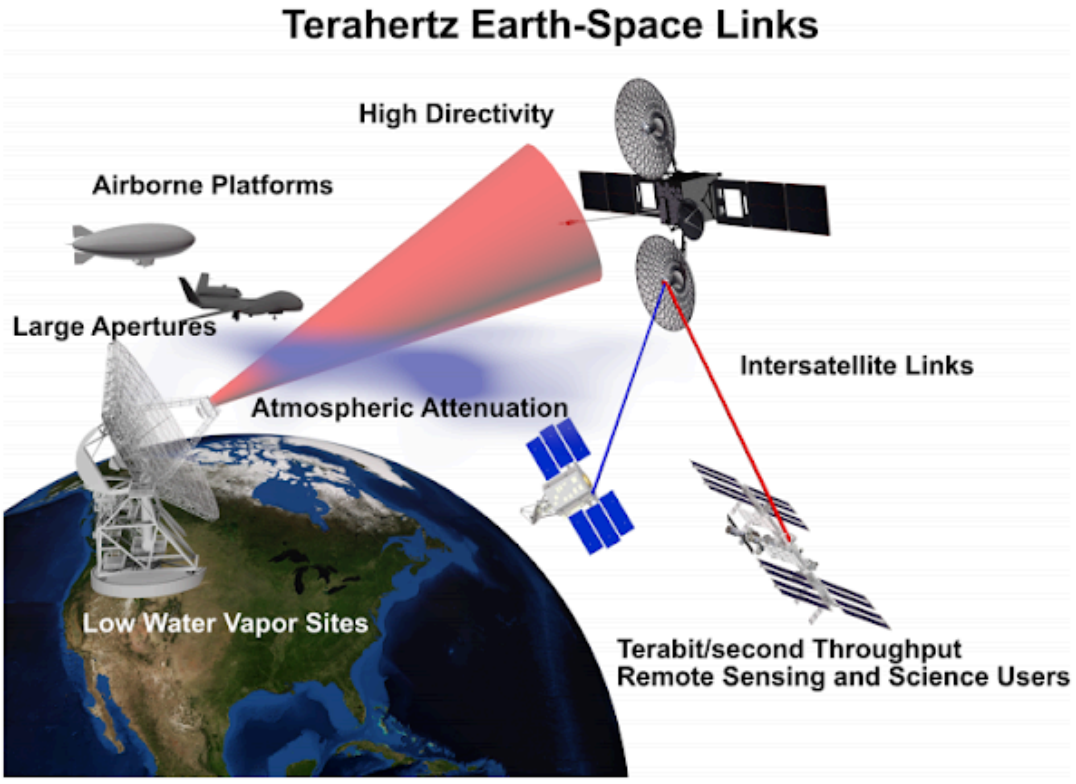

Figure 1.2.5.1 THz satellite link (3D Models source: NASA)

Despite traditional hesitations due to atmospheric interferences, observatories like the Atacama Large Millimeter/submillimeter Array (ALMA) in Chile have shown that these challenges can be mitigated in high-altitude, dry environments[29]. Emphasizing this potential, research [42] suggests that ground-to-satellite THz links might exploit untapped 125–1100-GHz bands, providing advantages such as frequency reuse and enhanced security [43]. Contrasting the limitations of current short-range THz applications, satellite-based THz links present promising solutions to meet the soaring bandwidth requirements of high-speed devices [44].

Wireless traffic, expanding at a 57% annual compound rate, is overtaking its wired counterpart [45]. This trend is exacerbated by the burgeoning need for commercial satellite services and data-intensive applications. Since 2020, the International Telecommunication Union (ITU) had projected that 3G and 4G networks would demand bandwidths ranging from 1.3 to 2.5 GHz [33]. This THz communication mode shares similarities with near-IR free-space optical satellite links, both aiming to secure more bandwidth and maintain a focused beam. Though optical bands boast advanced technology and allow compact apertures, they grapple with atmospheric disruptions. Conversely, while THz systems are challenged by atmospheric water vapor, they demonstrate superior performance under conditions like turbulence or cloud cover. Urgent areas for research in the THz realm include studying atmospheric perturbations on nanosecond timescales and understanding the impact of high-altitude clouds on THz transmissions. On the technology front, there's an acute need for low-noise, wide-bandwidth coherent receivers and further advancements in transmitters and integrated circuits.

1.2.6 Infrared radiation

Wavelength: 700 nm – 1 mm or*[1] 7×10^{-7} - 1×10^{-3}

Frequency: 300 GHz – 430 THz or 3×10^{11} - 4×10^{14}

Photon energy (eV): 1.7 eV – 1.24 meV or 2×10^{-22} - 3×10^{-19}

[1] In many references and sources in the internet the wavelengths can be given in a form of nm - mm instead of raised to the power of 10, the frequency instead of e.g GHz-THz in a form of raised to the power of 10 also, the photon energy the same.

Table 4 Telecommunication bands in the infrared (source: wikipedia)

Band	Descriptor	Wavelength range
O band	Original	1,260–1,360 nm
E band	Extended	1,360–1,460 nm
S band	Short wavelength	1,460–1,530 nm
C band	Conventional	1,530–1,565 nm
L band	Long wavelength	1,565–1,625 nm
U band	Ultralong wavelength	1,625–1,675 nm

The portion of the infrared spectrum used in optical communications is separated into seven bands based on the availability of light sources, transmitting/absorbing materials (fibers), and detectors. The C-band is the prevalent frequency band for long-distance communication networks. The S and L bands are based on less well-established technology and are not as extensively deployed.

Infrared waves, a segment of the electromagnetic spectrum, are invisible to the human eye but can be felt as heat. William Herschel discovered infrared light in 1800 after observing temperature variations across different colors in the visible spectrum, detecting the highest temperatures just beyond the visible red light. Devices like remote controls utilize infrared light waves, which span near-, mid-, and far-infrared. The range between 8 to 15 microns (μm) is particularly crucial for studying Earth's thermal energy. Infrared waves enable thermal imaging, allowing us to detect heat emissions from objects that our eyes cannot see, such as humans. Night-vision goggles and infrared cameras translate these waves into visible images, offering insights into warm objects. Astronomically, many celestial bodies, too faint in visible light, emit detectable infrared waves. The infrared spectrum has offered scientists

unique views, like Saturn's extensive auroras, captured by the Cassini spacecraft. Moreover, the longer wavelengths of infrared can traverse dense cosmic gas and dust, unmasking objects hidden from optical telescopes. The James Webb Space Telescope, equipped with infrared instruments, aims to uncover mysteries about the universe's origins. On Earth, infrared plays a pivotal role in monitoring surface temperatures, emitted as the planet absorbs solar radiation. Earth-observing satellites detect this infrared radiation, helping scientists monitor phenomena like forest fires and their aftermath, as demonstrated by instruments like the MODIS on the Aqua and Terra satellites. Infrared imaging provides valuable data on Earth's surface, revealing details like the structure of clouds based on their temperature. Both emission and reflection of infrared light from various objects, including animals and natural phenomena, underscore its significance in various scientific and practical applications. [47]

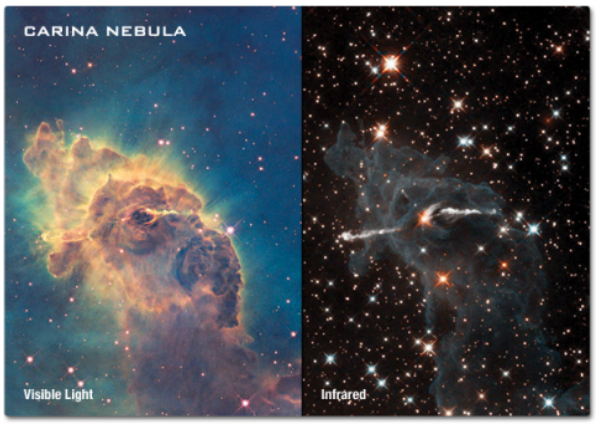

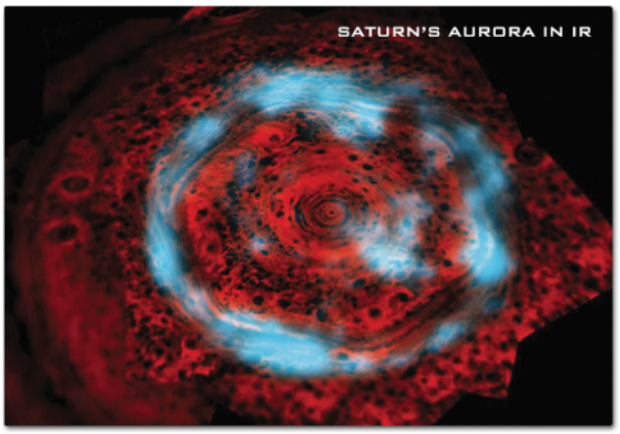

Figure 1.2.6.1 Carina Nebula in Infrared

Source:NASA, ESA,and the Hubble SM4 ERO Team

Figure 1.2.6.2 Saturn's aurora

Source: NASA, Cassini spacecraft

1.2.7 Visible radiation (light)

Wavelength: 400 nm – 700 nm

Frequency: 430 THz – 750 THz

Photon energy (eV): 3.3 eV – 1.7 eV

Table 5 Visible radiation colors, Source [33]

Color	Wavelength (nm)	Frequency (THz)	Photon energy (eV)
violet	380–450	670–790	2.75–3.26
blue	450–485	620–670	2.56–2.75
cyan	485–500	600–620	2.48–2.56
green	500–565	530–600	2.19–2.48
yellow	565–590	510–530	2.10–2.19
orange	590–625	480–510	1.98–2.10
red	625–750	400–480	1.65–1.98

Visible light represents a specific segment of the electromagnetic spectrum, detectable by the human eye, typically ranging between 380 to 700 nanometers in wavelength. Even though electromagnetic radiation encompasses a broad spectrum, our eyes, due to their biological limitations, are attuned only to this specific band, known as visible light. These wavelengths, when passing through a prism, diverge into distinct colors, from the shortest wavelength, violet, to the longest, red. The Sun remains our primary source of visible light, with its outer layer, the corona, observable during total solar eclipses as the Sun's brilliance is masked by the Moon. Interestingly, the color emitted by objects, like stars or even a torch flame, can indicate their temperature; for instance, our Sun emits predominantly yellow light due to its surface temperature of 5,500°C. This color-temperature relationship traces back

to observations where hotter objects tend to emit light at shorter wavelengths. Isaac Newton, in 1665, demonstrated how prisms could separate light into its constituent colors, each refracting differently based on its wavelength. Delving deeper into the spectrum of visible light from celestial bodies, scientists can discern absorption lines or specific patterns hinting at underlying properties of these objects. These patterns effectively serve as unique identifiers, much like fingerprints, indicating the presence of specific elements or molecules. Such spectral signatures extend beyond celestial studies; they're also applied on Earth, revealing unique reflectance signatures for various features. Another application of visible light in the realm of science is laser altimetry, an active remote sensing method.

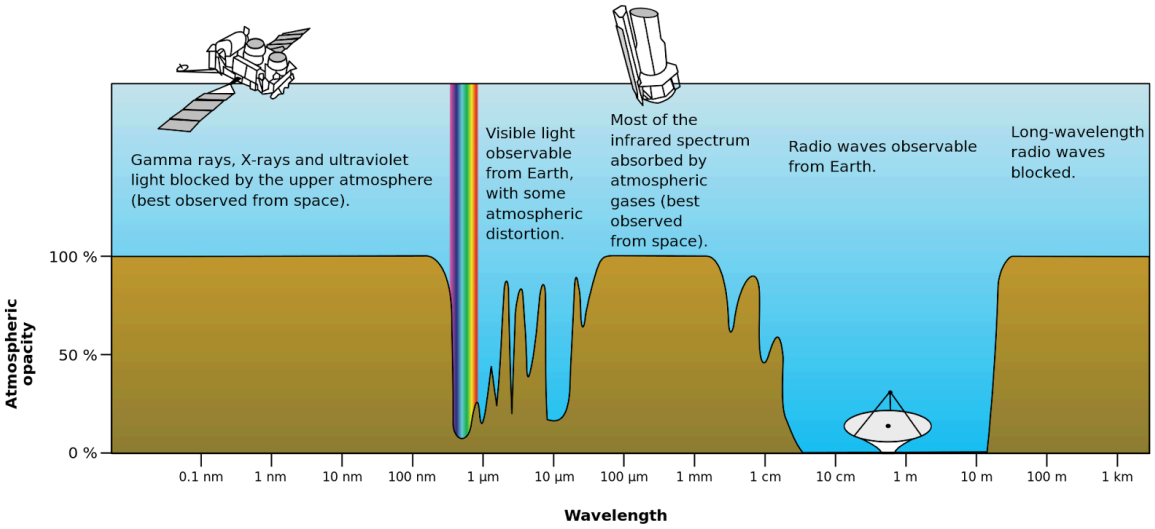

Figure 1.2.7.1 The Earth's atmosphere can obstruct certain electromagnetic radiation wavelengths.
However, when it **comes to visible light, it remains largely transparent.**
Source: NASA public

NASA has leveraged this technology, particularly with the GLAS instrument on the ICESat, to discern elevation changes in Earth's polar ice sheets, thus gauging water volume alterations in the form of ice. These lasers not only study ice elevations but also measure features like cloud heights, forest canopy structures, and even aerosol distributions from various environmental phenomena. All the process in remote sensing here occurs with spectroscopy technique, a study of the color spectrum that objects emanate, absorb, or reflect. By observing the emission and absorption lines of distant objects, this technique is essential in astronomy, allowing scientists to investigate their properties. These lines disclose chemical elements and molecules;

for example, Helium was identified for the first time in the Sun's spectrum. Moreover, by noting the frequency shift in these spectral lines, astronomers can ascertain the velocity of distant objects, which indicates whether they are moving toward or away from us. Utilizing high-dispersion diffraction gratings, astronomical spectroscopy achieves detailed spectral observations. [48], [49],[50]

1.2.8 Ultraviolet light

UV radiation resides between visible light and X-rays on the electromagnetic spectrum. UV radiation constitutes approximately 10 percent of the Sun's total electromagnetic radiation. Electric arcs, Cherenkov radiation, and specific illumination such as mercury-vapor lamps and tanning lamps are additional sources of ultraviolet radiation [51]. UV does not have the energy to ionize atoms, but it can initiate chemical reactions and cause numerous substances to fluoresce. Its interactions with organic molecules, which can result in absorption or changes in molecular energy states, have led to numerous practical applications, but not always involving heat [52].

The brief wavelength of UV light can cause DNA damage and sterilize surfaces upon contact. UV exposure can cause humans to develop suntans, sunburns, and an increased risk of developing skin cancer. If the Earth's atmosphere didn't filter out most of the UV radiation from the Sun, life on land might not be sustainable[51]. Nonetheless, some UV light (specifically UVB) is necessary for vitamin D formation in numerous terrestrial vertebrates, including humans [53]. Thus, the UV spectrum has both advantages and disadvantages for existence. Vision in humans typically begins around 400 nanometers (nm) away from the ultraviolet spectrum. However, under certain conditions, some individuals, particularly infants and young adults, may be able to perceive UV wavelengths as low as 310 nm [54][55]. On the other hand, birds, insects, and certain mammals can detect near-UV [56].

The term "ultraviolet" means "beyond violet" because UV radiation has a higher frequency and shorter wavelength than violet light.

In 1801, Johann Wilhelm Ritter, a German physicist, observed that invisible rays just beyond the violet end of the visible spectrum darkened paper immersed in silver chloride faster than violet light itself. Eventually, "ultraviolet" superseded "chemical rays"[57][58] as the most commonly used term. In 1878, it was discovered that short-wavelength light has a sterilizing effect, and by 1903, the most effective wavelengths were determined to be around 250 nm. 1960 saw the discovery of UV radiation's effect on DNA[15]. Later, in 1893, German physicist Victor Schumann discovered ultraviolet radiation below 200 nanometers, which he termed "vacuum ultraviolet" [59]. The spectrum of ultraviolet radiation, encompassing 10–400 nanometers, can be further subdivided according to ISO standard ISO 21348 [60]. There have been developments in UV spectrum detection devices[18]. Vacuum UV (shorter than 200 nm) is significantly absorbed by atmospheric oxygen, but the range of 150-200 nm can propagate through nitrogen. Therefore, this frequency range is utilized by scientific instruments in oxygen-free environments, such as pure nitrogen, eliminating the need for vacuum chambers. In the semiconductor manufacturing industry, 193-nm photolithography apparatus is an example of relevant technology. Depending on the discipline of study, the distinction between "hard UV" and "soft UV" can vary. In astrophysics, for instance, the limit could be the Lyman limit (91.2 nm), with "hard UV" being the more energetic segment [61]. However, this boundary may vary in various scientific or applied fields [62].

Ultraviolet radiation has a number of applications because of its ability to cause chemical reactions and stimulate fluorescence in materials.

The following gives some applications of specific UV wavelength bands.

- 13.5 nm: Extreme ultraviolet lithography
- 30–200 nm: Photoionization, ultraviolet photoelectron spectroscopy, standard integrated circuit manufacture by photolithography
- 230–365 nm: UV-ID, label tracking, barcodes
- 230–400 nm: Optical sensors, various instrumentation
- 240–280 nm: Disinfection, decontamination of surfaces and water (DNA absorption has a peak at 260 nm), germicidal lamps[38]

- 200–400 nm: Forensic analysis, drug detection
- 270–360 nm: Protein analysis, DNA sequencing, drug discovery
- 280–400 nm: Medical imaging of cells
- 300–320 nm: Light therapy in medicine
- 300–365 nm: Curing of polymers and printer inks
- 350–370 nm: Bug zappers (flies are most attracted to light at 365 nm)[85]

In conclusion of the Electromagnetic Spectrum sub-section, it is interesting to see also the risks and the properties of each energy [63].
The diagram-tree from coggle.it platform offers a quick view of these risks.
https://coggle.it/diagram/X165JU4r0mfkNtqg/t/electromagnetic-spectrum

1.3 Electromagnetic Spectrum and Space communication

As this thesis addresses mainly to communication systems and technology, the several types of radiation are used for communication signals are the Radio Waves with a range from very low frequency (VLF) to ultra-high frequency (UHF), the Microwaves which are essentially high-frequency radio waves and are particularly used for point-to-point communication and satellite communication e.g GPS and radar. It is included also the Infrared (IR) as it is still employed in certain communication contexts e.g audio systems, Short-range wireless communication between devices (e.g., IrDA standard), the Visible Light with some potential advantages in certain environments while also it is used the
Li-Fi via LED lights to transmit data by varying the intensity of the emitted light, which is detected and converted back into data by receivers, the Optical (Ultraviolet & Visible Light) Frequencies are used in fiber-optic communication. By transmitting data as light pulses through optical fibers, extremely high data rates and long-distance communication can be achieved without much loss of signal.
X-rays and gamma rays are not typically used for communication signals due to their ionizing nature and potential hazards.

For deep space communication, NASA and other space agencies rely predominantly on radio waves, specifically those in the microwave portion of the electromagnetic spectrum. This choice was based on the capacity of these waves to travel long distances without significant attenuation or absorption by interstellar matter, as well as their efficient penetration of the Earth's atmosphere upon return.
NASA's primary international array of giant radio antennas (Deep Space Network (DSN)) that supports interplanetary spacecraft missions, as well as a few that orbit Earth, predominantly employing S-band (2-4 GHz) and X-band (8-12 GHz) frequencies. Additionally, the DSN possesses Ka-band (26.5-40 GHz) communication facilities.

- S-band is employed for both uplink (transmitting commands to spacecraft) and downlink (receiving data from spacecraft). It is particularly advantageous for uplink because it is resistant to interference from the Earth's atmosphere, notably during rain.

- X-band: Used primarily for downlink due to its shorter wavelength, which allows for more precise data and tracking information.

- Ka-band: Provides even higher data rates than X-band and is used for specific missions that require transmitting large quantities of data back to Earth, such as high-resolution imaging missions.

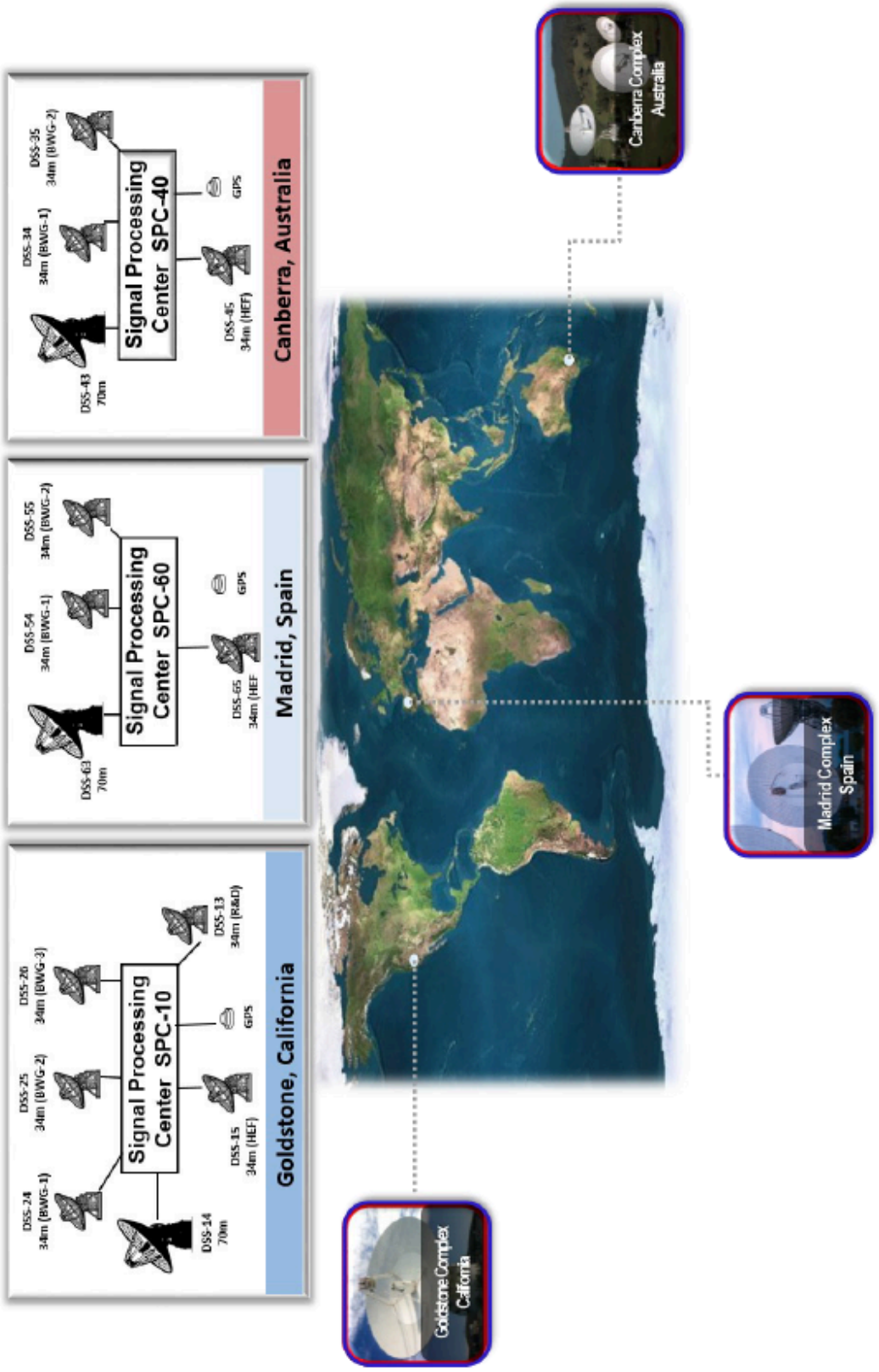

Figure 1.3.1 Deep Space Network, NASA

The Deep Space Network (DSN) actually is made up of three important tracking sites around the world that can help deep space missions around the world stay in touch and find their way. The three sites, Goldstone (USA), Madrid (Spain), and Canberra (Australia), are about 120 degrees apart in longitude. This allows flights above the Geosynchronous Earth orbit of 35,786 km (22,236 mi) to be tracked almost continuously. Each spot has big 34-meter and 70-meter antennas that can be turned and sensitive cryogenic receivers and big 20 kW transmitters. The DSN is open 24 hours a day, seven days a week, and 365 days a year. Operations on the network run more than 95% of the time every month, and most of the time they run more than 99% of the time.

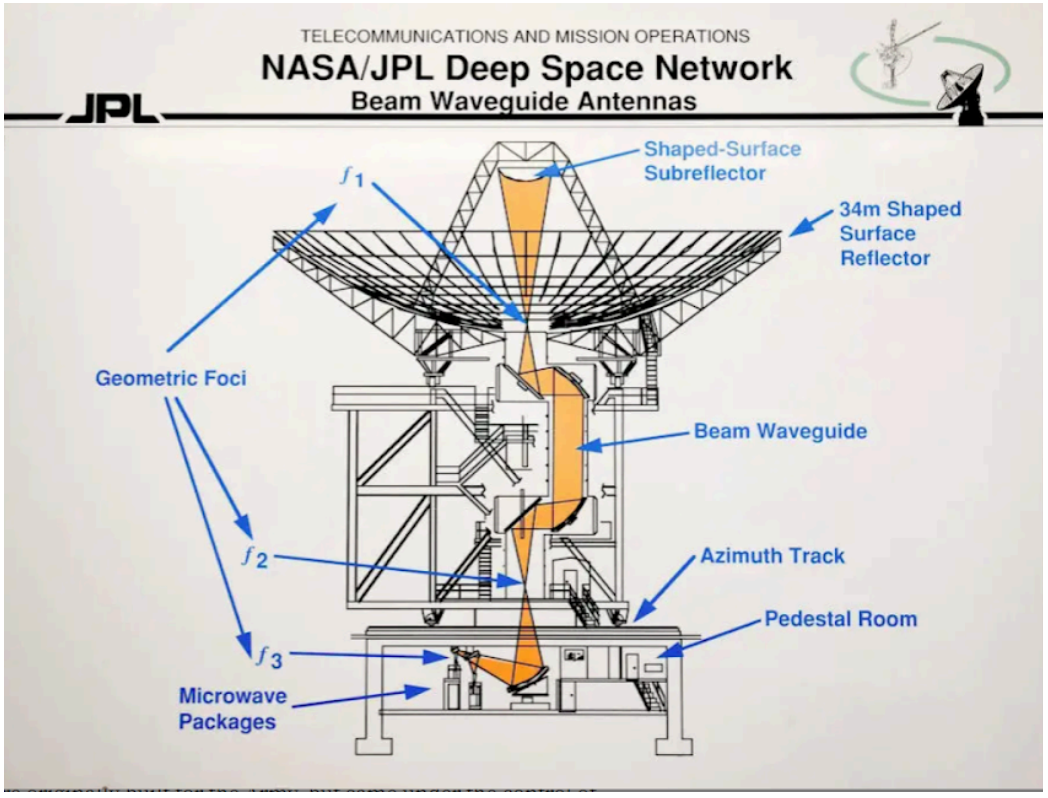

Figure 1.3.2 Shape of DSN antenna on the ground segment, Sourse: NASA

The DSN offers transmission services to a wide range of clients, such as:

- missions in deep space, including those that need to be very sensitive
- missions to the moon and beyond
- relay operations on Mars (providing services to people on the surface of Mars)
- missions to the Earth-Sun and Earth-Moon Lagrange points and missions in a Highly Elliptical Orbit (HEO).

Some of the standard services are about Data Transport, Command/Telemetry , Navigation, and Science services. Deep space communication presents although particular difficulties such the signal intensity which decreases with distance. As the spacecraft moves away from Earth, its signal becomes weaker, making message detection more difficult. Significant time disruptions can occur when communicating with distant spacecraft. Depending on their relative orbital positions, a transmission sent from Earth to Mars can take between four and twenty-four minutes to arrive. Moreover, if the Sun or other celestial bodies are in the line of sight between a spacecraft and the Earth (corresponding an other planet in our solar system we study), they can cause interference. Due to these factors, the antennas used by the Deep Space Network are immense (up to 70 meters in diameter) and are equipped with highly sensitive receivers.

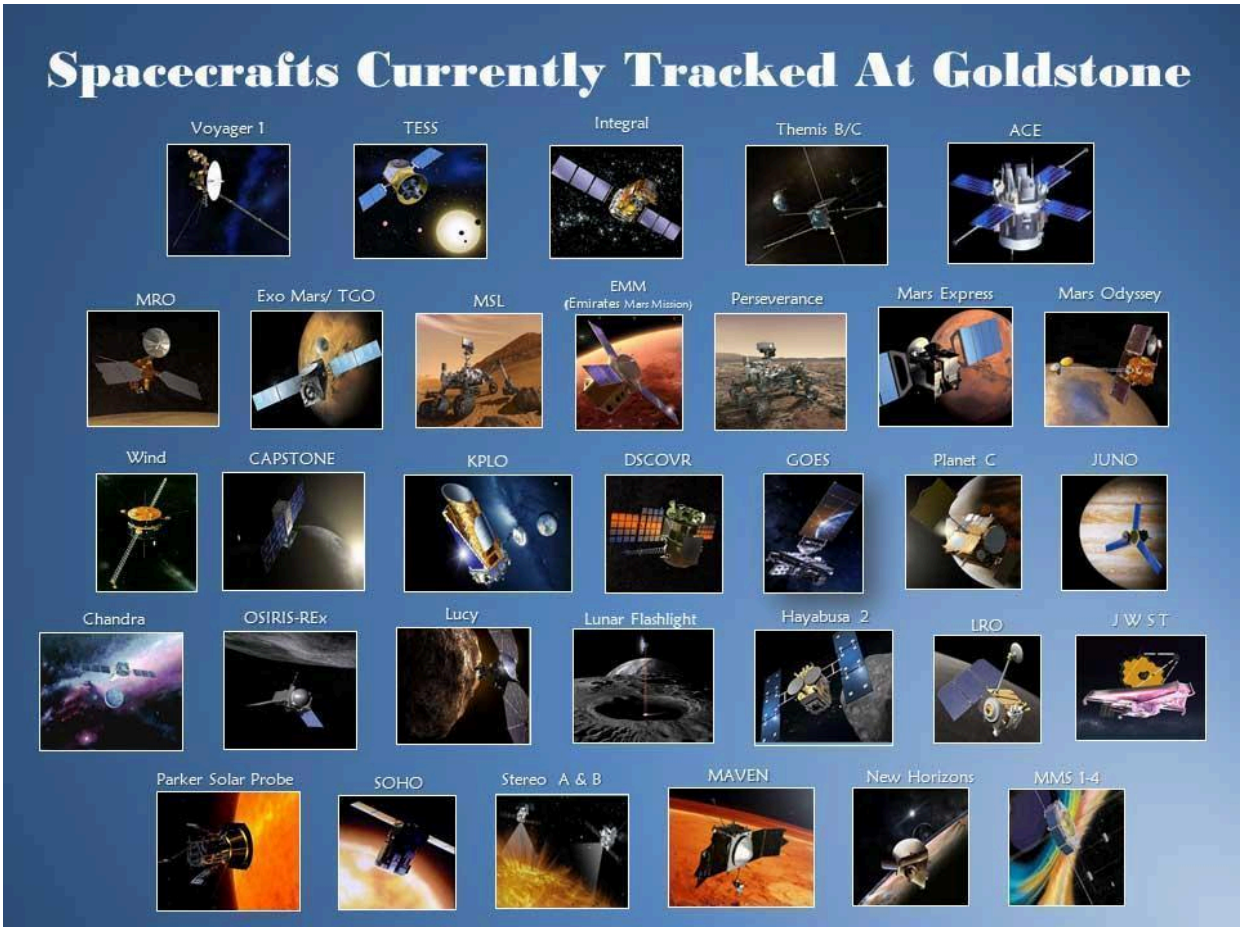

Figure 1.3.3. Spacecrafts that have tracked at Goldstone Complex / California

In addition, spacecraft are outfitted with high-gain antennas to narrowly direct their transmissions toward Earth, thereby increasing the likelihood that their feeble signals will be received. While radio waves are currently the primary method of deep space communication, there is ongoing research into the use of optical communication (lasers) in deep space. This method has the potential for much higher data rates, but there are obstacles to surmount, such as pinpointing the laser beam over extensive distances. Optical communication, often referred to as laser communication, is an emerging technology that uses light to transmit data. This method offers several advantages over RF communication, such as higher data transfer speeds and lower power consumption. However, it faces challenges like atmospheric disruptions and the need for precise pointing and tracking systems.FSO utilizes light to wirelessly transmit data, voice, and video across open spaces such as air, outer space, and vacuums. The transmission relies on sending light signals, and this light can be focused efficiently using LEDs or lasers.

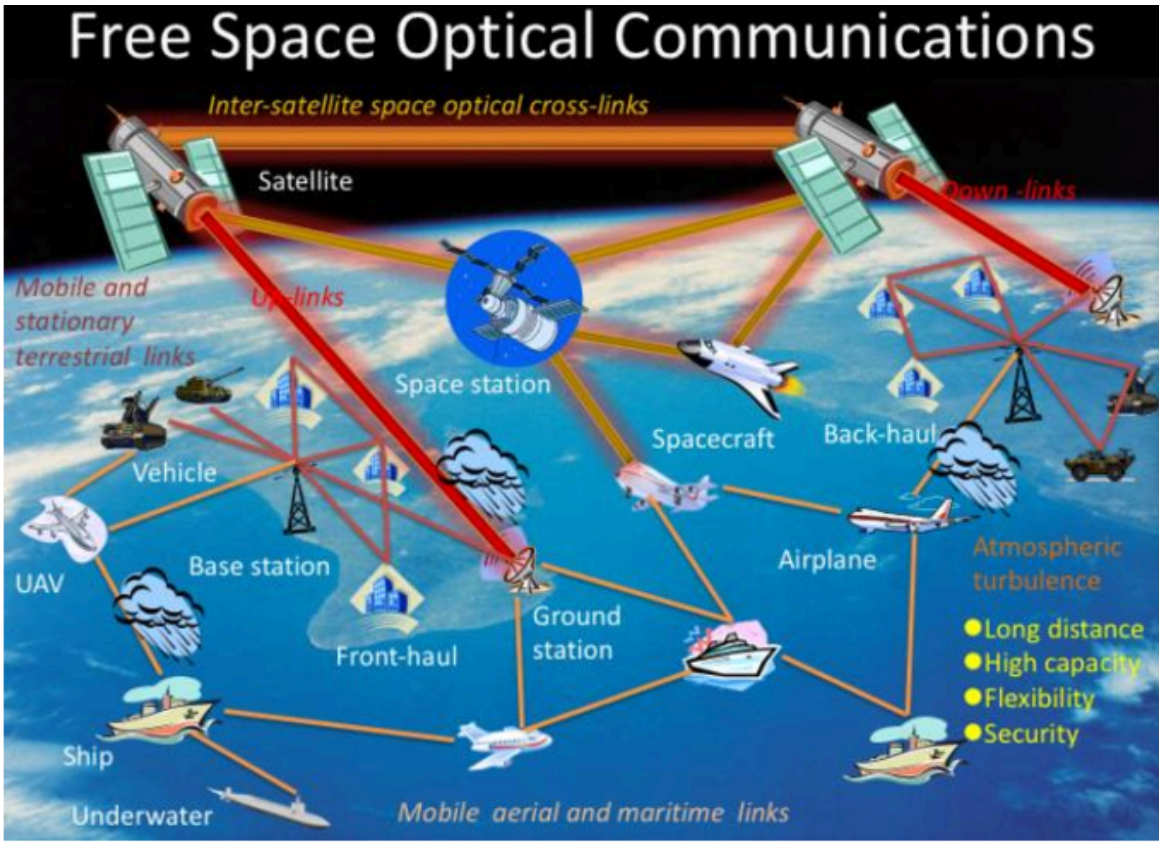

Figure 1.3.4. Free Space Optical Communication Network [58]

These lasers work on the principle of amplifying light through stimulated emission, making them powerful tools for transmitting data over considerable distances without the use of cables. The system's operation is similar to that of fiber-optic cable transmissions, with the significant distinction being that in FSO, light travels through open space instead of glass. The speed advantage comes from light's faster propagation through air than through glass. Overall, in FSO communication, light serves as the primary medium for conveying information over distances, making it essential for the system's functionality.

Free Space Optics (FSO) or optical communication has the potential also to be used in deep space applications. In fact, NASA and other space agencies have been investigating and testing the use of laser communication systems for deep space missions due to the potential advantages they offer over traditional radio frequency (RF) systems. Free Space Optics (FSO) is gaining traction as a potential solution for deep space communication due to its numerous advantages. For one, FSO systems promise significantly higher data rates than their RF counterparts, crucial for missions generating vast amounts of scientific data. Additionally, they can transmit this data more efficiently, consuming less power in the process.
Another compelling feature is the compactness of the required equipment; the antennas or telescopes needed for laser communication are considerably smaller than RF antennas, which translates to weight and volume savings on spacecraft. Moreover, the more focused nature of optical beams enhances the security against potential interception, offering a tighter communication beam than RF signals.

However, transitioning to FSO for deep space is not without its challenges. The accuracy demanded by FSO systems is immense, necessitating highly precise pointing mechanisms to ensure the laser beam's successful connection between the transmitting and receiving ends, especially considering the staggering distances involved in deep space communication. Furthermore, Earth's atmospheric conditions can disrupt laser signals, posing challenges for Earth-to-space or space-to-Earth communications — though this is not a concern for deep space-to-deep space links. Over extensive distances, the laser beam can also disperse, weakening the signal and demanding both powerful lasers and highly sensitive receivers to counteract this.

Recent tests and demonstrations have been positive. For example, the Lunar Laser Communication Demonstration (LLCD) (which also is referred to Section 5) on NASA's LADEE spacecraft in 2013, successfully showcased optical communication between the Moon and Earth. In summary, while FSO holds immense promise for revolutionizing deep space communication, it remains a technology in its developmental stages for such applications. Continued testing and refinement are essential for its adoption in deep space scenarios.

Section 2

The impact of the space environment on space vehicles (satellites, space capsules, probes, etc) and their communication systems.

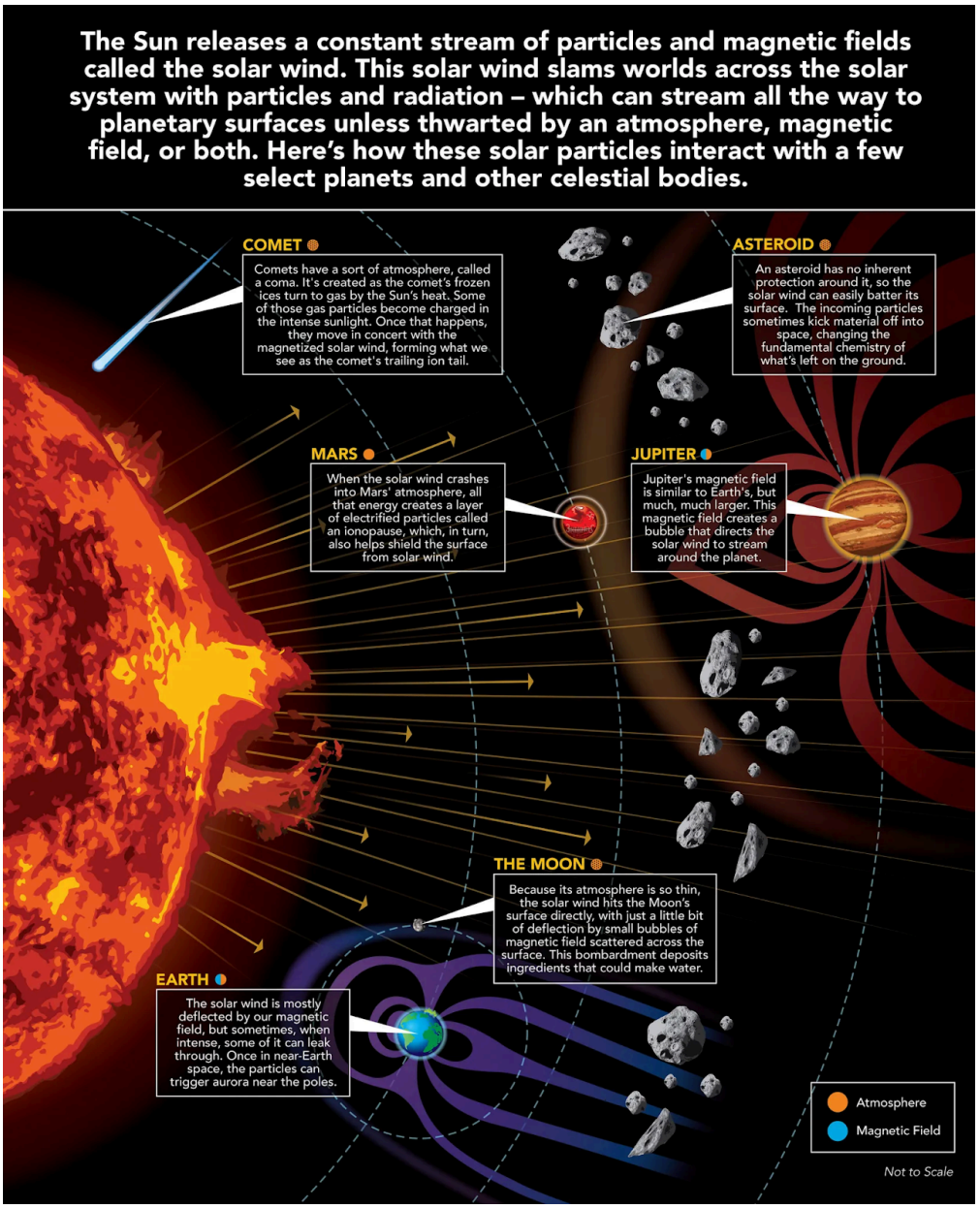

Figure 2 The Solar Wind Across Our Solar System

Many variables in space can negatively impact the operation and lifetime of space vehicles and their communication systems as the environment of space provide a unique set of effects of space radiation, noise, collisions, temperature extremes, microgravity, vacuum, magnetic fields, and geomagnetic storms.

In general, space radiation consists of galactic cosmic rays (GCRs), and solar energetic particles (SEPs), and if we are talking about Earth there is also trapped radiation in its radiation belts (e.g., Van Allen belts). This radiation can degrade the materials of space vehicles over time, reducing their mechanical strength and optical properties. It can also induce single-event upsets (SEUs), single-event latch-ups (SELs), and total ionizing dose (TID) effects in electronic components. It also can introduce noise in communication systems, reducing the signal-to-noise ratio as well as can damage or malfunction the electronic components of communication systems. Additionally, space debris, originating from sources like decommissioned satellites and rocket fragments, poses threats to space vehicles, with even minuscule debris capable of causing significant damage due to their high relative velocities. To dodge these threats, satellites often perform evasive maneuvers, which expend precious fuel. The vacuum of space presents an environment of thermal extremes, as the lack of an atmosphere prevents heat conduction, subjecting satellites to intense temperature fluctuations based on their orientation to the Sun.

This results in material stress, variations in system performance, and reduced battery life. Additionally, microgravity alters fluid dynamics and combustion processes in satellites. The vacuum of space can lead to material outgassing, potentially contaminating optical surfaces. Earth's magnetic fields and geomagnetic storms, stemming from solar interactions with the Earth's magnetosphere, can interfere with communication systems, induce surface charging on satellites, and disrupt navigation systems like GPS.

For satellites in low Earth orbit (LEO), atmospheric drag poses another challenge, reducing satellite altitude and necessitating fuel-intensive adjustments. In summary, the space environment offers a complex set of challenges for space vehicles and their communication systems, requiring comprehensive understanding and mitigation strategies to ensure their prolonged and effective operation. [64]

2.1 Space environment and typical effects on space systems and space communication systems

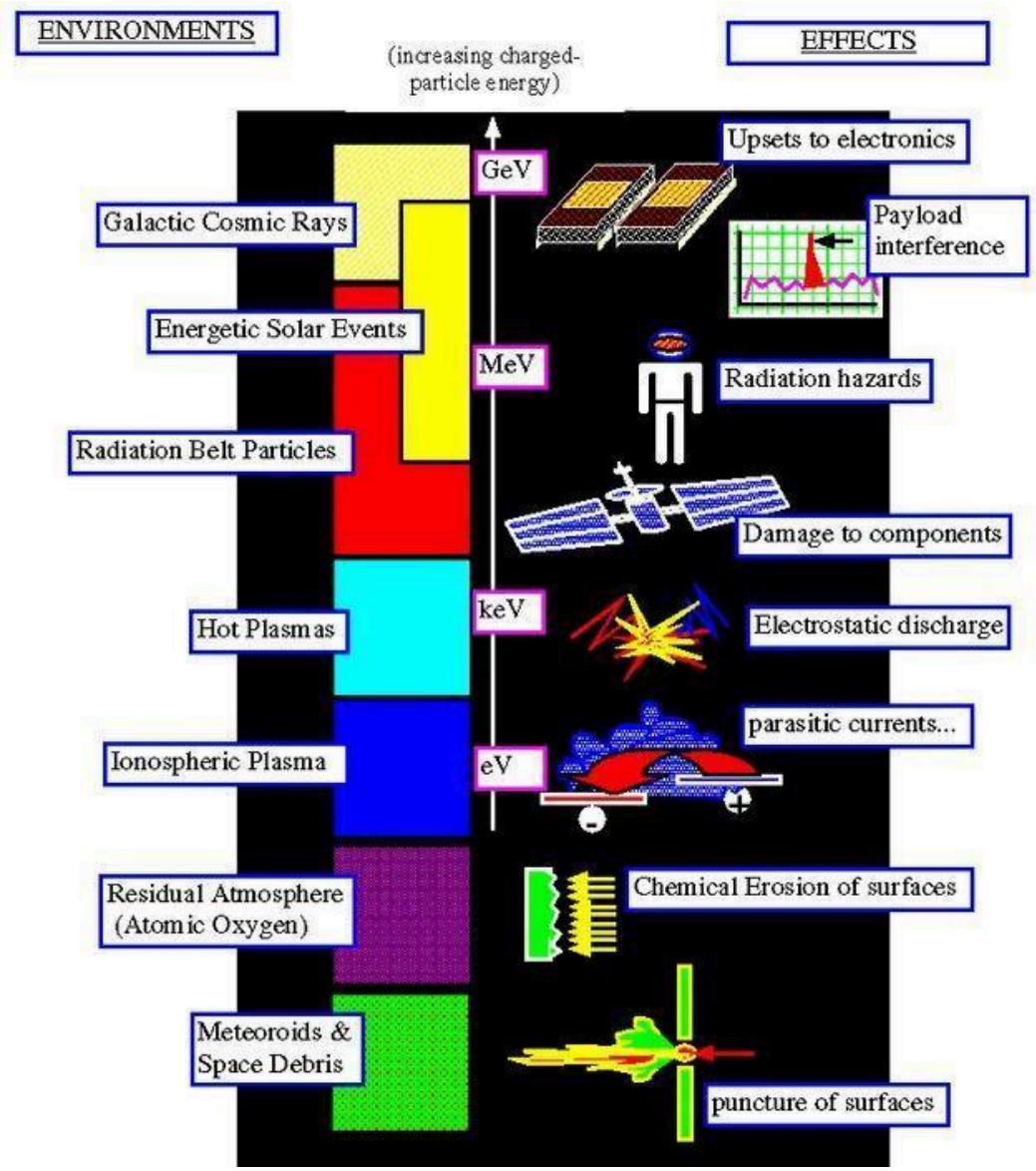

Figure 2.1.2 Space environment and typical effects on space systems in Earth orbit Source: (Boudjemai et al., 2015) [65]

Starting with Near-Earth space, besides it is about a region afflicted by high levels of space pollution, primarily in the form of space debris, Geospace, is another critical area near Earth, encompasses the upper atmosphere and magnetosphere,housing the Van Allen radiation belts. It's governed by the interactions between the Sun, the

solar wind, and our planet, making it intrinsically linked to heliophysics. Geospace's day-side magnetopause faces solar wind pressure, typically located at a distance of 10 Earth radii from Earth's center. Conversely, the solar wind stretches the magnetosphere on the night side, forming a magnetotail that can extend over 100–200 Earth radii[2]. During approximately four days each month, the Moon finds temporary respite from the solar wind as it passes through the magnetotail. This region, rich with electrically charged particles under the influence of Earth's magnetic field, can experience disturbances caused by solar wind, leading to geomagnetic storms with potential consequences for radiation belts, ionospheric activity, and technology on Earth and in space. Additionally, it gives rise to mesmerizing auroras in high-latitude regions.

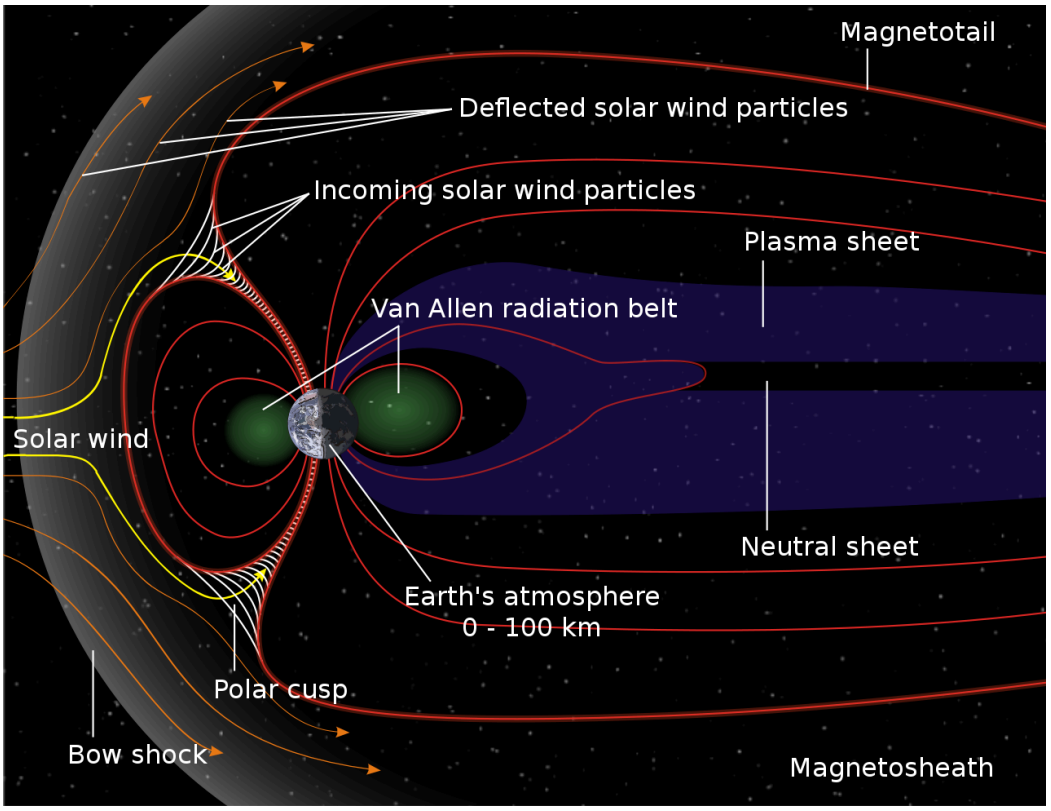

Figure 2.1.3 Magnetospheric Composition and dynamics plasma with charged particles, free elements (e.g hydrogen, helium, and oxygen, and electromagnetic fields). Source: NASA

[2] The plural "radii" simply refers to multiple radii, such as when discussing several circles or spheres with different sizes.

Although technically in outer space, the region within a few hundred kilometers above the Kármán line retains enough atmospheric density to affect satellites through significant drag and houses remnants of past space missions, potentially hazardous to spacecraft. Translunar space covers lunar transfer orbits, cislunar space encompasses lunar orbit and the Lagrange points, and geospace extends to high Earth orbits and beyond, encompassing cislunar space. The Hill sphere represents the region where Earth's gravitational influence prevails against solar perturbations and includes co-orbital space hosting Near-Earth Objects. [66], [67], [68], [69], [70]

2.2 Interplanetary space

On the other hand, interplanetary space is a vast expanse that extends billions of kilometers into space and is surrounded by a thin atmosphere - the heliosphere, which is shaped by the Sun's continuous passage of charged particles of solar wind. This solar wind has a particle density of between 5 and 10 protons per cubic centimeter and velocities between 350 and 400 kilometers per second and its region extends until it reaches the heliopause, where the galactic environment begins to take precedence over the Sun's magnetic field and particle flux. The location and intensity of the heliopause are subject to change based on the solar wind's activity levels, which impacts its ability to deflect low-energy galactic cosmic rays. This modulation effect is greatest during solar maximum. Despite its immensity, interplanetary space is predominantly a near-perfect vacuum, where particles have an average free path of about one astronomical unit, which corresponds to the distance between the Earth and its orbital plane. Interstellar space is not completely devoid of matter; it contains cosmic radiation, including ionized atomic nuclei and subatomic particles, as well as gas, plasma, dust, small meteors, and a variety of organic molecules identified by microwave spectroscopy. Notably, a faint swath known as the zodiacal light, created by an interplanetary dust cloud, is visible at night. In addition, interplanetary space contains the Sun's magnetic field and the magnetospheres generated by planets such as Jupiter, Saturn, Mercury, and Earth, each of which has its own magnetic field. The solar wind shapes these magnetospheres into a teardrop shape, extending a lengthy tail away from the planet. Particles from the solar wind and other sources can become confined within

these magnetic fields, forming regions similar to the Van Allen radiation belts. Planets without magnetic fields, such as Mars, gradually lose their atmospheres due to the solar wind's unimpeded impact. [71], 72]

2.3 Absence of atmosphere (vacuum)

Starting from the Earth's environment, as altitude increases, molecular density decreases in an almost exponential manner. The specific pattern of this variation is influenced by factors such as:latitude, time of day, and solar activity, e.g at an altitude of 36,000 km (the orbit of geostationary satellites), the pressure is below 10-13 Torr (measured in millimeters of mercury). In a vacuum environment, materials undergo processes like sublimation and outgassing, where the loss of mass is temperature-dependent. For instance, at 110°C, magnesium may experience a loss of 10^3 A/year, while at 170°C it's 10^3 cm/year, and at 240°C, it's 10^1 cm/year. Since temperatures exceeding 200°C are typical can be avoidable as long as excessively thin materials aren't utilized. The thermal loading that spacecraft experience affects various onboard systems, including radios and associated antennas, which are essential for spacecraft operations. However, the risk of gas condensation on cold surfaces is more concerning, leading to potential short circuits and degradation of thermo optical properties. This underscores the importance of avoiding highly volatile substances like zinc and cesium. Polymers also tend to decompose into volatile products. Conversely, a vacuum offers the advantage of shielding metals from corrosion. Yet, some materials, especially metals, can undergo diffusion upon high-pressure contact, causing cold welding and resulting in substantial friction on moving components such as bearings and mechanisms like solar generators and antennas. As a countermeasure, moving parts are enclosed within sealed pressurized enclosures, utilizing low evaporation and sublimation lubricants. Special materials, including ceramics and alloys like stellite, find application in bearing production. [73],[74],[75],[76],[77],[78]

2.4 Perfect vacuum

As we go deeper into Space (outer space), extremely low density and pressure characterize it by making it the closest physical approximation to a perfect vacuum. Even in interstellar space, where only a few hydrogen atoms per cubic meter exist, absolute perfection in a vacuum remains elusive. Due to gravitational attraction, objects like stars, planets, and moons retain their atmospheres, resulting in the density of atmospheric gas decreases as the distance from the object increases.

The Kármán line, where atmospheric pressure drops to approximately 32 millipascals (4.6106 psi) at 100 kilometers (62 miles), is a commonly used boundary for outer space. Beyond this point, the gas pressure becomes negligibly feeble in comparison to the pressure of solar radiation and the dynamic pressure of solar winds. Therefore, defining pressure becomes complicated. There are significant pressure, temperature, and composition gradients within the thermosphere that are influenced by space weather.

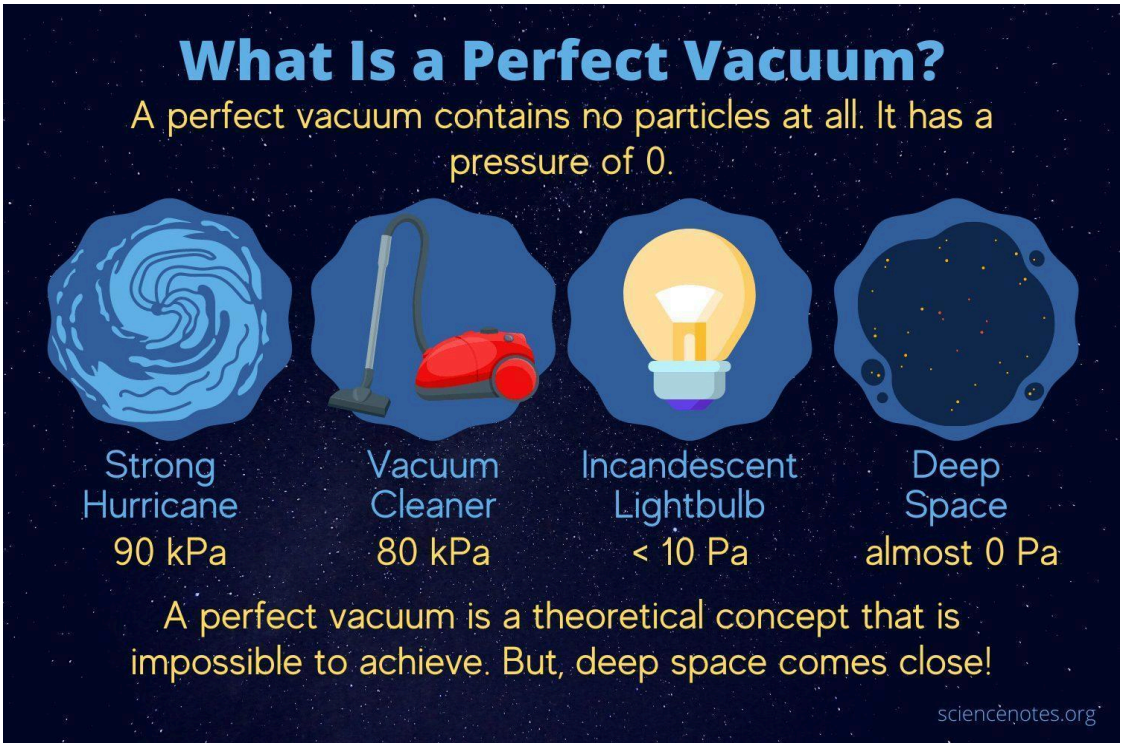

Figure 2.4.1 Perfect Vacuum

Astrophysicists prefer to characterize these environments using number density, which quantifies particles per cubic centimeter. Despite meeting the definition of outer space, the atmospheric density within a few hundred kilometers of the Kármán line remains high enough for satellites to experience significant drag. The entire observable universe is teeming with photons, also known as cosmic background radiation, and likely a similar number of neutrinos. The current temperature of this radiation is approximately 3 K (270.15 °C; 452.27 °F).

Table 6. The environment in Earth orbit and of interplanetary space

Space parameter	**Earth orbit (≤500km)**	**Interplanetary space**
Space vacuum		
Pressure (Pa)*)	10^{-6}-10^{-4}	10^{-14}
Residual gas (part/cm^{-3})	10^{5} H, 2×10^{6} He, 10^{5} N, 3×10^{7} O	1 H
Solar electromagnetic radiation		
Irradiance (W/m²)	1360	Different values[a)]
Spectral range (nm)	Continuum from 2×10^{-12} to 10^{2} m	Continuum from 2×10^{-12} to 10^{2} m
Cosmic ionizing radiation		
Dose (Gy/a) *)	0.1-3000[b)]	≤ 0.25 [c)]
Temperature (K)	100-400[a)]	> 4[a)]

2.5 Gravitational and magnetic fields

The dynamics of a space vehicle (satellites, space capsules, probes, etc) within a planet's gravitational field play a pivotal role, primarily shaping the trajectory of their center of mass. However, the uniformity of this gravitational field might be disrupted by the planet's non-spherical and uneven characteristics, akin to Earth's scenario, leading to deviations in the space vehicle's orbital path. Furthermore, if present, gravitational forces from celestial bodies like the sun and moon(s) can further impact the orbit. Regarding its effect on the space vehicle's orientation, the strength of a planet's gravitational field varies with altitude, implying that regions of the vehicle that are farther from the planet's center experience less gravitational attraction compared to closer regions. Due to the fact that the combined effect of this gravity gradient does not align with the satellite's center of mass, it generates a torque that influences the vehicle's attitude. The giant planets in the outer solar system, known for their rapid rotations, exhibit strong magnetic fields driven by dynamos, creating voids in the magnetized solar wind. Each planet contributes distinct characteristics to planetary magnetism. For instance, Jupiter possesses the largest magnetic moment, exceeding Earth's by over 20,000 times and tilting at about 10°, similar to Earth's. Saturn's dipole magnetic moment is around 600 times that of Earth, but its tilt is less than 1° relative to its rotation axis. Uranus and Neptune, the other gas giants, showcase unique magnetic fields due to their tilts and internal harmonic content. Uranus has anomalous tilts for its rotation and dipole axes. Although smaller, Neptune's magnetic moment is roughly 25 times greater than Earth's, with a tilt angle of 47°. The intricate harmonic nature of these magnetic fields challenges the accurate resolution of higher-degree coefficients from a single Voyager flyby.

Despite the absence of surface features reflecting deep interior motion, the gas giants' magnetic fields have been harnessed to deduce this information. Jupiter's magnetic field, particularly, has enabled precise determination of its rotation rate. Saturn's rotation period, approximately 10 hours and 33 minutes, remains somewhat uncertain. Uranus and Neptune, better suited for determining rotation periods through their magnetic fields, face limitations due to a short measurement baseline. Although smaller outer solar system bodies could possess magnetic fields, ongoing missions to Vesta, Ceres, and Pluto haven't included magnetic measurements.[79], [80] It is

given the example of the magnetic field of the Earth, denoted as H,which can be approximated as a magnetic dipole with a moment represented by M_E = 7.9 * 10^15 Wb m. This dipole's orientation forms an angle of 11.5 degrees with the Earth's axis of rotation and it generates an induction labeled as B, which can be divided into two distinct components, the normal and the radial.

Normal componant: $B_N = (M_E * \sin\theta) / r^3$ (Wb = m^2)

radial component: $B_R = (2M_E \cos\theta / r^3$ (Wb = m^2)

where "r" signifies the distance between the specific point and the Earth's center, while "u" represents the angle formed between the radius vector and the dipole's axis, utilizing the polar coordinates specific to the point in question within the dipole-associated reference system. For a geostationary satellite, the magnitude of the normal component varies from 1.03 x 10^7 to 1.05 x 10^7 Wb/m², and the radial component falls within the range of 0.42 x 10^7 Wb/m². The component perpendicular to the equatorial plane remains nearly constant at 1.03 x 10^7 Wb/m².

2.6 The impact of communication transmissions

The influence of communication transmissions is noteworthy as electromagnetic radiation emitted from antennas generates a discernible pressure, particularly if the transmission power is substantial. In the context of a radiating antenna, the resulting force, denoted as F, can be described by the equation: F - (dm/dt)c = - EIRP/c (N), where EIRP represents the effective isotropic radiated power in watts, and c stands for the speed of light in meters per second (3*10^8 m/s). The dm/dt has the meaning of the rate of change of momentum with respect to time. To illustrate, a satellite equipped with a 1 kW EIRP experiences a force F of approximately 0.3 * 10^5 N. When coupled with a lever arm of 1 meter, this imparts a torque of 3 * 10^6 Nm. This perturbation is particularly significant under conditions of high, concentrated transmitted power focused into a narrow beam. In such instances, it becomes imperative for the antenna axis to align with the center of mass or to incorporate two antennas with axes symmetrically positioned relative to the center. [81]

2.7 Thermal effects

Thermal effects on space vehicles arise due to differential exposure to solar radiation, causing the sunlit side to become warmer while the sides facing the cold expanse of space grow colder. Heat exchanges through conduction and radiation transpire, with convection inhibited by the vacuum environment. When e.g the satellite maintains a fixed orientation relative to the sun, it reaches a balance between absorbed solar power and radiated heat, resulting in an average temperature determined by the thermal equilibrium equation: Ps + P1 = Pr + PA, where PS signifies the power absorbed from direct solar flux (PS = αWSa, involving solar flux W, apparent surface Sa, and absorptivity α), P1 represents internal dissipated power, PR stands for radiated power, and PA accounts for stored or exchanged power during temperature shifts. [81], [82]

2.8 Cosmic particles

Cosmic particles, encompassing highly energetic electrons and protons, primarily originate from the sun and various space sources. Their density and energy are contingent upon factors such as altitude, latitude, solar activity, and time. The cosmic radiation predominantly comprises protons (constituting 90% of the particles) along with alpha particles, with energies within the gigaelectron-volt range. Despite their high energy, the flux of these particles is relatively low, approximately 2.5 particles per square centimeter per second.

The solar wind, in contrast, mainly consists of lower-energy protons and electrons. During periods of low solar activity, the mean proton density emanating from the sun is around 5 protons per cubic centimeter, traveling at velocities near 400 km/s. The corresponding flux at Earth's orbital level is approximately 2 x 10^8 protons per square centimeter, with an average energy spanning several kiloelectron-volts. Depending on solar activity, this flux can vary by up to a factor of 20. Intense solar activity leads to more frequent solar eruptions, releasing proton fluxes with energies ranging from several MeV to several hundreds of MeV. Occasional events, recurring every few years, can escalate proton energy levels to the gigaelectron-volt range.

When exposed to charged particles the metals and semiconductors then the atomic electron levels excited, while plastics become ionized and insulating minerals experience both effects.

Solar flares particularly impact the minority carriers in semiconductors, the light transmission of glasses, and specific polymers. Adequate shielding can safeguard the active components of electronic circuits in equipment from these impacts. Protective measures involve using equipment cases made from cast aluminum with wall thicknesses around a centimeter to house sensitive components. [83],[84],[85]

Section 3

This section explains the orbital elements and orbit satellite communication [86], [87],[88]

3.1 Orbital elements

Orbital elements, also known as Keplerian elements, are a set of parameters that can be used to characterize the orbit of one object around another (typically a planet around a star or a satellite around a planet). They are indispensable in celestial mechanics and satellite monitoring because they provide a concise description of an orbit. Together, these components provide a comprehensive description of an orbit, allowing one to anticipate the motion of the object orbiting the central body. However, these elements are subject to change over time as a result of gravitational perturbations from other bodies, atmospheric drag, and other factors. As such, they may require periodic updates to maintain their accuracy, particularly for objects in close proximity to large celestial bodies. The following constitutes the classical set of orbital elements for orbits around a central body:

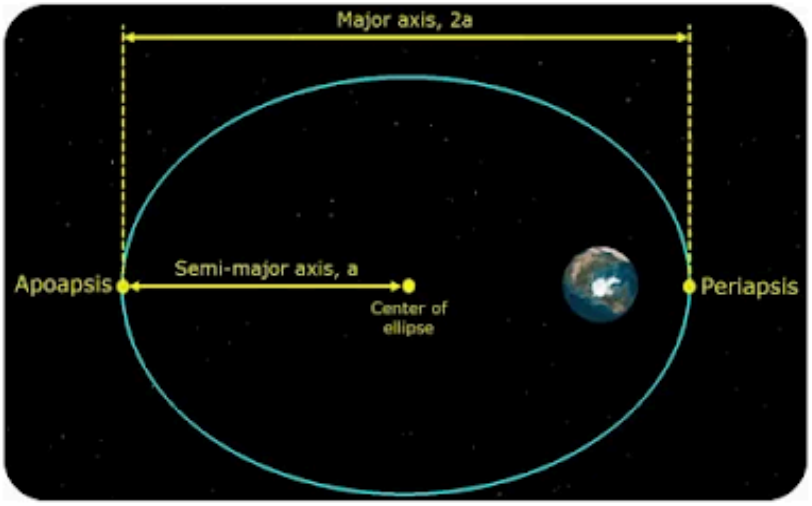

Figure 3.1.1. An ellipse with its periapsis, apoapsis, semi-major axis a, major axis 2a

1. Semi-major Axis (a): This describes the size of the ellipse. It's the distance from the center of the ellipse to either of its two foci. For circular orbits, this is equal to the circle's radius. $2a = (ra+rp) \rightarrow a = (ra+ rp) / 2$

- Periapsis - The point in an orbit that is closest to the central body.
- Apoapsis - The point in an orbit that is farthest from central body.
- rp is distance from center of the central body to periapsis
- ra is distance from center of the central body to apoapsis

2. Eccentricity (e): This is a measure of how much the orbit deviates from being circular. An eccentricity of 0 indicates a perfect circle, while an eccentricity close to 1 indicates a highly elongated ellipse.

$$e = \sqrt{1 - \frac{b^2}{a^2}}$$

The more eccentric the orbit (as e↑), the less circular the orbit.
An orbit is a trajectory with an e value less than 1 because an orbit is a closed path around a central body.

A trajectory with an eccentricity greater than or equal to 1 is an open trajectory, and the “orbiting” body will constantly move away from the central body.

For orbits or closed trajectories: $0 \leq e < 1$

- Circle: $e = 0$
- Ellipse: $0 < e < 1$

For open trajectories: e ≥ 1

- Parabola: e = 1
- Hyperbola: e > 1

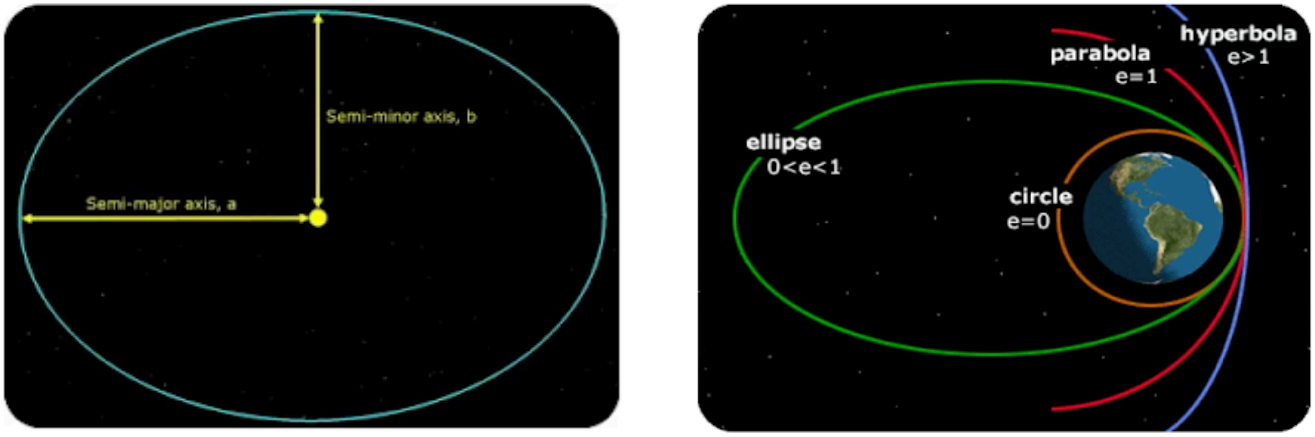

Figure 3.1.2. semi-major axis a, semi-minor axis b, and the right figure is about all the type of orbits according to eccentricity.

3. Inclination: This is the angle between the plane of the orbit and a reference plane, usually the equator of the central body. An inclination of 0° means the object orbits directly above the equator, while an inclination of 90° means it orbits from pole to pole.

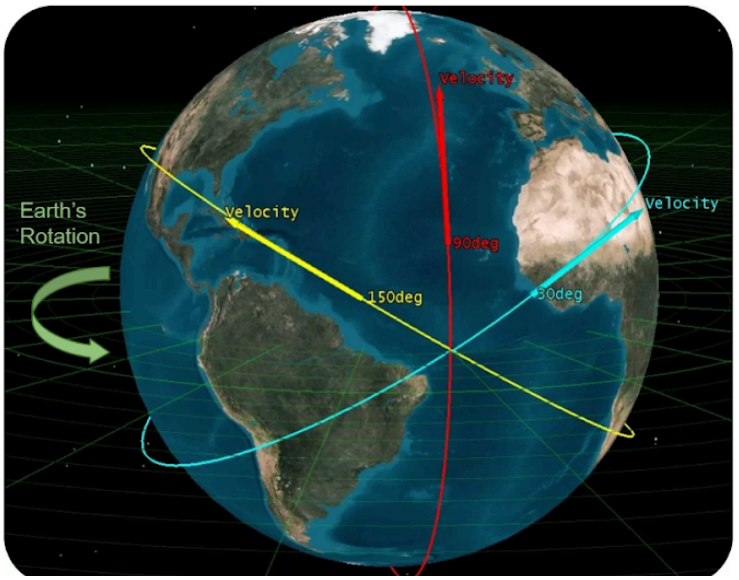

Figure 3.1.3. Inclinations (0° and 90°)

4. Longitude of the Ascending Node (Ω): This is the angle from a reference direction to the direction of the ascending node, where the orbiting object crosses the reference plane from south to north.

Figure 3.1.4. Orbiting from south to north

5. Argument of Periapsis (ω): This is the angle between the ascending node and the orbit's closest approach to the central body (called the periapsis or perigee for Earth orbiters).

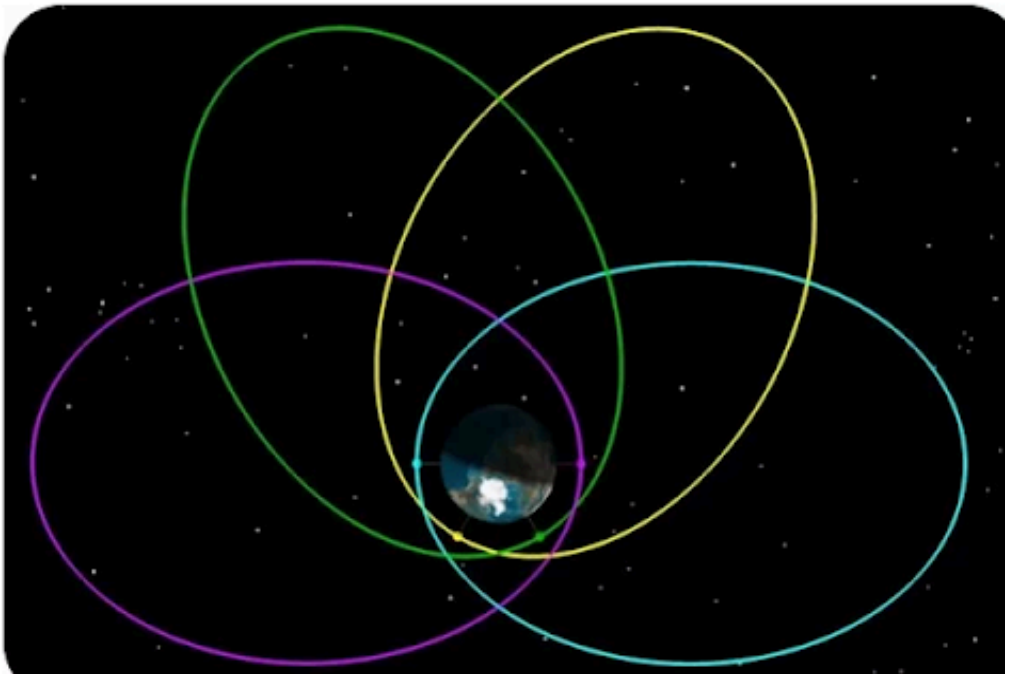

Figure 3.1.5. Periapsis (ω)

6. True Anomaly (v) or Mean Anomaly (M): This defines the object's current position in its orbit. The true anomaly is the angle between the direction of periapsis and the current position, measured at the central body. The mean anomaly, on the other hand, provides an average measure of the object's position, which is particularly useful for predicting its position at future times.

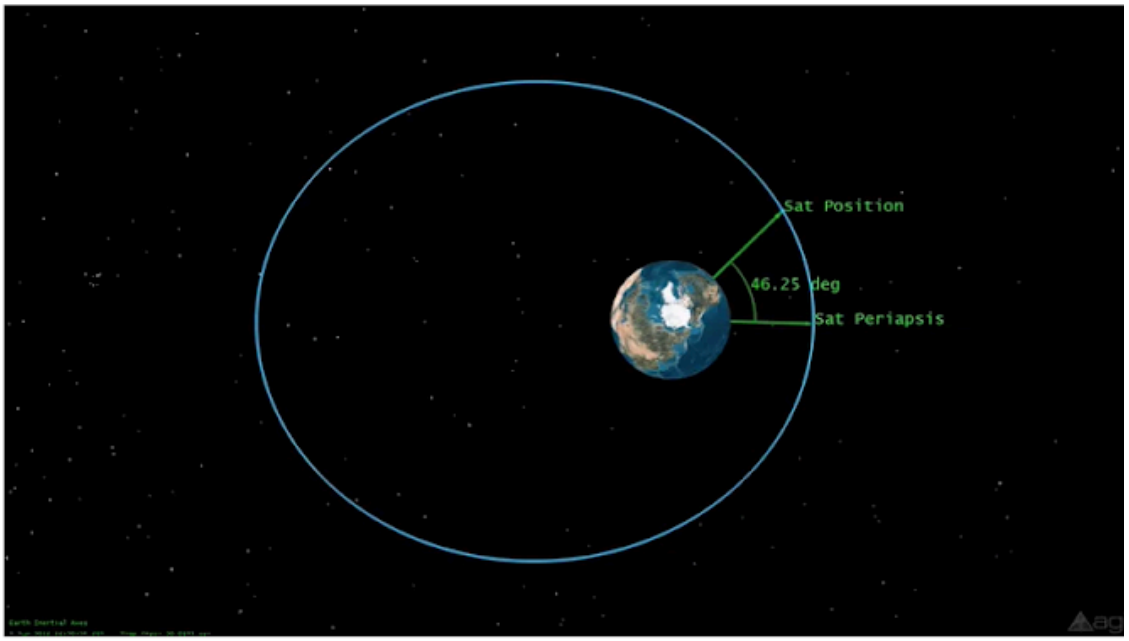

Figure 3.1.6. True Anomaly (v) or Mean Anomaly (M)

An example: the centripetal acceleration of a car around a circular track is:

$$a = v^2/r$$

And the force of gravity is:

1. $F = GMm/r^2 = ma$
2. $F/m=a = GM/r^2$
3. $GM/r^2 = v^2/r$
4. $v = \sqrt{(GM/r)}$

For a satellite at a 9,000 km altitude then will be:

$G = 6.674 \times 10\text{-}11\ m^3\ kg\text{-}1\ s^{-2}$

Mearth = 5.972 x 1024 kg

rsat = radius_earth + raltitude= 6,378.14+9,000 km=15,378.14 km

$v = \sqrt{(GM/r)} = 5.09$ km/s

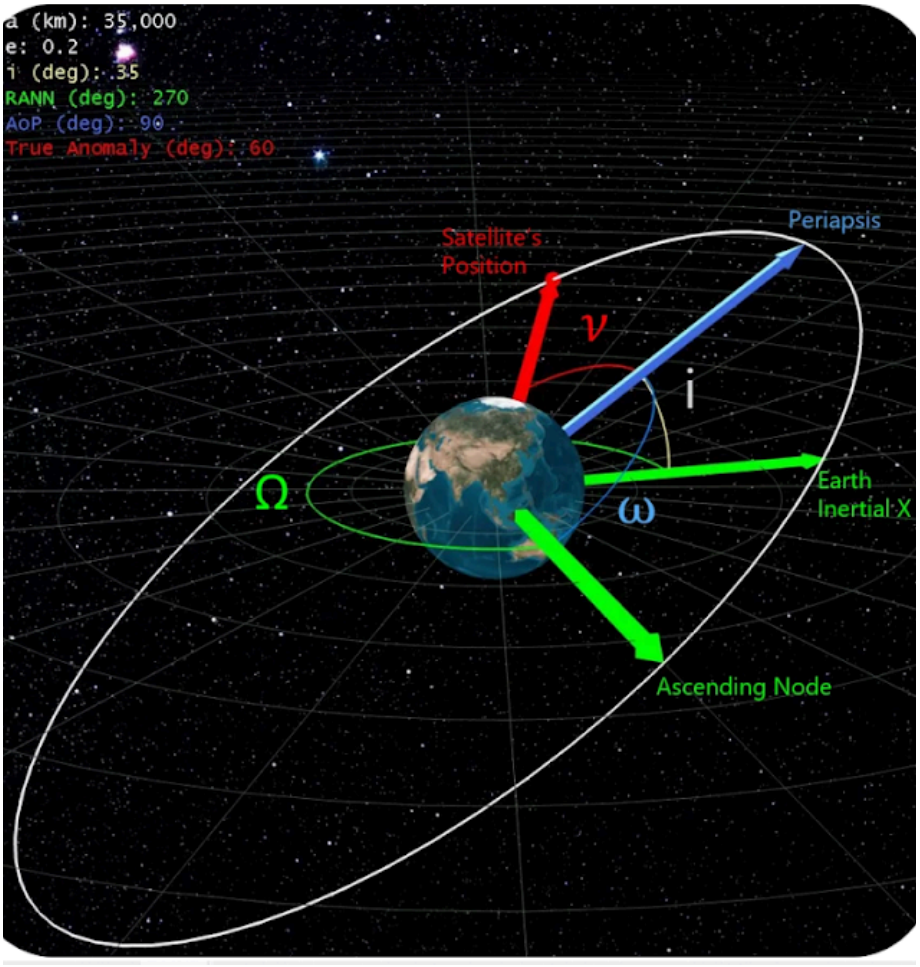

Figure 3.1.7. simulation

Orbits at lower altitudes have higher velocities.

Numerous distinct orbital configurations are delineated by a range of orbital elements. Prior to delving into particular orbital patterns, we shall elucidate Kepler's

three fundamental principles governing the motion of celestial bodies. More specific, by using a software like ANSYS, you can precisely determine the momentary path of a celestial body, such as a planet or satellite, by using these six specific parameters. In Cartesian terms, these include three positional parameters (X, Y, Z) and three for velocity (Vx, Vy, Vz). A more practical set of parameters exists that leverages Kepler's principles to forecast both the position and velocity of the orbiting entity. The Keplerian Orbital Elements as referred above also, are : two factors (semi-major axis 'a' and eccentricity 'e') , the orbit's magnitude and form; three (inclination 'i', right ascension of the ascending node 'Ω', and argument of perigee 'ω') indication of the orbit's spatial orientation; and the true anomaly. These parameters we can say that pinpoint the satellite's specific location within its orbit.

3.2 Kepler's Laws

Kepler's First Law

According to Kepler's First Law, the trajectory of a celestial body, such as a planet, is characterized by an elliptical path with the Sun being at one of the focal points. Its initial principle asserts that the trajectory traced by a satellite orbiting its central body (such as the Earth) takes the shape of an ellipse. This ellipse possesses two focal points (foci) designated as F1 and F2, visually depicted in the figure below.

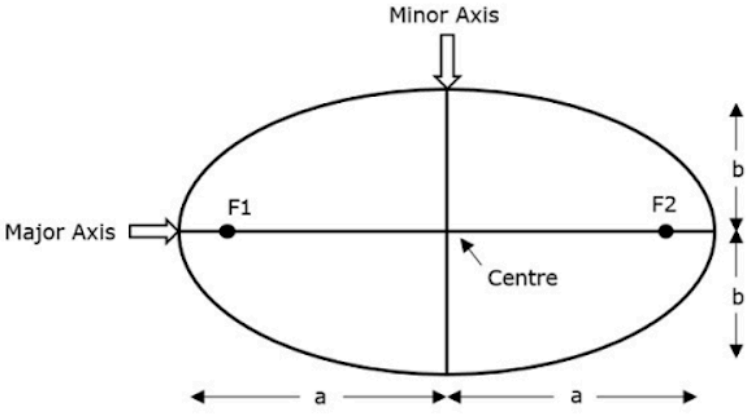

Figure 3.2.1 Kepler's First Law & trajectory of a celestial body

The sum of the distances from each foci to a point on the ellipse is constant. Here is a figure with the corresponding bodies (Sun, Earth, satellite).

An example of a spacecraft trajectory is the seven Venus flybys over nearly seven years to gradually shrink its elliptical orbit around the Sun, for a total of 24 orbits.

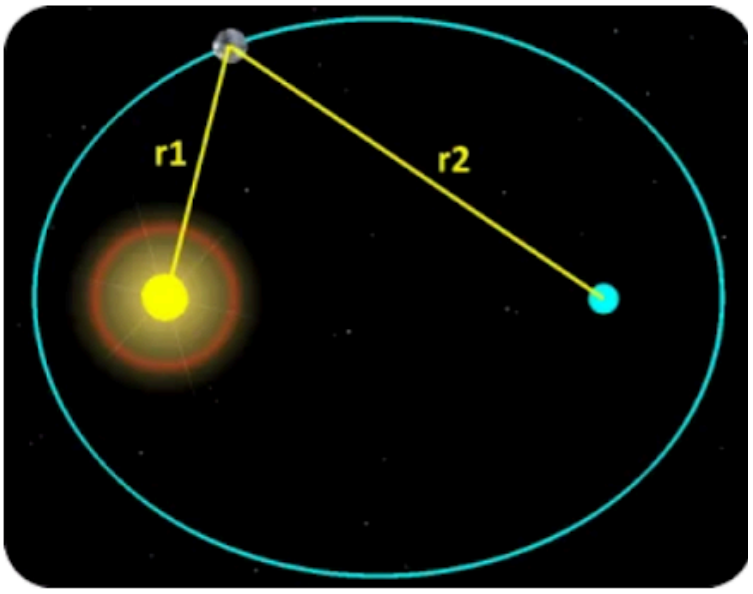

Figure 3.2.2 Sun, Earth, satellite

Kepler's Second Law

Kepler's Second Law says that as a planet or satellite moves around the Sun or its planet, it covers the same amount of area in the same amount of time. This means that when a satellite is nearer to Earth, it moves faster, and when it's farther away, it moves slower.

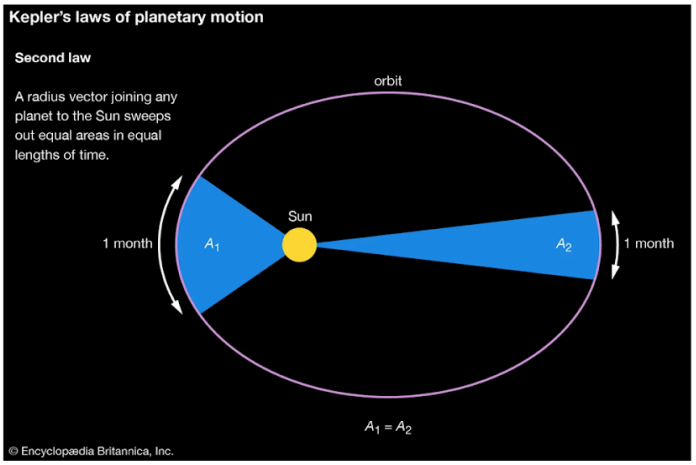

Figure 3.2.3 A1 = A2

Kepler’s Third Law

Kepler's Third Law states that the orbital periods of the planets are directly proportional to the cubes of the semi-major axes of their orbits. According to Kepler's Third Law, there is a direct relationship between the period of a planet's orbit around the Sun and the radius of its orbit, indicating that as the radius of the orbit increases, the period of the planet's orbit also increases at a rapid rate. Therefore, it can be observed that Mercury, being the planet closest to the Sun, completes a full orbit in a mere 88 days. The Earth has an orbital period of 365 days, whereas Saturn has a far longer orbital period of 10,759 days. Despite lacking knowledge of gravity at the time of formulating his three laws, Kepler's contributions proved important in Isaac Newton's subsequent development of the idea of universal gravitation. This theory effectively elucidates the enigmatic force underlying Kepler's Third Law. The contributions of Kepler and his theories have played a pivotal role in enhancing our comprehension of the dynamics inside our solar system. Moreover, they have served as a foundation for subsequent theories that provide more precise approximations of the orbits of our planets.

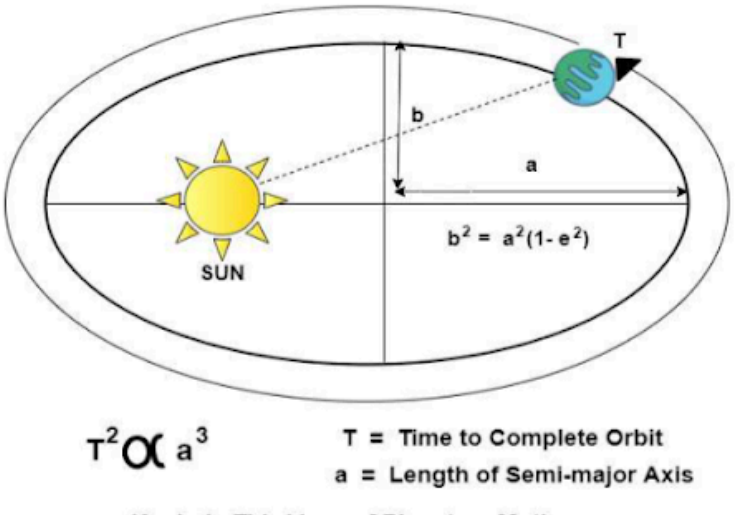

Figure 3.2.4 The Timeline Of Gravity.

Anjum, Arshia & Mishra, Sriman Sirsa Saran. (2020).

Coordinate Frames & Epoch

In order to accurately describe the characteristics of an orbit, it is necessary to establish a coordinate system and provide an epoch, or a particular point in time. This ensures that all orbital elements are defined within a consistent framework.

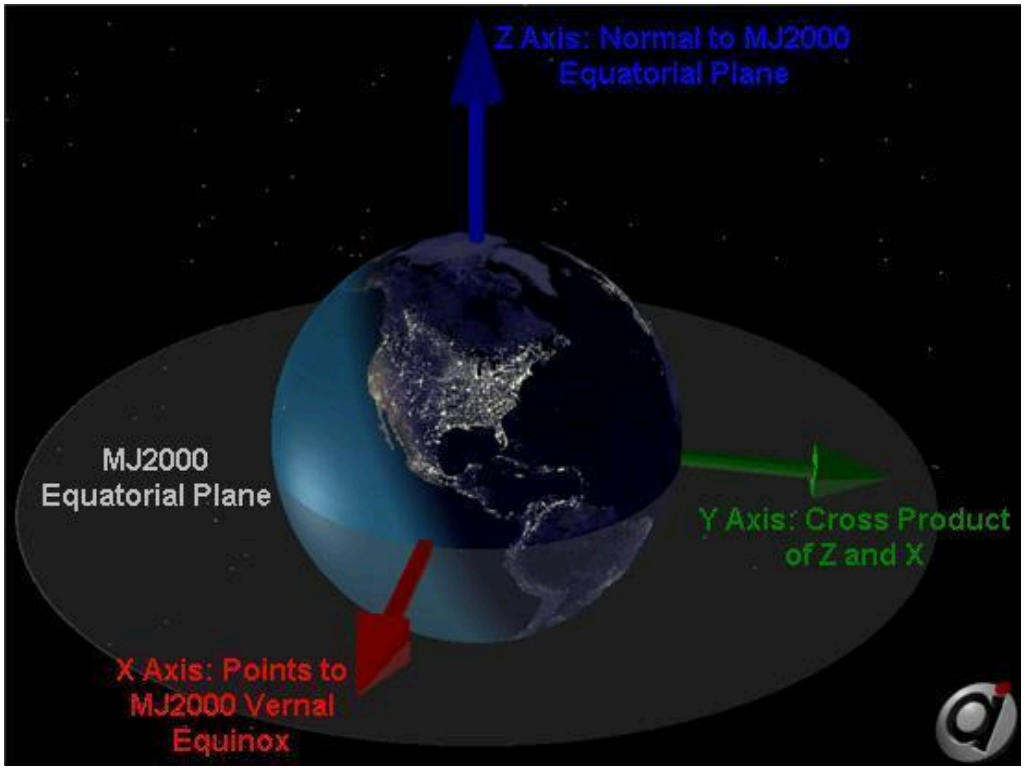

Figure 3.2.5. The Earth Centered Inertial (ECI) reference frame

Coordinate systems are mathematical frameworks used to represent and analyze the position and the velocity vectors.

3.3 Orbits - Hohmann transfer

The Hohmann transfer trajectory is a widely used method for moving a satellite from one circular orbit to another, as long as both orbits are in the same plane and have a common center. This transfer involves two distinct short bursts of propulsion, each causing a change in the satellite's speed. This specific type of movement is known for being highly efficient in terms of fuel consumption. The initial burst of propulsion is employed to adjust the satellite's original orbital path. The satellite then follows a specific elliptical path, referred to as a Hohmann ellipse, until it reaches the point farthest from the center of its orbit, known as apoapsis. At apoapsis, which aligns with the radius of the newly targeted orbit, a second burst of propulsion is used to fine-tune the satellite's trajectory and place it in a circular orbit with the adjusted radius.

Now, we'll examine several equations that can be used to find various unknown variables. The formula for calculating the semi-major axis of the Hohmann ellipse is given as: at = $(r_1 + r_2) / 2$, where r_1 stands for the radius of the initial orbit, and r_2 represents the radius of the subsequent orbit. To determine the total change in velocity, denoted as vTot, it's necessary to add up the separate velocity changes, v_1 and v_2.

$$\Delta v\text{Tot} = \Delta v_1 + \Delta v_2$$

$v\text{circ}_1$ and $v\text{circ}_2$ can be found by using the following equation for the velocity of a circular orbit:

$$\Delta v_1 = v_1 - v\text{circ}_1$$
$$\Delta v_2 = v\text{circ}_2 - v_2$$

$$v\text{circ}_{1,2} = \sqrt{(\mu / r_{1,2})}$$

v_1 and v_2 can be found by rearranging the energy equation for an orbit:

$$\varepsilon = (v2)/2 - \mu/r \rightarrow$$

$$v1,2 = \sqrt{(2(\varepsilon t + \mu/r1,2))}$$

where the energy of the Hohmann transfer ellipse is given by εt = -μ/2at

Hohmann transfers are characterized by their efficiency in terms of energy and fuel consumption for orbital transfers, but at the expense of a longer duration. In the context of time-constrained missions, it is possible to minimize transfer time by increasing fuel consumption. Utilizing a transfer ellipse that goes beyond the outer orbit, as opposed to employing an elliptical transfer orbit that merely reaches the outer orbit, will yield expedited transfer durations. This provides us with the overarching coplanar transfer.

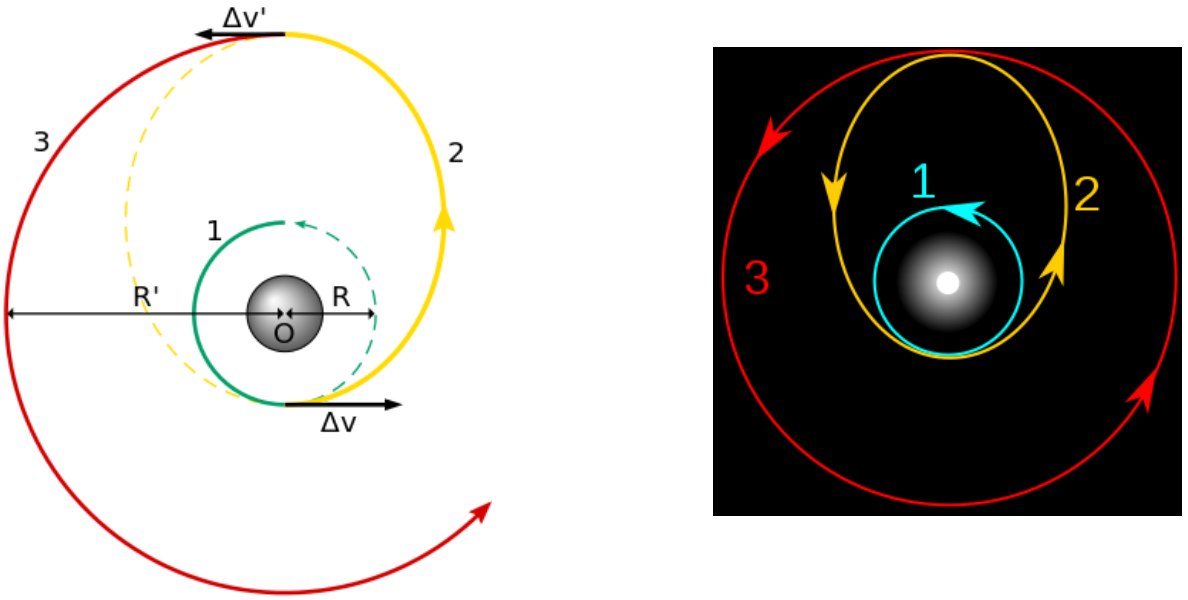

Figure 3.3.1 From an orbit to higher orbit

3.4 Oberth maneuver

The Oberth maneuver, coined by Hermann Oberth in 1927, is a significant concept in astronautics that involves the utilization of a spacecraft's engines to achieve additional acceleration while descending into a gravitational well. Hermann Oberth is renowned for his contributions to contemporary rocketry, making this move of particular importance in the field. The efficacy of this approach in augmenting the spacecraft's kinetic energy surpasses that of exerting an equivalent force in the absence of a substantial celestial body. The efficiency observed in spacecraft propulsion can be attributed to the Oberth effect, a phenomenon that elucidates the enhanced effectiveness of a spacecraft's engines while it operates at high velocities, particularly during the periapsis phase of its orbit. This is due to the maximization of the spacecraft's kinetic energy at this orbital position. In certain circumstances, it may prove advantageous to allocate fuel resources for the purpose of maneuvering the spaceship into a gravitational well, thereby optimizing the utilization of the Oberth effect. The efficacy of the Oberth maneuver is heavily contingent upon the propulsive capabilities exhibited by the engines of the spaceship. The utilization of high-thrust engines, such as liquid-propellant rockets, is more appropriate for this move owing to their capacity to produce a substantial impulse within a brief timeframe. This aspect has significant importance due to the spacecraft's proximity to the periapsis of its orbit being of a transient nature. On the other hand, low-thrust engines such as ion drives, which provide gradual acceleration of the spacecraft, are deemed less suitable for this particular maneuver.

In a depicted journey from Earth to Mars, a spacecraft uses the Oberth effect to efficiently increase its kinetic energy and enter a Hohmann transfer orbit with minimal fuel expenditure. Initially, it burns fuel close to Earth (at low periapsis) where it already has significant kinetic energy due to its orbit, requiring less additional energy to escape Earth’s gravity and enter a sun-centered orbit. As the spacecraft approaches Mars, it performs a deceleration burn at low altitude, again utilizing the Oberth effect, to allow Mars’ gravity to capture it into orbit. Proper alignment of the planets is crucial for the Hohmann transfer to be successful, leading to specific launch windows. This example illustrates the energy efficiency of utilizing gravity assists and strategic engine burns in space travel.

3.5 Orbit types

A general overview of the specified orbit types and their typical characteristics:

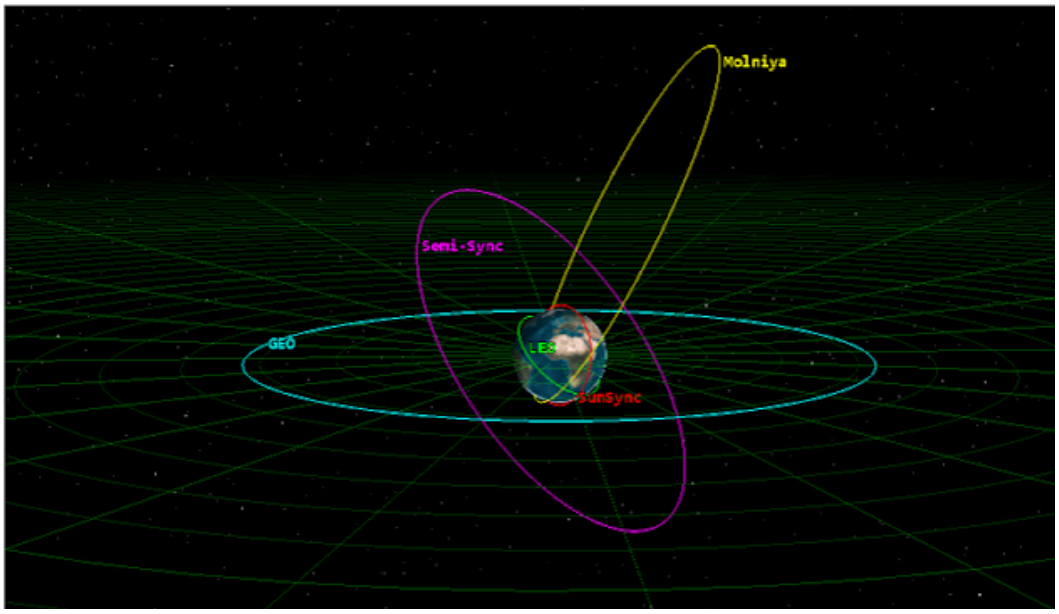

Figure 3.5.1 5 Types of Orbit

1. **Geostationary Orbit (GEO)**:

- Semi-major axis: Approximately 42,164 km from Earth's center (about 35,786 km above the equator).
- Period: 24 hours.
- Inclination: 0° (located directly above the equator).
- Eccentricity: Typically very close to 0 (circular orbit).
- Usage: Commonly used for telecommunication satellites because the satellite appears stationary relative to a fixed point on the Earth's surface.

2. **Semi-synchronous Orbit**:

- Semi-major axis: Typically around 26,560 km from Earth's center.
- Period: 12 hours.
- Inclination: Varies, but for some applications like GPS, it's approximately 55°.
- Eccentricity:Often near 0, but can vary.
- Usage: Often used for navigation satellites like the GPS constellation.

3. Sun-synchronous Orbit (SSO):

- Semi-major axis: Varies, but typically associated with Low Earth Orbits (around 700 km to 800 km above Earth's surface).
- Period: Varies based on altitude, but is designed to keep the satellite in constant sunlight.
- Inclination: Approximately 98°.
- Eccentricity: Near 0 (usually circular).
- Usage: Commonly used for Earth observation satellites as they can revisit any point on Earth at the same local solar time.

4. Low Earth Orbit (LEO):

- Semi-major axis: Ranges from just above Earth's surface up to an altitude of about 2,000 km.
- Period: Roughly 90 to 120 minutes, depending on the exact altitude.
- Inclination: Varies widely.
- Eccentricity: Can range, but many are near-circular.
- Usage: Used for a variety of purposes, including telecommunication (e.g., Starlink by SpaceX and OneWeb), Earth observation, and crewed space missions.

5. Molniya Orbit:

- Semi-major axis: Roughly 26,554 km from Earth's center.
- Period: 12 hours.
- Inclination: 63.4°.
- Eccentricity: High (about 0.7), which gives it a characteristic elongated appearance.
- Usage: Primarily used by Russian communication satellites to provide coverage to polar regions.

Of these orbits, Geostationary, Low Earth Orbit, and Molniya orbits are notably used for telecommunication. However, advancements in technology and the increasing demand for global internet coverage are leading to the proliferation of telecommunication satellites in LEO (like Starlink and OneWeb projects).

3.6 Orbits in satellite communications

Orbits play a pivotal role in the design and functionality of satellite communications and space vehicle navigations. Their selection and utilization are paramount in determining the efficacy of satellite-based communications, be it on an intercontinental scale on Earth or a broader interplanetary context within the solar system. For instance, geostationary orbits, due to their synchronous rotation with the Earth, are ideal for maintaining a fixed communication point, ensuring consistent signal reception in specific regions. On the other hand, low Earth orbits (LEOs) offer advantages in reduced latency and are the foundation of upcoming mega-constellations promising global broadband coverage. Venturing beyond Earth's immediate vicinity, interplanetary missions rely on Hohmann transfer orbits to move efficiently between planets within our solar system. The critical role of orbits transcends mere satellite positioning: it integrates complex aspects of orbital mechanics, satellite design, and mission objectives. For a comprehensive understanding of the intricate interplay between orbits and satellite communications, several foundational texts are recommended, including M. Richharia's "Satellite Communication Systems: Design Principles" and Bruce R. Elbert's "Introduction to Satellite Communication." Furthermore, journals such as the "International Journal of Satellite Communications and Networking" and "IEEE Transactions on Aerospace and Electronic Systems" frequently publish articles detailing the nuances of this relationship. If we want to understand how satellites will behave in space we need to utilize these laws, combined with Newton's law of gravitation, to design, launch, and maintain satellite systems and space vehicles.

Section 4

Fundamentals of Deep Space Communication

4.1 Basics of Radio Frequency (RF) Communication

Radio frequency (RF) communication is the primary method used also for deep space communication, leveraging electromagnetic waves to transmit information across vast distances. RF waves propagate through space at the speed of light, allowing communication between spacecraft and ground stations on Earth. The RF communication process involves converting data into a modulated signal that can be transmitted via an antenna on the spacecraft. This signal is then received by a ground station on Earth, where it is demodulated and processed to retrieve the original data. RF communication systems typically operate in the microwave region of the electromagnetic spectrum, which ranges from 300 MHz to 300 GHz. This frequency range is chosen because of its ability to penetrate Earth's atmosphere with minimal attenuation and interference. High-gain antennas, such as parabolic dishes, are used to focus and direct the transmitted signal, increasing its effective power and reception capabilities [94].

4.2 Challenges of Communicating Over Long Distances in Space

Communicating over long distances in space presents several unique challenges [95],[96],[97] including:

Signal attenuation: As a radio signal propagates through space, its power decreases with the square of the distance from the transmitter, leading to signal attenuation. To overcome this challenge, high-gain antennas and powerful transmitters are employed

to boost the signal strength, while highly sensitive receivers are used to detect weak signals at the ground station.

Signal attenuation refers to the decrease in signal power as it propagates through space. Attenuation is a critical challenge in deep space communication, as it can result in weak signals that are difficult to detect and process. High-gain antennas, powerful transmitters, and sensitive receivers are used to mitigate the effects of signal attenuation.

Doppler effect: The relative motion between the spacecraft and the ground station causes a frequency shift in the received signal, known as the Doppler effect. This shift must be taken into account during signal processing to ensure accurate data retrieval.

Latency: Due to the vast distances involved in deep space communication, there is a significant time delay, or latency, between the transmission and reception of signals. This latency can range from several minutes to hours, depending on the distance, and poses challenges for real-time communication and control. For instance, when Mars is at its closest, around 35 million miles away, there's roughly a four-minute delay. At its farthest, about 250 million miles away, this delay stretches to approximately 24 minutes. Consequently, astronauts would experience a wait time of between four and 24 minutes for their messages to arrive at mission control, and a similar duration for a reply. As NASA gears up for manned missions to Mars, its communication experts are devising methods to keep astronauts linked to Earth, all the while acknowledging that latency will be an inherent aspect of their exchanges.

Noise: Deep space communication systems encounter various sources of noise such as thermal noise from electronic components, cosmic noise from celestial bodies, and man-made interference, all of which can corrupt the transmitted signal and degrade communication quality. To combat this challenge, advanced error-correction techniques and signal processing algorithms are utilized to minimize the adverse effects of these unwanted signals or disturbances and ensure the accurate retrieval of the original data.

Bandwidth: Bandwidth refers to the range of frequencies used to transmit information in a communication system. It is a measure of the system's capacity to transmit data, with higher bandwidths enabling faster data transmission rates. In deep space

communication, bandwidth is a crucial factor that influences the system's ability to transmit large volumes of data, such as high-resolution images and scientific measurements, over long distances. Achieving sufficient bandwidth while maintaining signal quality is a key challenge in designing deep space communication systems. NASA employs various bands of electromagnetic frequencies to encode data, with each bandwidth having distinct capabilities. The capacity to transmit more data in a shorter time frame is inherent to higher bandwidths. While radio waves remain NASA's predominant communication medium, the agency is venturing into optical communications using infrared lasers. This new transmission method promises unparalleled data rates. The Laser Communications Relay Demonstration (LCRD) by NASA exemplifies the potential of optical communications. This mission is set to test the proficiency of optical links by relaying data between ground stations in California and Hawaii. Additionally, an optical terminal will be integrated into the space station to facilitate data relay to Earth through LCRD.

4.3 Satellite Systems

The satellite system consists of three main components:

1. the space segment,
2. the control segment,
3. the ground segment.

The **space segment** comprises a constellation of active and spare satellites.
A satellite is comprised of two main components, the payload and the platform. The payload encompasses both the receiving and transmitting antennas, as well as the accompanying electronic equipment that facilitates the transmission of carriers. Experiments have also been conducted pertaining to IP routers deployed on satellite platforms.

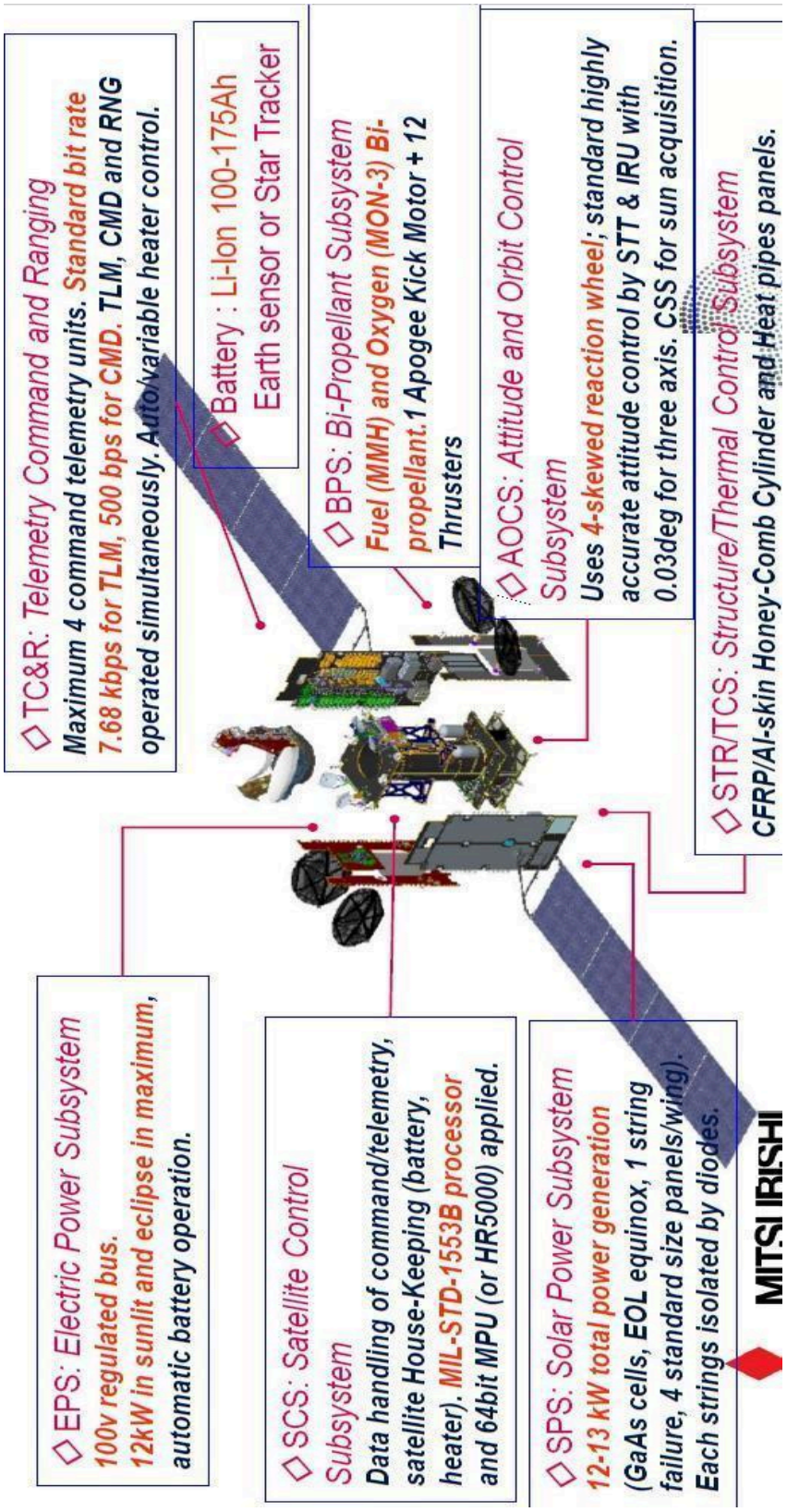

Figure 4.3.1: Satellite Structure (e.g Mitsubishi Electric DS-2000)

A transparent payload, also known as a bent pipe type, is used to amplify the power of the carrier signal and the frequency is downconverted. The power amplification necessary to increase the power level of the received carrier from a small magnitude of picowatts to the power level of the carrier supplied to the transmit antenna, which ranges from a few watts to a few tens of watts, typically falls within the range of 100-130 dB. In order to enhance the level of isolation between the input of the receiver and the output of the transmitter, it is necessary to implement frequency conversion. The division of the satellite payload bandwidth into multiple sub-bands and the amplification of carriers within each sub-band by dedicated power amplifiers is necessitated by limitations in technology power. The term used to refer to the amplifying chain associated with each sub-band is a satellite channel, also known as a transponder. The process of dividing the bandwidth is accomplished through the utilization of a collection of filters known as the input multiplexer (IMUX). The amplified carriers undergo recombination within the output multiplexer (OMUX).

The transparent payload is associated with a single-beam satellite system, wherein each transmit and receive antenna is responsible for generating a singular beam. Multiple-beam antennas could also be taken into consideration [99]. The payload would subsequently possess an equivalent number of inputs and outputs as the upbeams and downbeams. The process of directing carriers from an upbeam to a specific downbeam involves several methods, including routing through distinct satellite channels, transponder hopping based on the chosen uplink frequency, or utilizing onboard switching with transparent on-board processing. Subsequently, a multiple-beam regenerative payload is depicted, wherein the carriers of the uplink are subjected to demodulation. The presence of baseband signals enables the processing and routing of information from upbeam to downbeam through on-board switching at the baseband level. The process of frequency conversion is accomplished through the modulation of carriers generated on board at the downlink frequency. Subsequently, the carriers that have been modulated are amplified and transmitted to the intended recipient via the downbeam.

Every individual beam of a satellite antenna establishes a coverage area, commonly referred to as a footprint, on the surface of the Earth. The multi-beam antenna coverage area is determined by the aggregate beam coverage areas. A satellite may

possess multiple-beam antennas, each of which contributes to the overall coverage area of the satellite.

Bandwidth reuse, [104][105] which relies on the utilization of multibeam antennas, plays a crucial role in enabling high capacity for high-throughput satellites (HTS) and subsequently reducing the cost per bit for information transmission. The available bandwidth can be partitioned into three or four sub-bands, also known as three- or four-colour techniques, depending on the arrangement of the spot beams. This allows for the allocation of different sub-bands (colours) to different spot beams, ensuring that adjacent spot beams utilize distinct sub-bands (colours) to prevent interference between them.

The **control segment** encompasses the terrestrial facilities responsible for the control and surveillance of satellites, commonly referred to as tracking, telemetry, and command (TTC) stations. These facilities also manage the traffic and resources onboard communication network satellites.
The control segment of a satellite system, especially in the context of satellite constellations like the Global Positioning System (GPS), is responsible for the operation, management, and maintenance of the satellite fleet. This includes ensuring the health and functionality of each satellite, making sure they are in their designated orbits, and updating their software and data as required. The aspects of the control segment are:

1. Tracking: This involves continuously monitoring the position and velocity of each satellite in the constellation. This is crucial for satellite systems like GPS, where the precise location of each satellite must be known at all times to provide accurate location data to users.

2. Telemetry: Telemetry refers to the collection and transmission of data from the satellite back to the control centers on Earth. This data includes information about the satellite's health, its operational status, and other metrics that help the operators understand how the satellite is performing. If anomalies are detected, corrective measures can be taken.

3. Command: From the control centers, operators can send commands to the satellites. These commands might instruct a satellite to change its orientation, update its software, switch to backup systems in case of a malfunction, or even change its orbit.

The control segment infrastructure typically consists of:

1. Ground Antennas: These are large dish antennas that establish the uplink and downlink with satellites. They send commands to the satellites and receive telemetry data from them.

2. Control Centers: These are the facilities where operators monitor and control the satellite constellation. They process the telemetry data, decide on necessary actions, and send out commands to satellites.

3. Data Centers: These facilities store the vast amounts of data coming in from the satellites and also hold the software and databases that support the satellite system's operation.

4. Communication Links: These are essential for interconnecting all the parts of the control segment and ensuring that data can be sent and received in real-time.

For communication network satellites, there's an added complexity of managing the traffic and resources onboard. This means ensuring that bandwidth is allocated correctly, avoiding interference between channels, and efficiently handling the data traffic to and from Earth. In conclusion, the control segment plays a pivotal role in the smooth and efficient operation of satellite systems, ensuring they serve their intended purpose, whether it's navigation, communication, or any other application.

The **ground segment** encompasses all terrestrial stations, which are typically linked to the end user's terminal either through a terrestrial network or, in the case of small station VSATs, through a direct connection.

Stations exhibit differentiation based on their dimensions, which are contingent upon the magnitude of traffic to be transmitted via the satellite connection and the nature of the traffic, encompassing telephone, television, data, or multimedia Internet services. Historically, the most sizable antennas utilized in the Intelsat network were characterized by a diameter of 30 meters, as exemplified by Standard A. The smallest antennas, used for receiving signals from Direct Broadcast Satellites (DBSs), measure approximately 0.6 meters. Alternatively, there are even smaller antennas, measuring around 0.1 meters, which are utilized for mobile stations, portable stations, or handsets. Certain stations have the capability to both transmit and receive signals. There are additional stations that fall under the category of RCVO, such as receiving stations utilized for broadcasting satellite systems or distribution systems responsible for transmitting television or data signals. The diagram illustrates the standard configuration of an earth station, encompassing both transmission and reception functionalities. The ground segment consists of terrestrial traffic earth stations that vary in size based on the service type, ranging from a few centimeters to several meters.

Communication from space involves more than just aligning a spacecraft's antenna towards Earth. NASA boasts a comprehensive network of antennas spread across all seven continents to effectively capture transmissions from diverse spacecraft. To ensure optimal data reception, network engineers meticulously plan and establish robust communication links between these ground stations and various missions. They prepare antennas to communicate with spacecraft as they pass overhead. This spectrum of ground station antennas includes compact very high frequency antennas serving as auxiliary systems for the space station, and extends to a colossal 230-foot antenna designed to connect with distant missions like the Voyager spacecraft, which is situated over 11 billion miles away.

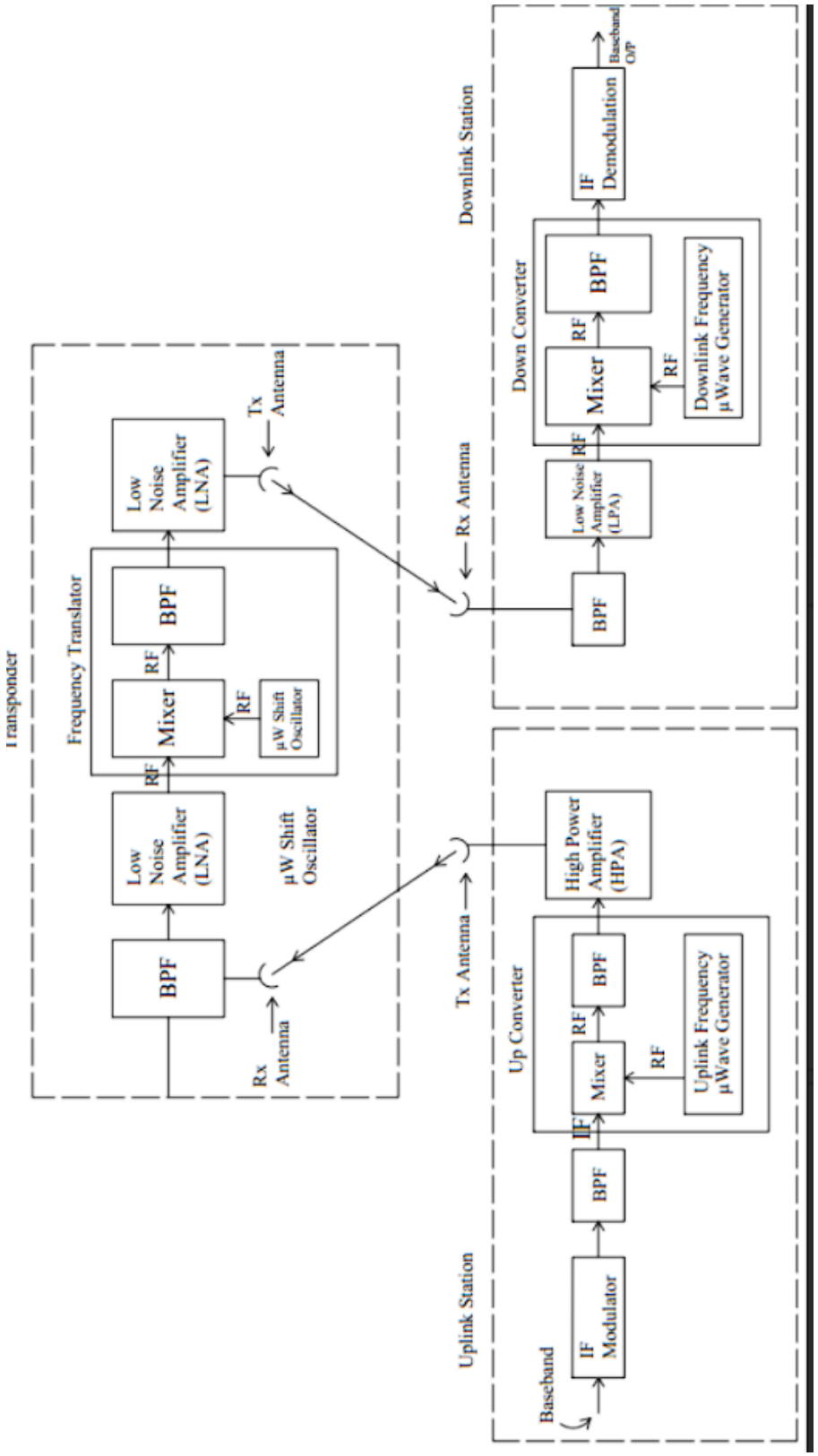

Figure 4.3.2 Transmit and receive block diagram

The size of the ground stations can vary depending on the type of service being considered, ranging from a few centimeters to several meters.
The classification of Earth stations can be categorized into three classes. These classes include user stations, interface stations, and service stations. User stations encompass devices such as handsets, portables, mobile stations, and VSATs, which enable customers to directly access the space segment. Interface stations, commonly referred to as gateways, serve the purpose of connecting the space segment to a terrestrial network. Lastly, service stations, such as hub or feeder stations, are responsible for the collection and distribution of information between user stations and the space segment.

The establishment of communication among users is facilitated by user terminals, which historically included devices like telephone sets, fax machines, and computers, and currently include laptops and smartphones. These terminals are connected to either the terrestrial network or the user station, such as a VSAT, or they may be integrated within the user station itself, particularly in the case of mobile terminals. The term "simplex connection" refers to the route taken by data from a source user terminal to a destination user terminal. There exist two fundamental schemes in telecommunications: single connection per carrier (SCPC) and multiple connections per carrier (MCPC). In the SCPC scheme, the modulated carrier is designed to accommodate only one connection. On the other hand, the MCPC scheme enables the modulated carrier to support multiple connections through time- or frequency-multiplexing techniques. In order for two users to engage in interactivity, it is necessary to establish a duplex connection between their terminals. This entails the establishment of two simple connections, with each connection facilitating communication in one direction.

Table 7. Difference between SCPC and MCPC

Specifications	**SCPC** single connection per carrier	**MCPC** multiple connections per carrier
Full form	Single Channel Per Carrier-single voice or data channel is modulated and transmitted over one RF carrier	Multiple Channels Per Carrier-Multiple voice and/or data channels are multiplexed(using TDM), modulated and transmitted over one RF carrier
Transmission format	Analog (voice channel) or Digital data (email,image/ text file)	Analog (voice channel) or Digital data (email,image/ text file
Multiplexing	Not provided	FDM or TDM
Modulation technique	FM or PSK(continuous/voice activated), voice activation is provided to save power when there is no voice activity	FM or PSK
Carrier Bandwidth(BW) usage	It can provide one connection and can use full bandwidth of transponder.	It can have multiplexed many connections over single carrier which uses full bandwidth of transponder. It efficiently uses bandwidth of transponder.
Capacity(Per MHz of transponder bandwidth)	more channels	less to medium channels depends on data rate of a system(VSAT)
Application	low data rate VSATs	High data rate VSATs
Burst transmission	Inefficient for such transmission.	Ideal for burst transmission e.g. packet based data transmission.

Dedicated connection	User pays for dedicated connection even if the connection is not used. SCPC DAMA implementation avoids this situation.	It does not need a dedicated channel for each of the connection.

Subsequently, it is imperative for every user terminal to possess the ability to transmit and receive data. The relationship between a service provider and a user is established via either a hub, which is responsible for aggregating services, or a feeder station, which is utilized for the dissemination of services, such as broadcasting. The term "forward connection" refers to the link that exists between a gateway, hub, or feeder station and a user terminal. The reverse connection refers to the connection that is established in the opposite direction of the initial connection. It can also be referred to as the return connection. Both the forward and return connections involve an uplink and a downlink, as well as the potential inclusion of one or more intersatellite links (ISLs).

Communication links refer to the channels or pathways through which information is transmitted between individuals, groups, or systems.
The connection between transmitting equipment and receiving equipment is established through the utilization of a modulated carrier, which can be in the form of either radio or optical signals. The evaluation of the transmitting equipment's performance is determined through the effective isotropic radiated power (EIRP), which is calculated by multiplying the power supplied to the antenna by the antenna's gain in the specified direction. The evaluation of the receiving equipment's effectiveness is quantified by the parameter G/T, which represents the ratio between the antenna's gain, G, in the specific direction under consideration, and the system's noise temperature, T. This ratio, known as the receiver's figure of merit, serves as a measure of the receiver's performance.

The various categories of links depicted in Figure **4.3.1** are as follows:

- The transmission of data from ground-based stations to satellites via uplinks.

- Downlink transmissions from satellites to earth stations are an essential component of satellite communication systems.

- Intersatellite links refer to the communication connections established between multiple satellites.

- Uplinks and downlinks are comprised of carriers that have been modulated with radio frequency, whereas ISLs have the capability to utilize either radio frequency or optical transmission methods. In addition to their ground stations, certain data-relay satellites of significant capacity employ optical links. Carriers undergo modulation through the utilization of baseband signals, which serve the purpose of transmitting information in communication systems.

- The measurement of link performance can be quantified by the C/N0 ratio, which represents the ratio of received carrier power (C) to the noise power spectral density (N0) and is typically expressed in hertz (Hz). The quality of service in digital communications is determined by the values of C/N0 for the links involved in the connection between the end terminals. This is specified in terms of the bit error rate (BER).

- The bandwidth, denoted as B, occupied by the carrier is another significant parameter to consider in the design of a link. The bandwidth is contingent upon factors such as the data rate of the information, the rate of channel coding (specifically forward error correction, or FEC), and the choice of modulation technique employed for carrier modulation.

- Adjust the carrier signal.

In the design of links, the trade-off between the power required by the carrier and the bandwidth occupied by the link is of utmost importance in achieving cost-effectiveness. The significance of power in satellite communications lies in its influence on the mass of the satellite and the size of the earth station, while the bandwidth is subject to limitations imposed by regulations. be determined using the formula provided by the Shannon-Hartley theorem. This theorem establishes the

upper limit for the rate of information transmission in a communication channel with a given bandwidth, taking into account the presence of noise.

It can be determined using the following equation:

The equation provided can be expressed as R = B log2(1 + S/N), where R represents the channel capacity, B represents the bandwidth, S represents the signal power, and N represents the noise power. Furthermore, the service provider, who leases satellite transponder capacity from the satellite operator, incurs charges based on the greater allocation of either power or bandwidth resources provided by the satellite transponder. The revenue of the service provider is determined by the quantity of established connections. Therefore, the goal is to optimize the throughput of the link under consideration in order to maximize revenue.

Maintaining an equitable distribution of power and bandwidth utilization.
In the context of a satellite system, multiple stations transmit their carriers to a specific satellite, thereby establishing the satellite as a network node. The methods employed by carriers to manage and regulate satellite access are commonly referred to as multiple-access techniques.

4.4 Multiple access techniques in deep space communication:

Multiple access techniques in deep space communication refer to the methods used to enable multiple spacecraft or ground stations to share communication resources efficiently. Here are some key points about these techniques [100], [101],[102],[103]:

1. Space Division Multiple Access (SDMA): SDMA is a technique that involves dividing the available space into sectors or beams, with each spacecraft or station allocated to a specific sector. This helps reduce interference and allows multiple users to communicate simultaneously in different spatial regions of deep space. SDMA can enhance the capacity and efficiency of communication in satellite networks.

2. Polarization Division Multiple Access (PDMA): PDMA is another technique used in satellite communications. It involves using different polarization states (e.g., horizontal and vertical) to transmit multiple signals simultaneously on the same frequency. This can help increase the data throughput in a satellite communication system by utilizing the polarization properties of electromagnetic waves.

3. Wavelength Division Multiple Access (WDM): While not specifically mentioned in the search results, WDM is a technique used in optical communications, including deep space optical communication. It involves multiplexing different data streams onto separate wavelengths of light, allowing for simultaneous data transmission on multiple optical channels.

4. Spread Spectrum Signals: In deep space communication, spread spectrum signals are often used to support multiple simultaneous communication links. This technique helps reduce interference and allows multiple spacecraft to communicate with ground stations or with each other in a coordinated manner.

5. Time-Division Multiple Access (TDMA): Although not directly related to deep space communication, TDMA is a common multiple access technique in shared-medium networks. It allows multiple users to share the same frequency channel by dividing time into slots, with each user transmitting during their allocated time slot.

6. Code Division Multiple Access (CDMA): CDMA is a technique applicable in various communication systems, including mobile satellite communications. It involves encoding data using unique codes for each user, allowing multiple users to share the same frequency without interference.

These multiple access techniques are crucial for ensuring efficient and reliable communication in deep space missions, where resources are limited, and signal quality is critical for the success of scientific exploration and data transmission. CDMA excels in bandwidth efficiency, security, and coverage area, while TDMA offers longer battery life due to intermittent data transmission. Each technology has its strengths and weaknesses, making them suitable for different applications in the wireless communication landscape.

Section 5

Latest Trends in Satellite Communication systems:

1. The James Webb Space Telescope (JWST), an unparalleled marvel in the realm of space observation, was launched in late December of 2021 and has recently reached its designated orbital point. A critical component of its mission will be the detailed study of far-off stars, as well as the meticulous survey of exoplanets, with particular attention to those that might harbor conditions suitable for life.

   The telescope also holds the ambitious objective of observing some of the most ancient and farthest celestial bodies in our observable universe. In its initial phases post-launch, all communications between NASA and the JWST were facilitated through its medium-gain antenna, which operates using the S-band microwave frequencies, ranging between 2–4 GHz.

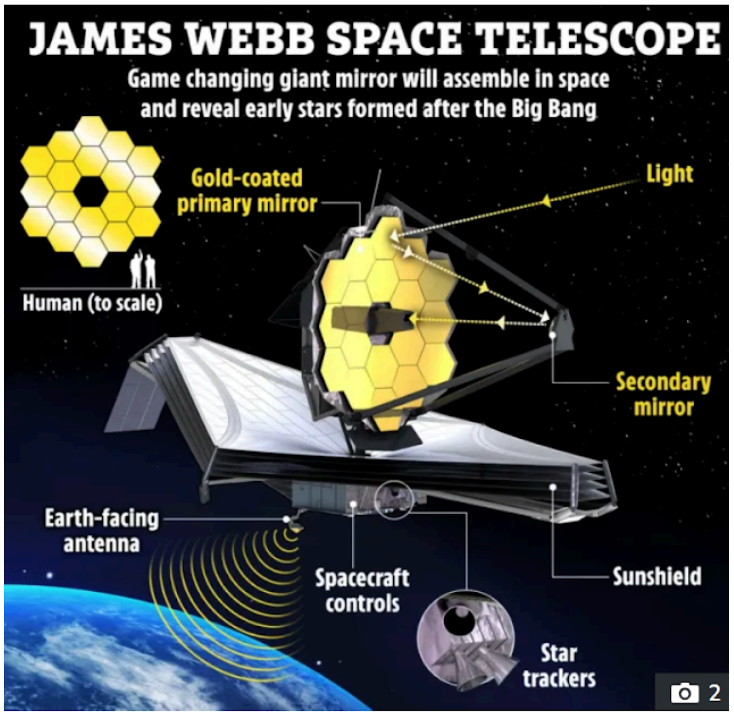

Figure 5.1 James Webb Telescope, Sourse NASA

However, a significant enhancement in communication capability is on the horizon. The high-gain antenna of the JWST, which functions in the higher frequency Ka-band (26.5–40 GHz), promises considerably faster data download speeds. This will be accomplished via NASA's Deep Space Network (DSN). Such a setup ensures that at least one station remains in line of sight with the JWST, irrespective of Earth's rotation.

The Ka-band antenna offers three distinct data transfer speeds. By default, it operates at an impressive 3.5 megabytes per second, a speed that notably surpasses the average download rate of a typical 4G mobile connection, which hovers around 1–1.25 megabytes per second. Furthermore, the system is designed with flexibility in mind: in the event of adverse weather conditions at a ground station, which could lead to signal interference, the antenna can switch to one of its two slower speeds to ensure consistent communication. As the JWST gears up to commence its scientific observations by mid-summer, NASA anticipates a steady influx of data, with the high-gain antenna slated to transmit a whopping 28.6 gigabytes of vital science data to Earth not once, but twice daily.

Before James Webb Space Telescope (JWST) achievement another has been taken place compared to conventional Radio Frequency (RF) systems, in 2013. The potential advantages of free space lasercom, compared to these (RF) systems, are significant, primarily due to its utilization of a shorter wavelength. A pivotal milestone in the journey toward establishing a fully operational deep-space lasercom system took place during a period from mid-October to mid-November in 2013. This marked the successful realization of a two-way lasercom link between a satellite orbiting the moon and multiple ground stations on Earth, as part of NASA's Lunar Laser Communication Demonstration (LLCD) project.

2. The LLCD project encompassed two key components: the space terminal known as the Lunar Lasercom Space Terminal (LLST) and the primary ground terminal named the Lunar Lasercom Ground Terminal (LLGT). The LLGT was a transportable system stationed at White Sands, NM, dedicated to the mission's objectives. The space terminal, an integral part of the Lunar Atmosphere and Dust Environment Explorer (LADEE) satellite, played a pivotal role in enabling laser communication. To ensure the success of the demonstration, additional ground stations located at Table

Mountain, CA, and Tenerife in the Canary Islands, Spain, were actively involved. The entire operation was meticulously coordinated and executed from the Lunar Lasercom Operations Center (LLOC) at MIT Lincoln Laboratory in Lexington, MA. It is worth noting that the development, construction, and operation of the LLST, LLGT, LLOC, and the overall LLCD system were carried out by dedicated teams from MIT Lincoln Laboratory. Oversight of the LLCD program rested with NASA Goddard Space Flight Center, while the LADEE satellite itself was the brainchild of NASA Ames Research Center (ARC). the Lunar Laser Communication Demonstration (LLCD) mission, despite its relatively short duration of 16 lunar days of operation spread over a month, managed to overcome major challenges traditionally associated with lasercom technology. These challenges included addressing issues related to the Earth's atmosphere and cloud interference, precise pointing and acquisition of signals, and predictive avoidance of potential obstacles. What's particularly remarkable is that LLCD demonstrated the feasibility of a nearly turn-key system, requiring only a minimal staff to operate effectively.

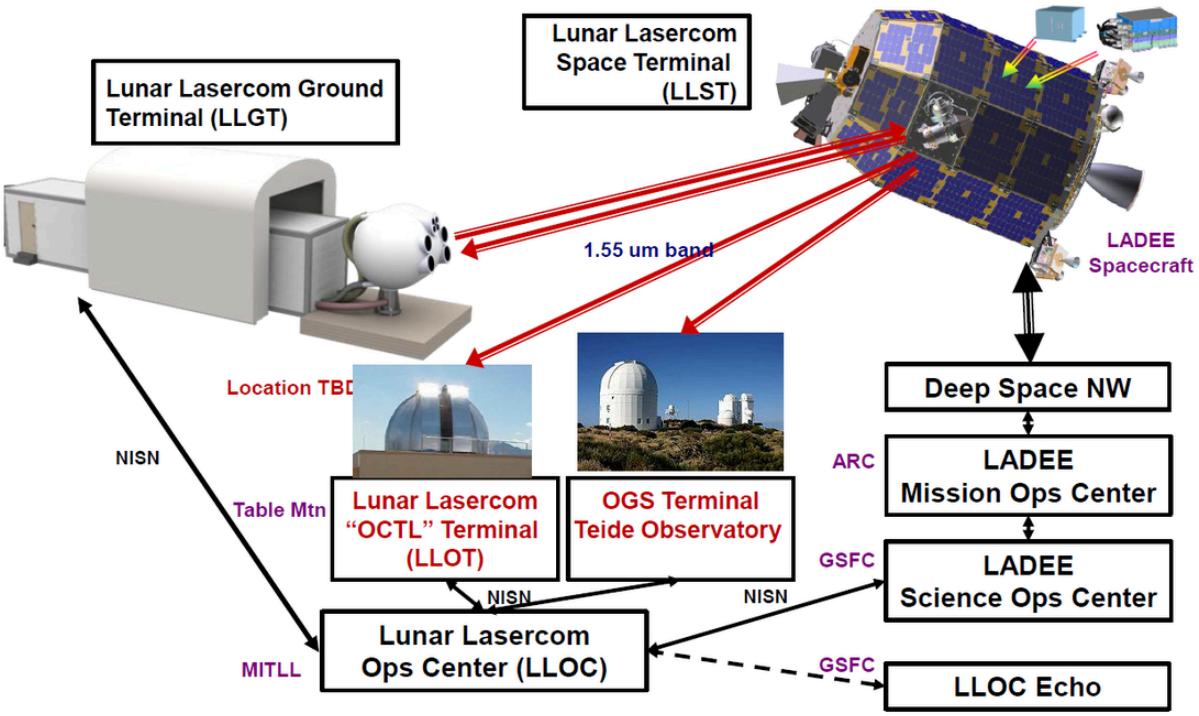

Figure 5.2 LLCD Architecture – Image: NASA Goddard

Referring to the lunar communication systems, a high effort to make sustainable communication systems between the Moon Mars and Earth is already happening in collaboration between the space government organizations and commercial companies such as NOKIA for example.

3. Nokia's mission involves developing groundbreaking technology that includes deploying an LTE/4G communication system on the lunar surface. This endeavor holds the promise of paving the way for a sustainable human presence on the Moon, aligning with NASA's Tipping Point program aimed at advancing commercial space capabilities to benefit future missions. NASA intends to leverage these innovations as part of its Artemis program, with the goal of establishing long-term lunar operations by the decade's end, in preparation for future missions to Mars. Thierry E. Klein, President of Bell Labs Solutions Research, shared insights into this ambitious initiative, highlighting Nokia's role in providing crucial communication capabilities through its LTE/4G network, a precursor to 5G technology.

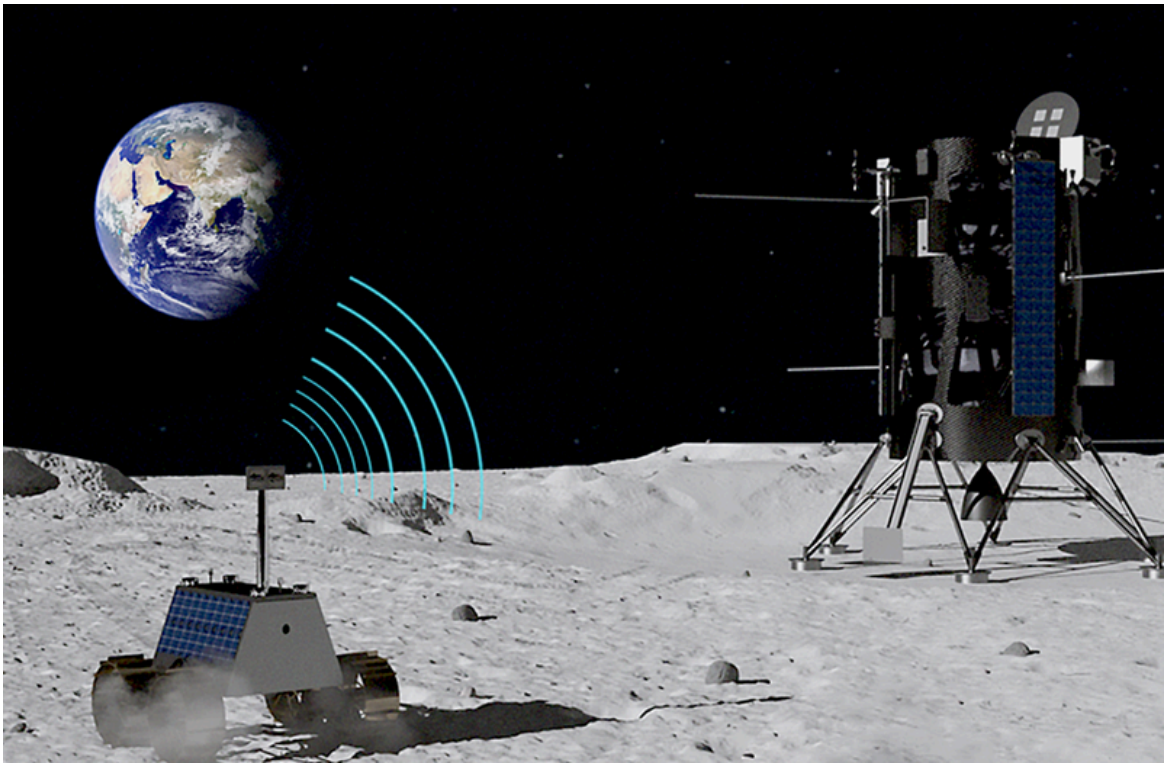

Figure 5.3 NOKIA LTE/4G communication system on the lunar surface. Source: NOKIA lab

Nokia's lunar network comprises an LTE Base Station equipped with integrated Evolved Packet Core (EPC) functions, LTE User Equipment, RF antennas, and high-reliability operations and maintenance (O&M) control software. This integrated cellular network has been meticulously designed to meet stringent size, weight, and power constraints for space payloads.

The mission's primary objectives include testing close proximity communication and longer-range communication between the lunar lander and rover. The system also includes custom-built O&M software for remote monitoring and configuration from Earth's mission control. The importance of this technological endeavor becomes evident when considering the need for robust communication capabilities for astronauts on the Moon and, eventually, Mars. These capabilities will support activities such as voice and video communications, telemetry and biometric data exchange, sensing applications, and remote robotics control.

Nokia's choice of LTE/4G technology is rooted in its proven performance and scalability, as well as its compatibility with the path to 5G deployment. The mission is scheduled for late 2022, with a duration of several weeks to validate network performance under lunar conditions. Rigorous testing has already taken place to ensure the equipment can withstand the harsh conditions of space, including vibration, shock, extreme temperatures, and radiation. Deploying a network on the Moon presents unique challenges related to radio propagation, as electromagnetic waves travel through the lunar surface without the need for an atmosphere. Nokia's system has undergone rigorous environmental and operational testing, positioning it to address the distinctive characteristics of lunar terrain, such as rock formations and craters. From a broader perspective, the innovations stemming from this initiative extend beyond space exploration and stand to benefit Nokia's customers by pushing the boundaries of technology. While Nokia has experience in building products for harsh environments like mining and industry, the challenges of operating complex electronics and software in space represent new frontiers for technological innovation.

4. The recent years in the space technology field we cross also the revolution of microsatellites. More specifically, The National Institute of Information and Communications Technology (NICT) has made a groundbreaking achievement by developing the world's smallest and lightest quantum communication transmitter,

known as SOTA. This compact device, weighing only 6 kilograms and measuring 17.8 cm in length, 11.4 cm in width, and 26.8 cm in height, was deployed on the microsatellite SOCRATES. The innovative technology successfully demonstrated the first-ever quantum communication experiment from space. During this experiment, SOTA transmitted laser signals from an altitude of 600 kilometers while traveling at a speed of 7 kilometers per second. Remarkably, these signals were received on Earth in a single-photon regime at an optical ground station in Koganei city, Japan, marking a major milestone in the development of a global and highly secure satellite communication network. This achievement paves the way for future advancements in global communication networks and represents a significant boost to the space industry. The results of this pioneering research were accepted for publication in Nature Photonics.

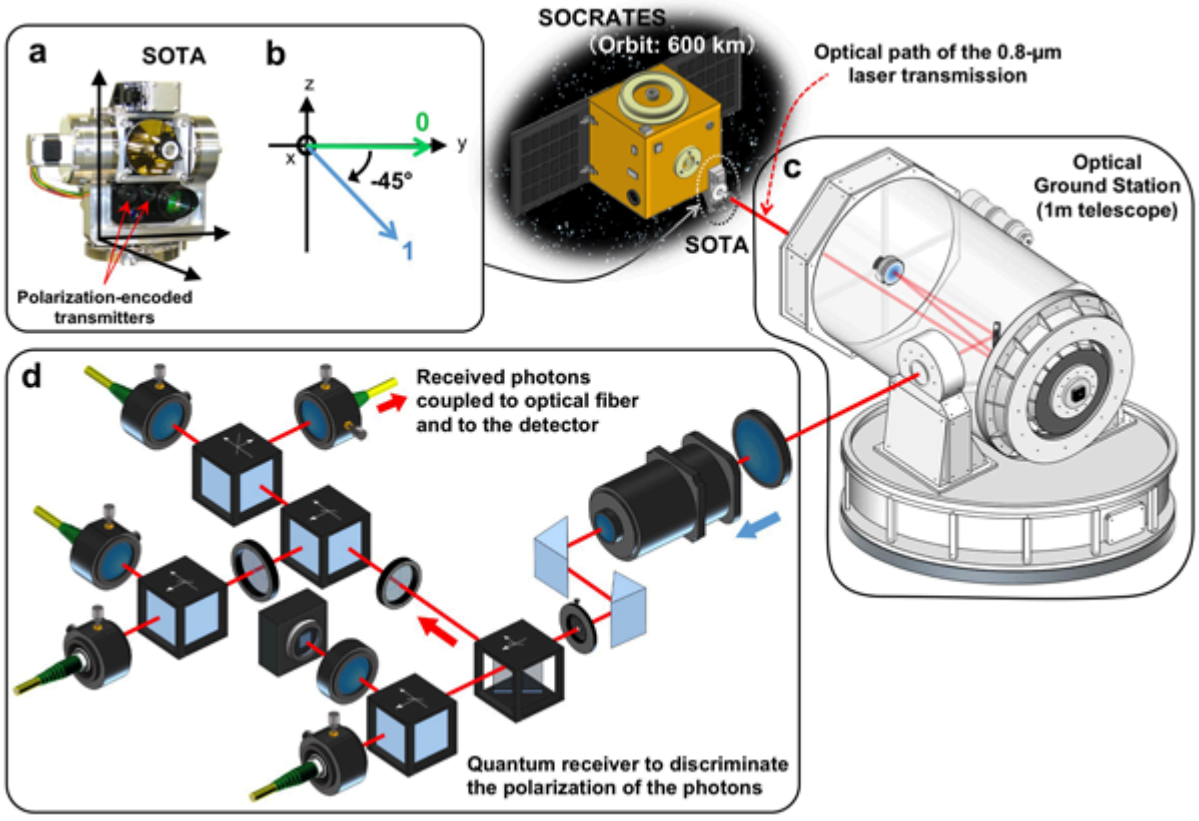

Figure 5.4 Description of the microsatellite SOCRATES and the NICT optical ground station situated in Koganei city. (a) Image of the laser communication terminal SOTA. (b) Polarization states used for encoding transmitted data bits. (c) Visual representation of the optical ground station. (d) Schematic illustration of the quantum receiver setup. Image credit: NICT.

The signal received by the 1-meter telescope from the satellite, known as SOCRATES, is exceptionally faint, with an average of just 0.1 photons per pulse. The National Institute of Information and Communications Technology (NICT) has developed groundbreaking technology to synchronize time and match the polarization reference frame between the satellite and the ground station directly from these weak Quantum Key Distribution (QKD) signals. Additionally, they have created a quantum receiver capable of detecting such delicate signals with minimal noise. This pioneering achievement marks the world's first quantum communication from a microsatellite weighing 50 kilograms. This development holds the potential to establish highly secure satellite communication links via quantum cryptography, preventing any information leakage. The breakthrough in this project demonstrates that satellite-based quantum communication can be realized with cost-effective and lightweight microsatellites. This advancement is expected to accelerate the practical application of quantum communication from space by numerous research institutes and companies. Moreover, the successful long-distance communication with minimal electric power usage opens up new possibilities for rapid deep-space optical communication with exploration spacecraft. Looking ahead, the plan is to further enhance transmission speed and tracking precision to maximize the secure key delivery from space to the ground through quantum cryptography. This endeavor aims to create a truly secure global communication network, addressing concerns posed by the development of quantum computers that could compromise information security. Advancements in technology have made it possible to launch small and cost-effective satellites into orbit, facilitating the development of satellite constellations for global communication networks. These constellations will face the challenge of transmitting vast amounts of data to Earth in short timeframes, especially as traditional radio frequency (RF) technology faces congestion and limitations. The field of quantum communication, particularly Quantum Key Distribution (QKD), is crucial for ensuring the security of future global communication networks. By leveraging satellites, QKD can significantly extend the range of secure key exchanges, as losses are lower than those in optical fibers. China's launch of a quantum communication satellite in 2016 demonstrated the potential of intercontinental-scale quantum cryptography. Japan's achievement with a much smaller satellite further underscores the feasibility of quantum communication technology implementation in space.

5. The Psyche mission also, with its primary goal of studying the metallic asteroid 16 Psyche, will serve as a platform to test the Deep Space Optical Communications (DSOC) technology. By using laser communication to transmit data via infrared photons, DSOC aims to achieve higher data rates and greater efficiency than traditional radio wave-based communication systems. If successful, this technology could revolutionize how we communicate with spacecraft in deep space, enabling more detailed and extensive scientific exploration.

The mission is planned for launch in 2022.

Spacecraft: The Psyche spacecraft will travel to the asteroid, orbiting it and collecting data using various scientific instruments, including magnetometers, multispectral imagers, and gamma-ray and neutron spectrometers.

Technology: DSOC uses a laser communication system to transmit data encoded in infrared photons, as opposed to traditional radio waves.

Advantages:

- **Higher Data Rates**: Using shorter wavelengths (infrared) allows for a higher frequency and more data to be transmitted in a given amount of time compared to radio waves.
- **Efficiency**: Optical communication systems can transmit more data with less power, making them more efficient, which is crucial for deep space missions where power is limited.
- **Bandwidth**: Optical systems offer greater bandwidth, enabling the transmission of higher-resolution images and more complex scientific data back to Earth.

How DSOC Works

- **Infrared Photons**: The DSOC system encodes data into infrared photons, which are then transmitted from the spacecraft to Earth.
- **Ground Station**: A sophisticated ground station with a large telescope and sensitive photon-counting detectors receives the optical signals.

Challenges:

- **Pointing Accuracy**: The laser beam must be precisely aimed at the receiving station on Earth, which is a significant challenge given the vast distances involved.
- **Atmospheric Interference**: Earth's atmosphere can scatter and absorb the laser signals, so the receiving stations are often located in high-altitude, dry locations to minimize this effect.

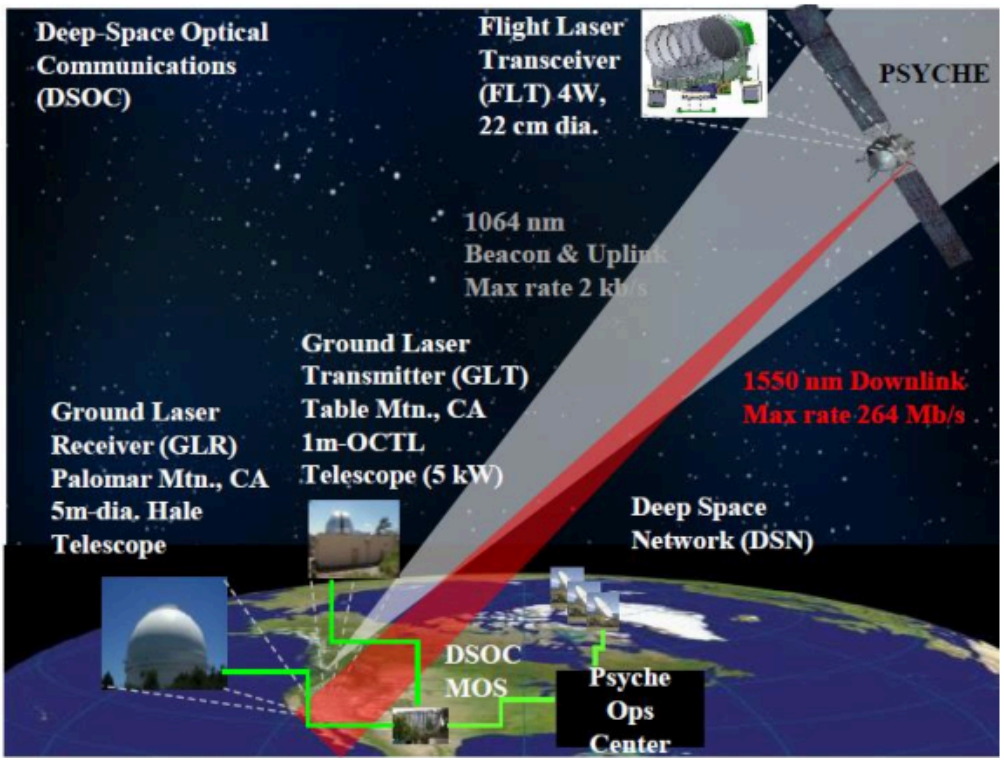

Figure 5.5 Psyche mission DSOC

The successful demonstration of DSOC on the Psyche mission could pave the way for future deep space missions to rely on laser communication systems, providing faster and more reliable data transmission. This technology is seen as a critical step forward in our ability to explore and understand the deeper regions of our solar system and beyond.

The Beginning of the Small Satellite Era

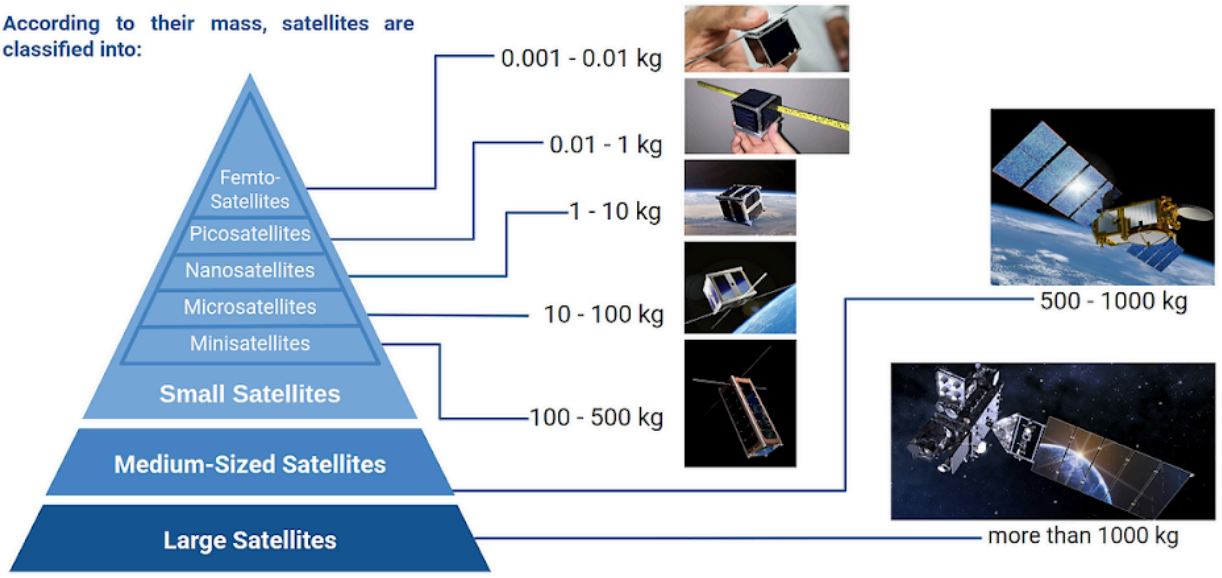

Figure 5.6 Image credit : Spacetech Analytics

The new paradigm in space exploration focuses on the development of satellites with reduced costs and shorter production timelines. This shift enables satellite manufacturers to lower expenses and minimize the size of electronic components, making satellite launches more accessible to various entities, including corporations, academic institutions, educational establishments, and private individuals.

Within the realm of satellite technology, small satellites are typically defined as those with a mass not exceeding 300 kg (1,100 lb). CubeSats, a specific category of small satellites, adhere to predefined criteria governing their physical dimensions, shape, and mass. These stringent standards contribute to cost reduction by allowing for the mass production of standardized components, making the engineering and development of CubeSats more cost-effective compared to highly customized small satellites. The use of standardized shapes and sizes also reduces expenses related to transportation and deployment in space.

CubeSats are available in various dimensions based on the standardized CubeSat "unit," known as 1U, which measures 10 cm on each side and has a mass ranging

from approximately 1 to 1.33 kg. While the 1U CubeSat is the most common, larger sizes like 1.5U, 2U, 3U, 6U, and 12U have gained popularity, offering increased flexibility for CubeSat missions. These small satellites have successfully demonstrated inter-satellite communication links and the ability to control relative distances using onboard propulsion, essential for future constellation projects. They have also contributed to various scientific endeavors, such as monitoring Earth's solar irradiance and radiation budget for climate change studies, exploring the plasma environment in orbit, measuring space radiation levels for space weather tracking, and mapping the Sun's X-ray flux. Notably, these achievements have led to the development of instruments for operational missions conducted by organizations like the United States National Oceanic and Atmospheric Administration (NOAA).

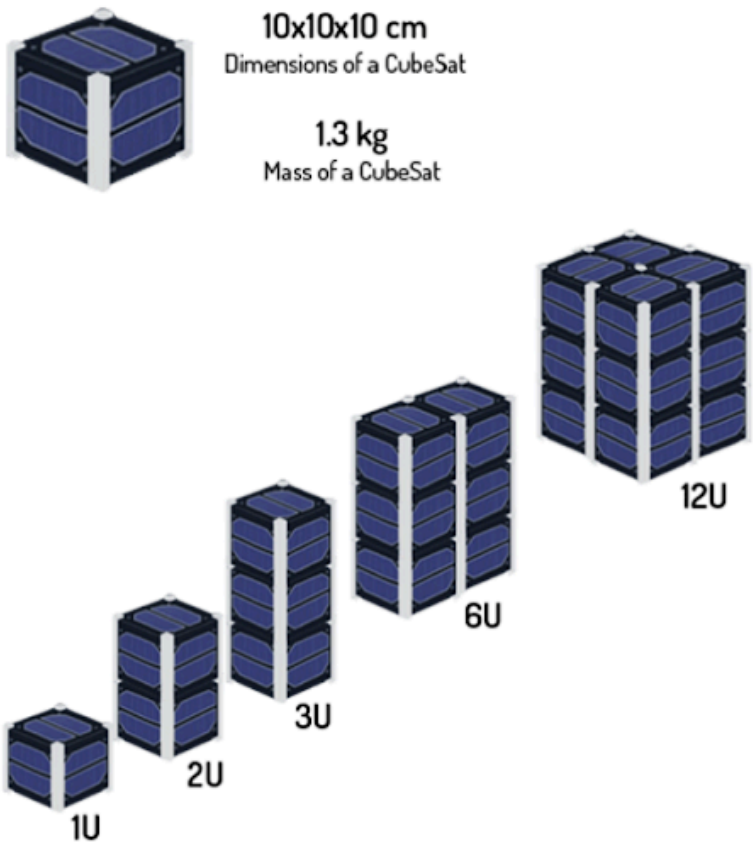

Figure 5.7 cubesats

To facilitate communication with CubeSats, space agencies maintain networks of tracking ground stations following international standards set by the International

Telecommunication Union (ITU) and the Consultative Committee for Space Data Systems (CCSDS). These networks use specific frequency ranges, such as S-band and X-band, for tracking, telemetry, and command (TT&C) operations. The integration of S-band and X-band ground stations by private tracking networks aligns with the trend of reduced station costs. Currently, CubeSats primarily use UHF or S-band payload telemetry subsystems, allowing for the retrieval of several hundred megabits of data per day. However, these frequencies have limited data volume capabilities due to recommended spectral occupation bandwidth restrictions. To address this limitation, the utilization of a portion of the Industrial, Scientific, and Medical (ISM) S-band, particularly the 2400-2483.5 MHz range, could enhance telemetry capacity, though it is susceptible to interference. To improve transmission rates, there is interest in acquiring compact S-band TT&C transceivers and X-band transmitters tailored for CubeSats.

The integration of X-band transmitters in CubeSats has emerged as a solution to meet the increasing demand for higher data transfer rates, offering capacities ranging from 6 to 14 Gbit per pass and compatibility with 3U configurations. These transmitters are cost-effective, consume minimal power, and feature compact antenna designs. Modulation and coding schemes play a significant role in optimizing performance, with OQPSK modulation and convolutional coding employed for effective data transmission. Variable Bit Rate (VBR) can enhance download capacity during a pass, provided the ground station receiver can handle predictable bit rate switching.

Machine learning (ML)

Also, Machine learning (ML), fundamental technology in wireless communications, has shown its value in accelerating complex optimization procedures, both in general wireless communications and SatCom. The European Space Agency (ESA) initiated AI-related projects in SatCom to explore AI's applicability in satellite communications, leading to SATAI and MLSAT projects. However, both projects faced challenges, including the need for large training datasets and limited examination of ML techniques. NASA has also explored cognitive radio (CR) in satellite communications. Moreover, AI has been proposed for optimizing space–air–ground

integrated networks (SAGINs), but it's considered a new topic requiring further improvement.

Despite significant progress, AI applications in SatCom are still evolving, with most studies based on theoretical simulations. Real-world implementation faces challenges related to computational intensity and hardware limitations in space. However, the availability of commercial AI chipsets has enabled practical AI usage onboard satellites.

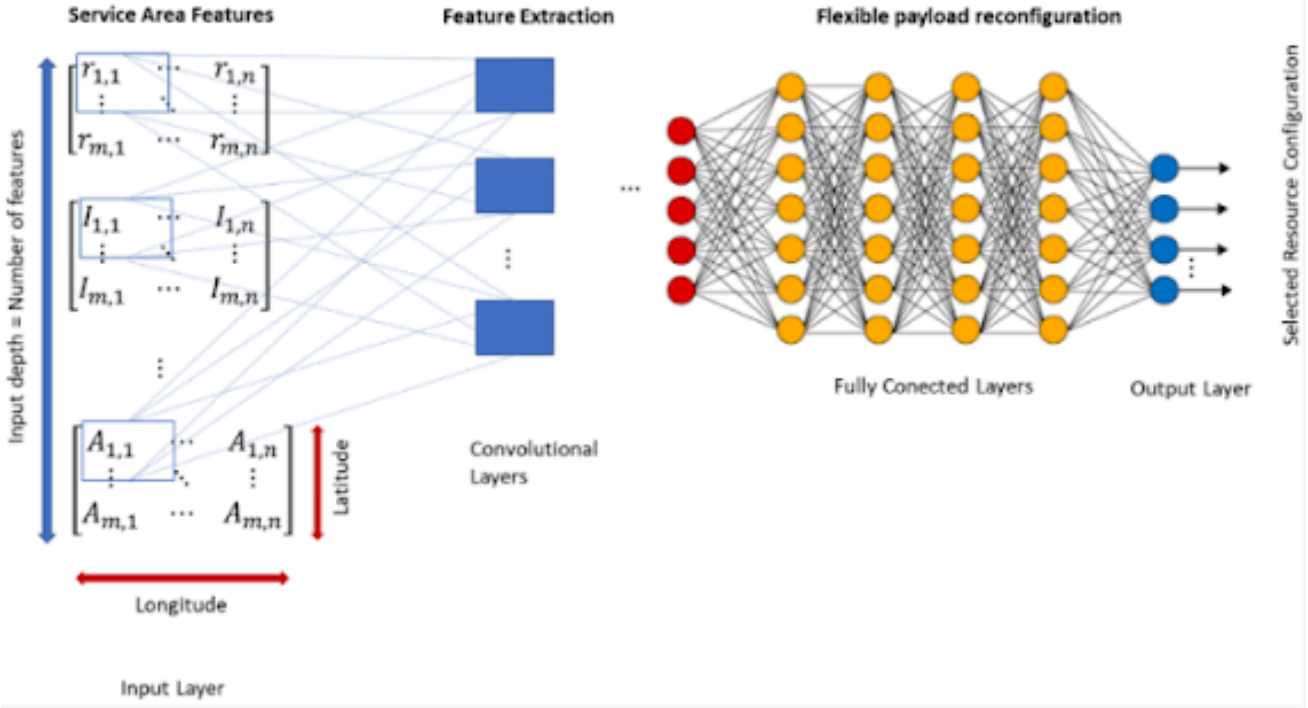

Figure 5.8 convolutional neural networks [107]

A convolutional neural network (CNN) is a deep learning architecture that has found applications in a wide range of fields, including radio frequency (RF) interface and flexible payload reconfiguration. In this context, a CNN can be employed to enhance the adaptability and efficiency of RF systems within satellite or communication payloads. The CNN can be used to analyze and process RF signals, making it possible to perform tasks such as signal classification, modulation recognition, interference detection, and adaptive reconfiguration.

Here's how it works:

1. Signal Processing: RF signals received by the satellite's RF interface are digitized and fed into the CNN. The CNN consists of multiple layers of neurons designed to automatically extract features from the input signals.

2. Feature Extraction: The initial layers of the CNN extract low-level features from the RF signals, such as edges, patterns, or spectral characteristics. These features are learned from a large dataset during the training phase.

3. Pattern Recognition: Deeper layers of the CNN learn to recognize higher-level patterns and structures within the RF signals. This includes identifying modulation schemes, signal types, and any anomalies or interference.

4. Classification and Decision Making: The output layer of the CNN provides a classification of the RF signal or the presence of any issues. For example, it can determine if the incoming signal is a specific type of communication protocol or if it's suffering from interference.

5. Adaptive Reconfiguration: Based on the CNN's analysis and classification, the satellite's RF interface can be dynamically reconfigured to optimize performance. This might involve adjusting the receiver's parameters, switching to a different antenna, or altering the transmission protocol.

By employing a CNN in RF interface flexible payload reconfiguration, satellites and communication systems can adapt to changing conditions and requirements autonomously. This technology can improve the overall efficiency, reliability, and resilience of RF systems in space applications.

Section 6

Provides communication protocols and standards

6.1 ITU (International Telecommunication Union)

(the bands have been referred also in Section 2)

The ITU manages the global radio-frequency spectrum, ensuring the harmonized and efficient use of frequencies both on Earth and for space services, such as satellites. The frequencies allocated for space services, like satellite communication or space research, are part of the same electromagnetic spectrum that is used for terrestrial (on-Earth) services.

When discussing space and satellite communications specifically, there are certain frequency bands that are commonly referred to. Here are some of the ITU's designated frequency bands used for space services:

- L-band (1 to 2 GHz): Used for GPS and other satellite navigation systems, mobile satellite services, and some satellite broadcasting.
- S-band (2 to 4 GHz): Used for weather radar, some communications satellites, and mobile satellite services.
- C-band (4 to 8 GHz): Commonly used for satellite communication, especially for fixed satellite services. It's less susceptible to rain fade compared to higher bands.
- X-band (8 to 12 GHz): Employed for satellite communications, radar, and satellite telemetry.
- Ku-band (12 to 18 GHz): Popular for satellite broadcasting and direct-broadcast satellite services.
- K-band (18 to 27 GHz): Used in satellite communications. Some satellite broadband services operate in this band.
- Ka-band (26.5 to 40 GHz): Increasingly used for high-speed satellite broadband and communication services.

- V-band (40 to 75 GHz): There's growing interest in this band for future high-capacity satellite services.
- Q/V-band (33 to 75 GHz): Considered for future high-throughput satellite systems and satellite-to-satellite links.

These frequency bands are part of the larger electromagnetic spectrum that the ITU manages. Within each band, specific allocations are made for different services—terrestrial, spaceborne, or others. The goal is to ensure that these services can operate without harmful interference from each other. In summary, the frequencies used for space services are part of the same spectrum as those on Earth. The allocation and management by the ITU ensure organized and interference-free operations globally.

In the case of Earth, the ITU (International Telecommunication Union) designations for frequency bands and radar bands are frameworks used to categorize and specify different portions of the electromagnetic spectrum and the key differences between the ITU frequency bands and the ITU radar bands (the bands are referred also in the section 1) are:

ITU Frequency Bands: These are general classifications for frequency ranges in the electromagnetic spectrum. They cover all potential uses of those frequencies, not just radar, like all electromagnetic wave applications, including television, radio broadcasting, satellite communication, and more.
ITU Radar Bands: These are specific classifications within the ITU frequency bands that are designated for radar applications, such as weather radar, air traffic control, maritime radar, and other radar applications.

Many ITU radar bands fall within a specific ITU frequency band. For instance, the S-band for radar falls within the UHF frequency range. However, not all frequencies within an ITU frequency band are used for radar applications.
However, the ITU radar band designations are often used in technical and industry contexts where radar applications are discussed because they provide clarity regarding the specific radar technology in use while the ITU frequency bands, being

more general, are used in a broader range of contexts including regulation, broadcasting, and general communication technology discussions.
It's important to note that while the ITU designations provide a standardized framework, variations might exist in some contexts or regions.

6.2 Consultative Committee on Space Data Systems (CCSDS)

The Consultative Committee for Space Data Systems (CCSDS) is a 1982-founded international organization dedicated to the development of spaceflight data and information systems standards. Its primary objective is to improve cross-support and interoperability between various space agencies, as well as to expedite operations by standardizing techniques, practices, and data formats.

Members of the CCSDS include prominent international space agencies, such as NASA (United States), ESA (European Space Agency), Roscosmos (Russia), and CNSA (China National Space Administration). Once approved, individual agencies may employ these recommendations for space data system standards.

CCSDS has made significant contributions to a variety of fields, including data transmission, space link services, mission operations, and information management, ensuring that the developed standards address a broad spectrum of space communication requirements. Numerous space missions have utilized CCSDS-developed standards, which have helped to facilitate international collaboration and reduce the cost and danger of space missions.

6.2.1 Space Internetworking Services Area

The work of the CCSDS is supported by the Space Internetworking Services Area (SIS), which offers services and protocols to address networked interactions in a variety of contexts. These contexts include interactions between spacecraft and earth-based resources; interactions among spacecraft; interactions between spacecraft and landed elements; and interactions within heterogeneous spacecraft.

The SIS Domain focuses on communication services and protocols that are not dependent on any particular connection technology (as a lower layer bound) or any application-specific semantics (as an upper layer bound). This includes the majority of the OSI reference model, from the network layer up to the application layer. The SIS Area can accept a wide variety of latency, interactivity, and directionality settings; however, not all protocols are suitable for use in all contexts—statement Regarding the Granting of Permission to Reproduce for Publications.

6.2.2 Spacecraft Onboard Interface Services Area

The Spacecraft Onboard Interface Services Area (SOIS) helps the CCSDS with its work by providing standard development activities. The goal of these activities is to improve the design and development of spacecraft flight segment data systems by a large amount. This will be done by defining generic services that will make it easier for flight software to talk to flight hardware and will allow interoperability and reuse for both agencies and industrial contractors. Statement about Reproduction Permission for Publications.

6.2.3 Mission Operations and Information Management Services Area

The goal of the Mission Operations and Information Management Services (MOIMS) Area is to deal with all of the flight execution phase applications that are needed to run the spacecraft and its ground system according to mission goals, as well as the detailed information management standards and processes that go with them. The main focus of this Area is on the "mission operations" tasks that happen on a timescale set by the space vehicle's flight path. Mission operations are often done by a dedicated community, while "mission utilization" is usually done at times that are useful for users and is usually done by a different community. The MOIMS Area makes sure that there are application guidelines that make it easy for "mission operations" systems and "mission utilization" systems to share information about space missions. Statement about Reproduction Permission for Publications.

6.2.4 Area of System Engineering

The job of the CCSDS is helped by the System Engineering Area (SEA), which does the following:

- Communications, tactics, and cross-support for space missions as a whole.
- Coordination and working together with the other areas on decisions and options for architecture.
- Helping the CESG make sure that all area work plans are consistent with the architecture that has been set up.
- Putting together the working groups and BoFs that CCSDS needs to move its work forward.

6.2.5 Cross Support Services (CSS) Area

Cross Support Services (CSS) looks at how one organization makes space network resources available to another organization for "cross support." So, the goal of the CSS Area is to define what services are needed at different cross-support interface points and how organizations that want to work together to complete a mission can expose, plan, and use those services.

6.2.6 Space Link Services Area

The Space Link Services Area (SLS) helps the CCSDS do its job by creating efficient communication methods that all participating agencies can use for space links. A space link ties a spaceship to its support system on Earth or to another spaceship. The next generation of space flights for agencies needs better telecommand and telemetry than what is currently available. These new needs include higher data rates, better link performances, and better range systems, as well as lower cost, mass, and power, and higher security.

More specifically, the SLS Area focuses on levels 1 and 2 of the OSI protocol stack, which are RF and modulation, channel coding, and the data link layer for both long-haul (like spacecraft to ground) and short-haul (like orbiter to lander) links. The SLS area also handles two other tasks: data compression to speed up end-to-end data sharing and ranging to find an object's exact orbit. There are expert working groups in this area, and their goal is to come up with specific suggestions. Most of

the time, one suggestion will cover one layer or sub-layer of the OSI. This stacking of suggestions allows for the most flexibility and compatibility with commercial protocols like TCP/IP.

Note: The CCSDS Experimental Specification (Orange Books) says that it is part of a study or development project based on future needs. Because of this, it is not a Standards Track document. Experimental Recommendations are meant to show that something is technically possible before a "hard" requirement comes up. If a hard need comes up in the future, experimental work can be moved quickly to the Standards Track.

Several of the papers below may need patent licenses. Look for the "Patent Licensing" entry to find the information you need about the patent that is in the paper. This paper is for the ISO patent declaration form that goes with it.

6.3 Space Communications Protocol Specifications (SCPS)

The Consultative Committee on Space Data Systems (CCSDS) created the Space Communications Protocol Specifications (SCPS) to enhance the efficacy of Internet protocols in space environments. More than 1000 space missions have flown with CCSDS-developed standards.

6.3.1 SCPS protocol Hierarchy components

1. SCPS-FP—A set of extensions to FTP to make it more bit efficient and to add advanced features such as record updates within a file and integrity checking on file transfers.
2. SCPS-TP—A set of TCP options and sender-side modifications to improve TCP performance in stressed environments including long delays, high bit error rates, and significant asymmetries.

3. The SCPS-TP options are TCP options registered with the Internet Assigned Numbers Authority (IANA) and hence SCPS-TP is compatible with other well-behaved TCP implementations.
4. SCPS-SP—A security protocol comparable to IPsec
5. SCPS-NP—A bit-efficient network protocol analogous to but not interoperable with IP
6. The SCPS protocol that has seen the most use commercially is SCPS-TP, usually deployed as a Performance Enhancing Proxy (PEP) to improve TCP performance over satellite links.

6.4 Consultative Committee on Space Data Systems (CCSDS) PROTOCOLS

6.4.1 Space Internetworking Services Area

1. *CCSDS 702.1-B-1* (IP over CCSDS Space Links)
    a. This Recommendation defines a mechanism for transferring IP Protocol Data Units (PDUs) using CCSDS Space Data Link Layer protocols.
2. *CCSDS 702.1-B-1* Cor. 1 (Technical Update 1 to CCSDS 702.1-B-1, published in September 2012)
    a. This Technical update details modifications made to CCSDS 702.1-B-1, IP over CCSDS Space Links (Blue Book, Issue 1, September 2012).
3. *CCSDS 706.1-G-2* (Applications for Motion Imagery) This document provides a common reference and framework for developing digital video and motion imagery standards for space missions and a foundation for future recommendations for using international standards to share or distribute video and motion imagery between spacecraft elements and ground distribution systems.
4. *CCSDS 706.2-G-2* (Voice Communications)

    a. This CCSDS Informational Report covers human spaceflight voice communications.
5. *CCSDS 714.0-B-2* (Transport Protocol Specification for Space Communications (SCPS))
    a. The four Space Communications Protocol Specification (SCPS) Recommendations describe a set of protocols that work the same way as the protocols of the Internet on Earth (FTP/TCP/IP) and can be used together. The SCPS protocols have been made better so that they can be used in space without the problems that come with using Internet protocols there. This Recommendation describes the SCPS protocol suite's transport-layer protocols and services. Space Communications Protocol Specification (SCPS) Transport Protocol (SCPS-TP) specification: - adds optional support for Selective Acknowledgements (SACK) and Explicit Congestion Notification (ECN); - defines semantics to extend SCPS-TP signaling to allow optional inclusion of vendor- and community-specific options. The CCSDS reviews its products regularly to make sure they are still relevant. This Recommended Standard will still be used until June 2022.
6. *CCSDS 720.1-G-4* (Part 1: Introduction and Overview of the CCSDS File Delivery Protocol (CFDP))
    a. This Report gives an overview of the CCSDS File Delivery Protocol (CFDP) and its ideas, features, and traits.
7. *CCSDS 720.2-G-4* (Part 2 of the Implementers Guide for the CCSDS File Delivery Protocol (CFDP))
    a. This Report has information that will help implementers understand the details of the protocol and choose the best choices. It also has ideas and recommendations about things that are important for implementation. This Report also includes implementation reports from different member agencies, reports on testing the implementations and protocol, and the requirements on which the CFDP is built.
8. *CCSDS 720.3-G-1* CCSDS File Delivery Protocol (CFDP)—Part 3: Interoperability Testing Final

a. This Informational Report talks about the results of CFDP interoperability tests done by CCSDS Agencies and explains what they mean.

9. *CCSDS 720.4-Y-1* till CCSDS 720.6-Y-1
    a. These 6 notebooks serve as a guide for individuals involved in planning, participating in, or assessing inter-Agency evaluations of the CFDP Store and Forward Overlay (SFO) Procedures and the CFDP Protocol, as outlined by the CCSDS Record.
10. *CCSDS 722.1-M-1* (CFDP over Encapsulation Service)
    a. This CCSDS Recommended Practice describes how to use the CCSDS File Delivery Protocol (CFDP) over the CCSDS Encapsulation Service for Earth-to-spacecraft, spacecraft-to-Earth, and spacecraft-to-spacecraft communications. It defines CFDP communications over the Encapsulation Service. The CFDP service of the underlying layers is reconciled with the Encapsulation Service service.
11. *CCSDS 727.0-B-5* (CFDP CCSDS File Delivery Protocol)
    a. The CFDP Recommended Standard describes a protocol for file transmission to and from spacecraft data storage that can be used in many mission configurations. The protocol provides file management capabilities to govern the storage medium in addition to file delivery. A new SANA Checksum Types registry supports checksum algorithm selection, and compatibility testing has updated/clarified certain language.
12. *CCSDS 730.1-G-1* (Solar System Internetwork (SSI) Architecture)
    a. The CCSDS Informational Report describes the Solar System Internetwork's top-level design. This document specifies the SSI's features, elements, principles, and processes in accordance with the 2010 Space Internetworking Strategy Group and Interagency Operations Advisory Group SSI Operations Concept.
13. *CCSDS 730.2-G-1* (Reasons for Streaming Services over Bundle Protocol)
    a. This document discusses Bundle Protocol real-time video streaming concepts and logic. Video streaming over Bundle Protocol have been

tested. A standard test configuration for video and streaming data testing and benchmarking is also given.

14. *CCSDS 734.0-G-1* (Space DTN rationale, scenarios, and requirements)
    a. This Informational Report provides background and explanation for CCSDS Recommendations for a Delay-Tolerant Networking protocol suite. The reasoning, scenarios/use cases, and needs for a space internetworking DTN service are described.
15. *CCSDS 734.1-B-1* (CCSDS Licklider Transmission Protocol (LTP))
    a. This Recommended Standard defines CCSDS Licklider Transmission Protocol (LTP) and service. LTP offers various reliability techniques over a data link communication service.
16. *CCSDS 734.2-B-1* (A CCSDS bundle protocol specification)
    a. The RFC 5050 Bundle Protocol is extended to accommodate space application Delay/Disruption Tolerant Networking (DTN) in this Recommended Standard. Feedback from the second draft issue was included into the current issue.)
17. *CCSDS 734.3-B-1* (Schedule-Aware Bundle Routing)
    a. This Recommended Standard specifies Schedule-Aware Bundle Routing (SABR) for Delay-Tolerant Networking (DTN) bundle forwarding in the space environment. SABR provides dynamic route computation in an environment with a stable topology but time-varying connectivity when connectivity instances are scheduled rather than opportunistic.
18. *CCSDS 735.0-G-1* (Asynchronous Message Service)
    a. This Informational Report provides additional perspectives on the motivation, design, implementation, and deployment of Asynchronous Message Service (CCSDS 735.1-B-1) in space flight missions.
19. *CCSDS 766.1-B-3* (Digital Motion Imagery)
    a. This Recommended Standard gives a shared point of reference and a framework for standards for digital moving images. It also gives suggestions for how international standards can be used to capture and send moving images between spacecraft and ground systems. With this change, H.265 is now supported.
20. *CCSDS 766.2-B-1* (Voice and Audio Communications)

a. This Recommended Standard describes the technologies, services, and service interfaces for real-time or almost real-time voice and audio communications between terrestrial facilities and space systems to support the mission activities of space flight.

b.

6.4.2 Spacecraft Onboard Interface Services Area

1. *CCSDS 811.1-O-1 CAST Flight Software as a CCSDS Onboard Reference Architecture*
   The goal of this Experimental Specification is to build and implement a Flexible and Unified Flight Software Architecture (FUHSI) of China Academy of Space Technology (CAST) to provide standard basic service support for future spacecraft avionics systems.

2. *CCSDS 850.0-G-2 Spacecraft Onboard Interface Services*
   This Informational Report talks about the idea behind the Spacecraft Onboard Interface Services (SOIS) and why it makes sense. It is meant to give an introduction and overview of the SOIS services idea, which is the basis for the detailed CCSDS SOIS recommendations, as well as a summary of the individual service recommendations and why they were made. The ideas in this Informational Report are the basis for the CCSDS's efforts to standardize services and generic support services that will be used in the flight section of spacecraft systems.

3. *CCSDS 851.0-M-1 Spacecraft Onboard Interface Services--Subnetwork Packet Service*
   This Recommended Practice describes the services and service interfaces that the Spacecraft Onboard Interface Services (SOIS) Subnetwork Packet Service offers.
4. *CCSDS 852.0-M-1 Spacecraft Onboard Interface Services--Subnetwork Memory Access Service*
   This Recommended Practice describes the services and service interfaces that the Spacecraft Onboard Interface Services (SOIS) Subnetwork Memory Access Service offers.
5. *CCSDS 853.0-M-1 Spacecraft Onboard Interface Services--Subnetwork Synchronisation Service*
   The Recommended Practice describes the services and service interfaces that the Spacecraft Onboard Interface Services (SOIS) Subnetwork Synchronisation Service offers.

6. *CCSDS 854.0-M-1 Spacecraft Onboard Interface Services--Subnetwork* Device Discovery Service
   The Recommended Practice defines the services and service interfaces provided by the Spacecraft Onboard Interface Services (SOIS) Subnetwork Device Discovery Service.
7. *CCSDS 855.0-M-1 Spacecraft Onboard Interface Services--Subnetwork Test Service*
   This Recommended Practice describes the services and service interfaces that the Spacecraft Onboard Interface Services (SOIS) Subnetwork Test Service offers.
8. *CCSDS 870.10-Y-1 MO Services and SOIS Electronic Datasheets*
   This report looks at Application Layer interoperability for missions by using standards made by the Mission Operations and Information Management Services (MOIMS) and the Spacecraft Onboard Interface Services (SOIS) Areas. The goal is to make sure that interactions are well-defined, well-understood, and don't cause any problems. This study also gives a brief look at three different ways that different missions may choose to integrate MOIMS and SOIS.
9. *CCSDS 876.0-B-1 Spacecraft Onboard Interface Services--XML Specification for Electronic Data Sheets*
   This Recommended Standard describes the XML Specification for SOIS Electronic Data Sheet (SEDS). The SEDS is used to describe online, over the SOIS Subnetwork Services, the data interfaces that flight hardware, like sensors and actuators, offer.
10. *CCSDS 880.0-G-3 Wireless Network Communications Overview for Space Mission Operations*
    This Informational Report gives basic information and explanations to support the CCSDS Best Practices for networked wireless communications to help space missions. It looks at the possibilities and benefits of using wireless communications technology on board space missions. It also describes a set of driving use cases in the space domain and evaluates how existing technologies and related commercial standards on Earth can be used to meet the needs of space-based use cases. There is also useful lesson information meant to help the reader understand the basics of wireless transmission and networking, as well as any problems that might come up when wireless networks are set up.
11. *CCSDS 881.0-M-1 Spacecraft Onboard Interface Services--RFID-Based Inventory Management Systems*
    This paper gives suggestions for how to use the Radio Frequency Identification (RFID) protocol and communication standards to help with inventory management for space missions.
12. *CCSDS 881.1-B-1 Spacecraft Onboard Interface Services--RFID*

This Recommended Standard describes tag-encoding options that add to an older ISS Inventory Management System tag-encoding schema that was set up for early flight studies but are still compatible with it.

13. *CCSDS 882.0-M-1 Spacecraft Onboard Interface Systems--Low Data-Rate Wireless Communications for Spacecraft Monitoring and Control*
    This CCSDS Recommended Practice shows how low-data-rate wireless communication technologies can be used to help with spacecraft testing on the ground and flight tracking and control.
14. *CCSDS 883.0-B-1 Spacecraft Onboard Interface Services-High Data Rate Wireless Proximity Network Communications*
    This Recommended Standard outlines the transmission protocol and standards for wireless proximity networks that can be used to help with space missions.

6.4.3 Mission Operations and Information Management Services Area

1. *CCSDS 500.0-G-4 Navigation Data--Definitions and Conventions*
2. *CCSDS 500.2-G-3 Navigation Data Messages Overview*
3. *CCSDS 502.0-B-3 Orbit Data Messages*
4. *CCSDS 502.1-Y-1 Orbit Data Messages V2.0 Test Plan/Report*
5. *CCSDS 503.0-B-2 Tracking Data Message*
6. *CCSDS 503.0-B-2 Cor. 1 Technical Corrigendum 1 to CCSDS 503.0-B-2, Issued June 2020*
7. *CCSDS 504.0-B-1 Attitude Data Messages*
8. *CCSDS 504.0-B-1 Cor. 1 Corrigendum 1 to CCSDS 504.0-B-1, Issued May 2008*
9. *CCSDS 505.0-B-3 XML Specification for Navigation Data Messages*
10. *CCSDS 508.0-B-1 Conjunction Data Message*
11. *CCSDS 508.0-B-1 Cor. 1 Corrigendum 1 to CCSDS 508.0-B-1, Issued June 2013*
12. *CCSDS 508.0-B-1 Cor. 2 Technical Corrigendum 2 to CCSDS 508.0-B-1, Issued June 2013*
13. *CCSDS 508.1-B-1 Re-entry Data Message*
14. *CCSDS 508.1-B-1 Cor. 1 Technical Corrigendum 1 to CCSDS 508.1-B-1, Issued November 2019*
15. *CCSDS 509.0-B-1 Pointing Request Message*

16. *CCSDS 509.0-B-1 Cor. 1 Technical Corrigendum 1 to CCSDS 509.0-B-1, Issued February 2018*
17. *CCSDS 520.0-G-3 Mission Operations Services Concept*
18. *CCSDS 520.1-M-1 Mission Operations Reference Model*
19. *CCSDS 521.0-B-2 Mission Operations Message Abstraction Layer*
20. *CCSDS 521.1-B-1 Mission Operations Common Object Model*
21. *CCSDS 522.0-B-1 Mission Operations--Common Services*
22. *CCSDS 522.1-B-1 Mission Operations Monitor & Control Services*
23. *CCSDS 523.1-M-1 Mission Operations Message Abstraction Layer--JAVA API*
24. *CCSDS 523.2-M-1 Mission Operations Message Abstraction Layer--C++ API*
25. *CCSDS 524.1-B-1 Mission Operations--MAL Space Packet Transport Binding and Binary Encoding*
26. *CCSDS 524.2-B-1 Mission Operations--Message Abstraction Layer Binding to TCP/IP Transport and Split Binary Encoding*
27. *CCSDS 524.3-B-1 Mission Operations--Message Abstraction Layer Binding to HTTP Transport and XML Encoding*
28. *CCSDS 524.4-B-1 Mission Operations--Message Abstraction Layer Binding to ZMTP Transport*
29. *CCSDS 529.0-G-1 Mission Planning and Scheduling*
30. *CCSDS 540.0-G-1 Telerobotic Operations*
31. *CCSDS 551.1-O-2 Correlated Data Generation*
32. *CCSDS 610.0-G-5 Space Data Systems Operations with Standard Formatted Data Units: System and Implementation Aspects*
33. *CCSDS 620.0-B-2 Standard Formatted Data Units — Structure and Construction Rules*
34. *CCSDS 621.0-G-1 Standard Formatted Data Units — A Tutorial*
35. *CCSDS 622.0-B-1 Standard Formatted Data Units — Referencing Environment*
36. *CCSDS 630.0-B-1 Standard Formatted Data Units — Control Authority Procedures*
37. *CCSDS 631.0-G-2 Standard Formatted Data Units — Control Authority Procedures Tutorial.*

38. *CCSDS 632.0-B-1 Standard Formatted Data Units — Control Authority Data Structures*
39. *CCSDS 641.0-B-2 Parameter Value Language Specification (CCSD0006 and CCSD0008)*
40. *CCSDS 641.0-G-2 Parameter Value Language — A Tutorial*
41. *CCSDS 643.0-B-1 ASCII Encoded English (CCSD0002)*
42. *CCSDS 644.0-B-3 The Data Description Language EAST Specification (CCSD0010)*
43. *CCSDS 645.0-G-1 The Data Description Language EAST—A Tutorial*
44. *CCSDS 646.0-G-1 The Data Description Language EAST—List of Conventions*
45. *CCSDS 647.1-B-1 Data Entity Dictionary Specification Language (DEDSL)—Abstract Syntax (CCSD0011)*
46. *CCSDS 647.2-B-1 Data Entity Dictionary Specification Language (DEDSL)—PVL Syntax (CCSD0012)*
47. *CCSDS 647.3-B-1 Data Entity Dictionary Specification Language (DEDSL)—XML/DTD Syntax (CCSD0013)*
48. *CCSDS 647.4-O-1 Data Entity Dictionary Specification Language (DEDSL)--XML/XSD Syntax*
49. *CCSDS 650.0-M-2 Reference Model for an Open Archival Information System (OAIS)*
50. *CCSDS 651.0-M-1 Producer-Archive Interface Methodology Abstract Standard*
51. *CCSDS 651.1-B-1 Producer-Archive Interface Specification (PAIS)*
52. *CCSDS 651.2-G-1 Producer-Archive Interface Specification (PAIS)--A Tutorial*
53. *CCSDS 652.0-M-1 Audit and Certification of Trustworthy Digital Repositories*
54. *CCSDS 652.1-M-2 Requirements for Bodies Providing Audit and Certification of Candidate Trustworthy Digital Repositories*
55. *CCSDS 660.0-B-2 XML Telemetric and Command Exchange--Version 1.2*
56. *CCSDS 660.1-G-2 XML Telemetric and Command Exchange (XTCE)-Element Description*
57. *CCSDS 660.2-G-2 XML Telemetric and Command Exchange (XTCE)*

58. *CCSDS 661.0-B-1 XML Formatted Data Unit (XFDU) Structure and Construction Rules*

6.4.5 Area of System Engineering

1. *CCSDS 301.0-B-4 Time Code Formats*
2. *CCSDS 311.0-M-1 Reference Architecture for Space Data Systems*
3. *CCSDS 312.0-G-1 Reference Architecture for Space Information Management*
4. *CCSDS 313.0-Y-3 Space Assigned Numbers Authority (SANA)—Role, Responsibilities, Policies, and Procedures*
5. *CCSDS 313.1-Y-2 CCSDS SANA Registry Management Policy*
6. *CCSDS 313.2-Y-2 Procedures for SANA Registry Specification*
7. *CCSDS 315.1-Y-1 CCSDS URN Namespace Policy*
8. *CCSDS 320.0-M-7 CCSDS Spacecraft Identification Field Code Assignment Control Procedures*
9. *CCSDS 320.0-M-7 Cor. 1 Corrigendum 1 to CCSDS 320.0-M-7, Issued November 2017*
10. *CCSDS 350.0-G-3 The Application of Security to CCSDS Protocols*
11. *CCSDS 350.1-G-3 Security Threats against Space Missions*
12. *CCSDS 350.4-G-2 CCSDS Guide for Secure System Interconnection*
13. *CCSDS 350.6-G-1 Space Missions Key Management Concept*
14. *CCSDS 350.7-G-2 Security Guide for Mission Planners*
15. *CCSDS 350.8-M-2 Information Security Glossary of Terms*
16. *CCSDS 350.9-G-1 CCSDS Cryptographic Algorithms*
17. *CCSDS 351.0-M-1 Security Architecture for Space Data Systems*
18. *CCSDS 352.0-B-2 CCSDS Cryptographic Algorithms*
19. *CCSDS 356.0-B-1 Network Layer Security Adaptation Profile*
20. *CCSDS 357.0-B-1 CCSDS Authentication Credentials*
21. *CCSDS 371.0-G-1 Application and Support Layer Architecture*
22. *CCSDS 500.1-G-2 Delta-DOR--Technical Characteristics and Performance*

23. *CCSDS 506.0-M-2 Delta-Differential One Way Ranging (Delta-DOR) Operations*
24. *CCSDS 506.1-B-1 Delta-DOR Raw Data Exchange Format*
25. *CCSDS 506.3-M-1 Delta-DOR Quasar Catalog Update Procedure*
26. *CCSDS A13.1-Y-1 CCSDS Recommended Procedures for Cloud-Based Interoperability Testing*

6.4.6 Cross Support Services (CSS) Area

Cross Support Services (CSS) looks at how one organization makes space network resources available to another organization for "cross support." So, the goal of the CSS Area is to define what services are needed at different cross-support interface points and how organizations that want to work together to complete a mission can expose, plan, and use those services.

1. *CCSDS 901.0-G-1 Space Communications Cross Support--Architecture Description Document*
2. *CCSDS 901.1-M-1 Space Communications Cross Support--Architecture Requirements Document*
3. *CCSDS 902.0-G-1 Extensible Space Communication Cross Support--Service Management--Concept*
4. *CCSDS 902.1-B-1 Cross Support Service Management--Simple Schedule*
5. *CCSDS 902.1-B-1 Cor. 1 Technical Corrigendum 1 to CCSDS 902.1-B-1, Issued May 2018*
6. *CCSDS 902.12-M-1 Cross Support Service Management—Common Data Entities*
7. *CCSDS 902.13-M-1 Abstract Event Definition*
8. *CCSDS 902.2-B-1 Cross Support Service—Management Communications Planning Information Format*
9. *CCSDS 910.2-G-1 Standard Terminology, Conventions, and Methodology (TCM) for Defining Data Services*
10. *CCSDS 910.3-G-3 Cross Support Concept — Part 1: Space Link Extension*
11. *CCSDS 910.4-B-2 Cross Support Reference Model—Part 1: Space Link Extension Services*

12. *CCSDS 911.1-B-5 Space Link Extension-Return All Frames Service Specification*
13. *CCSDS 911.2-B-4 Space Link Extension-Return Channel Frames Service Specification*
14. *CCSDS 911.5-B-4 Space Link Extension-Return Operational Control Fields Service Specification*
15. *CCSDS 912.1-B-5 Space Link Extension-Forward CLTU Service Specification*
16. *CCSDS 912.11-O-1 Space Link Extension--Enhanced Forward CLTU Service*
17. *CCSDS 913.1-B-2 Space Link Extension--Internet Protocol for Transfer Services*
18. *CCSDS 914.0-M-2 Space Link Extension--Application Program Interface for Transfer Services--Core Specification*
19. *CCSDS 914.0-M-2 Cor. 1 Corrigendum 1 to 914.0-M-2, issued September 2015*
20. *CCSDS 914.1-G-1 Space Link Extension—Application Program Interface for Transfer Services—Summary of Concept and Rationale*
21. *CCSDS 914.2-G-2 Space Link Extension—Application Program Interface for Transfer Services—Application Programmer's Guide*
22. *CCSDS 915.1-M-2 Space Link Extension—Application Program Interface for Return All Frames Service*
23. *CCSDS 915.2-M-2 Space Link Extension—Application Program Interface for Return Channel Frames Service*
24. *CCSDS 915.5-M-2 Space Link Extension—Application Program Interface for Return Operational Control Fields Service*
25. *CCSDS 916.1-M-2 Space Link Extension—Application Program Interface for the Forward CLTU Service*
26. *CCSDS 916.3-M-2 Space Link Extension—Application Program Interface for the Forward Space Packet Service*
27. *CCSDS 920.0-G-1 Cross Support Transfer Service Specification Framework*
28. *CCSDS 921.1-B-2 Cross Support Transfer Service—Specification Framework*
29. *CCSDS 921.2-M-1 Guidelines for the Specification of Cross Support Transfer Services*

30. *CCSDS 921.2-M-1 Cor. 1 Technical Corrigendum 1 to CCSDS 921.2-M-1, Issued March 2019*
31. *CCSDS 922.1-B-2 Cross Support Transfer Services—Monitored Data Service*
32. *CCSDS 922.2-B-2 Cross Support Transfer Service-Tracking Data Service*
33. *CCSDS 922.27-O-1 Cross Support Transfer Service-Return CFDP PDU Service*
34. *CCSDS 922.3-B-1 Cross Support Transfer Service—Forward Frame Service*
35. *CCSDS 927.1-B-1 Terrestrial Generic File Transfer*

6.4.7 Space Link Services Area

1. *CCSDS 120.0-G-4 Lossless Data Compression*
2. *CCSDS 120.1-G-3 Image Data Compression*
3. *CCSDS 120.2-G-2 Low-Complexity Lossless and Near-Lossless Multispectral and Hyperspectral Image Compression*
4. *CCSDS 120.3-G-1 Spectral Pre-Processing Transform for Multispectral & Hyperspectral Image Compression*
5. *CCSDS 121.0-B-3 Lossless Data Compression*
6. *CCSDS 122.0-B-2 Image Data Compression*
7. *CCSDS 122.1-B-1 Spectral Preprocessing Transform for Multispectral and Hyperspectral Image Compression*
8. *CCSDS 123.0-B-2 Low-Complexity Lossless and Near-Lossless Multispectral and Hyperspectral Image Compression*
9. *CCSDS 123.0-B-2 Cor. 1 Technical Corrigendum 1 to CCSDS 123.0-B-2, Issued February 2019*
10. *CCSDS 123.0-B-2 Cor. 2 Technical Corrigendum 2 to CCSDS 123.0-B-2, Issued February 2019*
11. *CCSDS 123.0-B-2 Cor. 3 Technical Corrigendum 3 to CCSDS 123.0-B-2, Issued February 2019*
12. *CCSDS 124.0-B-1 Robust Compression of Fixed-Length Housekeeping Data*
13. *CCSDS 130.0-G-4 Overview of Space Communications Protocols*

14. *CCSDS 130.1-G-3 TM Synchronization and Channel Coding - Summary of Concept and Rationale*
15. *CCSDS 130.11-G-2 SCCC-Summary of Definition and Performance*
16. *CCSDS 130.12-G-2 CCSDS Protocols over DVB-S2-Summary of Definition, Implementation, and Performance*
17. *CCSDS 130.2-G-3 Space Data Link Protocols--Summary of Concept and Rationale*
18. *CCSDS 130.3-G-1 Space Packet Protocols*
19. *CCSDS 131.0-B-4 TM Synchronization and Channel Coding*
20. *CCSDS 131.2-B-2 Flexible Advanced Coding and Modulation Scheme for High Rate Telemetry Applications*
21. *CCSDS 131.21-O-1 Serially Concatenated Convolutional Codes—Extension (SCCC-X)*
22. *CCSDS 131.21-O-1 Cor. 1 Technical Corrigendum to CCSDS 131.21-O-1, Issued May 2021*
23. *CCSDS 131.3-B-2 CCSDS Space Link Protocols over ETSI DVB-S2 Standard*
24. *CCSDS 131.31-O-1 CCSDS Space Link Protocols over ETSI DVB-S2X Standard*
25. *CCSDS 131.31-O-1 Cor. 1 Technical Corrigendum to CCSDS 131.31-O-1, Issued September 2021*
26. *CCSDS 131.5-O-1 Erasure Correcting Codes for Use in Near-Earth and Deep-Space Communications*
27. *CCSDS 132.0-B-3 TM Space Data Link Protocol*
28. *CCSDS 133.0-B-2 Space Packet Protocol*
29. *CCSDS 133.1-B-3 Encapsulation Packet Protocol*
30. *CCSDS 140.1-G-1 Real-Time Weather and Atmospheric Characterization Data*
31. *CCSDS 141.0-B-1 Optical Communications Physical Layer*
32. *CCSDS 141.1-M-1 Atmospheric Characterization and Forecasting for Optical Link Operations*
33. *CCSDS 141.10-O-1 Optical High Data Rate (HDR) Communication-1550 NM*
34. *CCSDS 141.11-O-1 Optical High Data Rate (HDR) Communication--1064 NM*
35. *CCSDS 142.0-B-1 Optical Communications Coding and Synchronization*

36. *CCSDS 200.0-G-6 Telecommand Summary of Concept and Rationale*
37. *CCSDS 210.0-G-2 Proximity-1 Space Link Protocol--Rationale, Architecture, and Scenarios*
38. *CCSDS 211.0-B-6 Proximity-1 Space Link Protocol-Data Link Layer*
39. *CCSDS 211.1-B-4 Proximity-1 Space Link Protocol--Physical Layer*
40. *CCSDS 211.2-B-3 Proximity-1 Space Link Protocol--Coding and Synchronization Sublayer*
41. *CCSDS 230.1-G-3 TC Synchronization and Channel Coding—Summary of Concept and Rationale*
42. *CCSDS 230.2-G-1 Next Generation Uplink*
43. *CCSDS 231.0-B-4 TC Synchronization and Channel Coding*
44. *CCSDS 232.0-B-4 TC Space Data Link Protocol*
45. *CCSDS 232.1-B-2 Communications Operation Procedure-1*
46. *CCSDS 232.1-B-2 Cor. 1 Technical Corrigendum 1 to CCSDS 232.1-B-2, Issued September 2010*
47. *CCSDS 350.5-G-1 Space Data Link Security Protocol--Summary of Concept and Rationale*
48. *CCSDS 355.0-B-2 Space Data Link Security Protocol*
49. *CCSDS 355.1-B-1 Space Data Link Security Protocol--Extended Procedures*
50. *CCSDS 401.0-B-32 Radio Frequency and Modulation Systems—Part 1: Earth Stations and Spacecraft*
51. *CCSDS 413.0-G-3 Bandwidth-Efficient Modulations--Summary of Definition, Implementation, and Performance*
52. *CCSDS 413.1-G-2 Simultaneous Transmission of GMSK Telemetry and PN Ranging*
53. *CCSDS 414.0-G-2 Pseudo-Noise (PN) Ranging Systems*
54. *CCSDS 414.1-B-3 Pseudo-Noise (PN) Ranging Systems*
55. *CCSDS 415.0-G-1 Data Transmission and PN Ranging for 2 GHz CDMA Link via Data Relay Satellite*
56. *CCSDS 415.1-B-1 Data Transmission and PN Ranging for 2 GHz CDMA Link via Data Relay Satellite*
57. *CCSDS 421.0-G-1 Report of the Proceedings of the RF and Modulation Subpanel Meeting at the Ames Research Center, April 11-20, 1989*
58. *CCSDS 431.1-B-1 Variable Coded Modulation Protocol*

59. *CCSDS 431.1-B-1 Cor. 1 Technical Corrigendum 1 to CCSDS 431.1-B-1, Issued February 2021*
60. *CCSDS 700.0-G-3 Advanced Orbiting Systems, Networks and Data Links: Summary of Concept, Rationale and Performance*
61. *CCSDS 700.1-G-1 Overview of the Unified Space Data Link Protocol*
62. *CCSDS 732.0-B-4 AOS Space Data Link Protocol*
63. *CCSDS 732.1-B-2 Unified Space Data Link Protocol*
64. *CCSDS B20.0-Y-1 Proceedings of the CCSDS RF and Modulation Subpanel 1E Meeting at the German Space Operations Centre September 20-24, 1993*
65. *CCSDS B20.0-Y-2 Proceedings of the CCSDS RF and Modulation Subpanel 1E on Bandwidth-Efficient Modulations*

MATLAB examples

A. Communications in Space with the use of MATLAB

1. Satellite Communication Link Design:

The initial step is determining if satellites can establish communication with each other or ground stations, emphasizing the importance of orbit propagation, satellite-ground station visibility, and communication link analysis.

2. Link Budget Analysis:

Once satellite positions are confirmed and communication links are feasible, a detailed link budget analysis is undertaken. While Excel is a common tool, it lacks graphical capabilities and poses challenges in sharing designs among teams or organizations.

3. Waveform Design:

Upon confirming viable links through budget analysis, waveforms for specific standards are designed. This involves generating waveforms and conducting end-to-end simulations.

4. Accessing Satellite Data:

Building ground stations is costly and labor-intensive. New services, such as Amazon Web Services ground station, offer an alternative by allowing users to interface with satellites and extract data without establishing their own expensive ground stations.

5. System Workflows and Standards:

It's crucial that satellite communication (satcom) systems support emerging application areas and have the flexibility to adapt. This involves integrating models throughout the development lifecycle, emphasizing code generation and in-the-loop simulations. A key challenge is adhering to evolving international standards, vital due to rising global collaborations and increasing system complexity. Standards ensure the safety, reliability, and quality of contributions from various developers.

6. Integration with Onboard Systems:

Beyond communication, integrating satcom with other onboard satellite systems is crucial. The necessity for high fidelity simulations varies depending on the development phase. MATLAB and Simulink facilitate subsystem development and integration, which is especially valuable given the tightening budgets in contemporary satellite programs.

7. Orbit Visualization and Link Analysis with MATLAB:

MATLAB enables users to define satellites with orbital elements and attach antennas to transmitters or receivers, pointing them towards fixed Earth points. This can be visualized in both 2D and 3D, showing fields of view and when links are operational. An example showcased a multi-hop satellite communication link between India and Australia using two satellites, highlighting the times data can be transferred between the two ground stations.

8. Simulating Large Constellations:

With companies launching numerous satellites for global cell coverage, swift simulation of these vast constellations is vital. MATLAB provides capabilities to visualize these constellations efficiently and to determine paths through them between two ground stations.

A significant challenge in the industry is the lack of a standard link budget format. This inconsistency makes exchanging information between teams problematic. The link budget analyzer app offers customization to address this issue. Modern satellite communication systems frequently use cross-links for global coverage. This app supports multi-hop links, allowing users to analyze each link in the chain.

Some challenges during designing wireless communication systems for space applications are the:

- High Complexity: Space systems have to cover long distances (leading to significant path loss) with limited power, resulting in a low signal-to-noise ratio. The movement of many space systems can lead to higher Doppler shifts.
- Implementation: Systems in space often operate on low power and require standalone embedded device implementations, like FPGAs or GPUs. Hand coding and verifying these can be challenging and time-consuming.
- Testing: Testing systems in space is not practical for most projects. Relying solely on over-the-air testing can uncover multi-subsystem issues too late, increasing the importance of simulations.

Impacts of the Challenges: Due to the interactivity of subsystems in complex space communications systems, several design iterations might be necessary, leading to delays and higher costs. Hand coding can introduce errors, which, if discovered late, can be costly and time-consuming to fix.

Debugging and verification, especially for hand-coded systems, consume a lot of time. Testing is paramount, and late-stage errors can be expensive to remedy. The statistics in 2020 gave that 68% of FPGA projects were delayed, with over half the project time spent on verification. The solution is to use a Unified Wireless Design Platform.

To address these challenges, a unified wireless design platform can provide the tools needed for the efficient design, implementation, and testing of satellite communication systems.

Simulink as a Unified Design Platform: allows multi-domain simulation for all subsystems. This enables exploration of design options, risk reduction, performance enhancement, or cost-saving solutions. Using automatic code generation, the development time can be significantly reduced. Continuous testing and verification help in identifying design problems early, saving time and money. Simulink enables multi-domain simulations, which facilitates cross-domain optimizations. It supports automatic code generation from models for prototyping and implementation.With Simulink, all communication subsystem models are on one platform, promoting easy handling, testing, integration, and collaboration.

Benefits of Using Simulink:

1. Simplified Collaboration: With everything in one platform, sharing and collaboration become more efficient, preventing confusion from missing documentation.

2. Automatic Code Generation: Allows engineers to focus on algorithm and structure design. Additionally, it supports continuous testing to identify design issues early.

3. Saves Time and Money: Reduces design iterations and streamlines the design-to-implementation process.

4. Multi-domain Simulation: Demonstrates a multi-domain simulation model including models for antenna array, RF, and digital signal processing algorithms. It showcases the effectiveness of beamforming for custom antenna arrays.

Making a Wireless System Architecture:

1. Design challenges in allocating power gain budgets across a system and the importance of considering the system as a whole for optimal design.
2. Highlight the role of multi-domain simulation in managing complexity and optimizing designs.

Building a Multi-domain Simulation:

1. Antenna Modeling: Using the antenna designer app, users can select from built-in models or create custom ones. The radiation patterns can be incorporated into simulation models.

2. RF Design: The RF budget analyzer app provides a platform for basic architecture layouts. Users can define parameters like gain, noise figure, and more, either from their own designs or manufacturer datasheets.

3. Baseband System: There are functions available to model RF impairments and Doppler shifts in the digital domain, as well as for compensating these impairments.

Implementation:

- The multi-domain simulation model can be used in prototyping and implementation through automatic code generation.
- The model can directly communicate with RF test equipment and software-defined radio platforms to support rapid prototyping.

Concluding Remarks:

- MATLAB and Simulink offer a comprehensive environment to build simulations for all communication subsystems.
- Users can significantly cut down development time via automatic code generation.
- Continuous testing ensures early problem detection, saving both money and project time.
- Resources, training courses, white papers, videos, and consulting services are available to assist users.

B. Satellite scenario modeling and satcom simulation using MATLAB Satcom Toolbox.

Satcom Design Challenges:

- Determining of the type of satellite constellation and orbit (e.g., polar, equatorial, circular).
- Assessing visibility and link analyses, crucial initial stages.
- Conducting power budget analyses: considering factors like antenna sizes, HPA powers, back offs, and digital pre-distortion.
- Designing waveforms and transceivers with considerations for RF or optical communications and carrier tracking loops.
- Navigating the array of satcom standards, including DVB-S, 5G, various satnav standards like GPS, Galileo, and GLONASS, and the CCSDS for telecommand and telemetry.

1. Scenario Construction:

To simulate satellite communication scenarios, demonstrating how to set up ground stations, model an aircraft's path, incorporate a satellite constellation, and analyze communication links.

- A simulation scenario is initiated by defining a start time, stop time, and sample time.
- A viewer is created to visualize the simulation

2. Ground Stations Creation:

- Two airports, JFK in New York City and LF Wade International in Bermuda, are defined using their latitude and longitude.
- These airports are designated as ground stations, and this pattern of coding is frequently repeated.

3. Aircraft Path Modeling:

- An aircraft's path between JFK and Bermuda is mapped out using simple latitude and longitude values.

- A geo trajectory is then generated, which automatically adjusts the pitch and roll (orientation) of the aircraft.
- The position and orientation of the aircraft over its flight path are calculated and prepared in a timetable format for integration into the satellite scenario.

4. Aircraft Integration:

- The aircraft is represented as a "satellite" and added to the scenario. Its orientation is adjusted using a north, east, and down coordinate frame.

5. Satellite Constellation Addition:

- The Iridium satellite constellation, consisting of six orbital planes with 11 satellites each, is added.
- Conical sensors are incorporated for visibility analysis, determining which satellites can "see" the ground stations or aircraft.

6. Visibility Analysis:

- The satellites' visibility to both JFK and LF Wade is calculated.
- The aircraft's visibility from the satellites is visualized, ensuring there's always at least one satellite in view throughout the simulation.

7. Link Analysis:

- A transmitter is set up on the aircraft by specifying its output power and frequency.
- Receivers are created with antennas; the Iridium satellites are given a custom
  48-beam antenna to represent their 48 different spot beams.
- The link between the aircraft and satellites is established and analyzed over time.
- Link quality, represented by EBN 0, is evaluated, noting how it decreases as the
  aircraft moves away from the airport and must rely on satellite communication.

8. Link Margin Analysis:

- The link margin deteriorates but remains positive.
- When an aircraft is in sight of Bermuda, it directly communicates with the airport, and the link margin improves as it nears the airport.

9. Iridium Satellites:

- Multiple Iridium satellites have an antenna pattern resembling jellyfish.
- Solid green lines signify a complete connection.

The Iridium satellite constellation offers voice and data services, including L band coverage for satellite phones, two-way satellite messaging for Android smartphones, and communication devices across the entire globe. Owned and operated by Iridium Communications, the system also markets its services and equipment. The idea was initiated by Bary Bertiger, Raymond J. Leopold, and Ken Peterson in the late 1980s, and Motorola developed it between 1993 and 1998, after which it became operational and open for commercial use. The system comprises 66 active satellites, ensuring worldwide coverage, and additional reserves in case of malfunctions. Positioned in low Earth orbit at about 781 kilometers and inclined at 86.4°, their near-polar route and inter-satellite communication guarantee uninterrupted service, including hard-to-reach places like poles and oceans, irrespective of ground station locations.

10. Link Budget Analysis:

- While many use Excel for link budgets, MathWorks offers an app for this purpose.
- The app enables analysis of up, down, and cross-links and can be customized.
- Users can create custom plots and export MATLAB scripts from an analysis for various testing, including parameter sensitivity sweeps.
- The app offers a feature for easy availability analysis, including modeling specific losses.

11. Waveform Generation:

- The toolbox supports a wide range of standards including DVB-S2, RCS2, and optical communications.
- The block diagram highlights processing at both the bit and waveform level.
- Generation of waveforms for optical and GPS communications is discussed.
- For CCSDS RF waveform generation, all coding and modulation schemes are covered.

12. End-to-End Link Simulation:

- The foundation of waveform simulation is the channel model.
- The p dot 618 model calculates various parameters, including Earth-space propagation losses.
- Channels can also be modeled that filter signals at the waveform level, like the simplified Rician channel.
- Optical communications can model a deep space optical Poisson channel.
- The Satcom Toolbox is open MATLAB code, allowing users to understand, debug, and customize the algorithms.

13. 5G NTN (Non-Terrestrial Networks):

- Satellite communications play a significant role in 5G and will be even more prominent in 6G.
- A 3GPP 38.811 channel is set up, with Doppler shift added due to satellite movement.
- An example demonstrates throughput as a function of SNR, all open in MATLAB code.

14. GPS Simulation:

- A comprehensive example of GPS starts with satellites in orbit and their downlink waveforms.
- It incorporates different delays, signal aggregation, synchronization, decoding, and position estimation.

15. Live Satellite Data Access:

- AWS Ground Station offers a "ground station as a service" for users needing live satellite data.
- MATLAB offers an example and APIs for accessing this data, which can be utilized for various applications, from receiver verification to satellite control.

16. Conclusion:

The Satcom Toolbox provides:

- Orbit propagation and visualization capabilities.
- An app for static link budgets that can be dynamically adjusted.
- Support for various standards for waveform generation and receiver designs.
- Extensive analysis capabilities, including bit error rate calculations and throughput calculations.

Here is the pdf file of presentation by Mike McLernon, Principal Technical Marketing Manager, Wireless Communications MathWorks:
chrome-extension://efaidnbmnnnibpcajpcglclefindmkaj/https://www.mathworks.com/content/dam/mathworks/mathworks-dot-com/company/events/webinar-cta/3999200-Presentation.pdf

C. How to evaluate the link budget for optical inter-satellite communication, as well as uplink and downlink with the use of satellite communication tool.

Optical satellite communication offers benefits like broader bandwidth, no need for licensing, faster data transfer, and reduced energy use compared to satellite communication using radio frequency. In this scenario, the link budget assessment for both uplink and downlink takes into account atmospheric influences, such as absorption and scattering.

Given Parameters:

The performance of an optical communication system is commonly evaluated in terms of link margin. A positive link margin indicates that the link has enough power to overcome the attenuation. A negative link margin indicates that the received signal is too weak to function properly. To compute the link margin in dB, use this equation:

$$LM = Prx - Preq$$

where:

- Prx is the received signal power in dBm.
- $Preq$ is the required signal power to achieve a specific bit error rate (BER) at a given data rate in dBm.

This example considers the receiver sensitivity as —35.5 dBm for on-off keying modulation with a 10 Gbps data rate and 10^{-12} BER, as defined in the following paper:

Liang, Jintao, Aizaz U. Chaudhry, Eylem Erdogan, and Halim Yanikomeroglu. “Link Budget Analysis for Free-Space Optical Satellite Networks.” In *2022 IEEE 23rd International Symposium on a World of Wireless, Mobile and Multimedia Networks (WoWMoM)*, 471–76. Belfast, United Kingdom: IEEE, 2022. https://doi.org/10.1109/WoWMoM54355.2022.00073.

```
Preq = -35.5; % Required signal power in dBm
Ptx = 17.5;   % Transmitted power in dBm

% Configure the ground station, satellites, and link
characteristics
% Set the ground station characteristics with parabolic
telescope
gs = struct;
gs.Height = 1;                % Height above the mean sea
level in km
gs.OpticsEfficiency = 0.8;    % Optical antenna efficiency
gs.ApertureDiameter = 1;      % Antenna aperture diameter in m
gs.PointingError = 1e-6;      % Pointing error in rad

% Set the satellite A characteristics with parabolic telescope
satA = struct;
satA.Height = 550;            % Height above the mean sea
level in km
satA.OpticsEfficiency = 0.8;  % Optical antenna efficiency
satA.ApertureDiameter = 0.07; % Antenna aperture diameter in m
satA.PointingError = 1e-6;    % Pointing error in rad

% Set the satellite B characteristics with parabolic telescope
satB = struct;
satB.OpticsEfficiency = 0.8;  % Optical antenna efficiency
satB.ApertureDiameter = 0.06; % Antenna aperture diameter in m
satB.PointingError = 1e-6;    % Pointing error in rad

% Set the link characteristics
link = struct;
link.Wavelength = 1550e-9;    % m
link.TroposphereHeight = 20;  % km (Typically ranges from 6-20
km)
```

```
link.ElevationAngle = 50;      % degrees
link.SatDistance = 1000;       % Distance between satellites in
km
link.Type = downlink;
% "downlink"|"inter-satellite"|"uplink"
% When the Type field is set to "uplink" or "downlink", you
must specify
% the CloudType field, as defined in [5] table 1
link.CloudType = Thin cirrus;
```

Analyze Link Budget

Assess the link budget for communication through the optical inter-satellite link, uplink, or downlink, based on the 'Type' field value in the link structure. When considering uplink and downlink, the optical link exists between the ground station and satellite A. Meanwhile, the inter-satellite link is established between satellite A and satellite B. This example, by default, computes the link budget for the downlink.

```
if link.Type=="downlink"
    % satellite A to ground station
    tx = satA;
    rx = gs;
elseif link.Type=="uplink"
    % Ground station to satellite A
    tx = gs;
    rx = satA;
else % "inter-satellite"
    % satellite A to satellite B
    tx = satA;
    rx = satB;
end
```

Link Budget for Inter-Satellite Link

An optical inter-satellite link is the link between two satellites. In this case, satellite A and satellite B. The propagation medium is the vacuum of space. To compute the received power for an optical inter-satellite link in dB, use this equation:

$$Prx = Ptx + OEtx + OErx + Gtx + Grx - LPtx - LPrx - LPS$$

where:

- Pt is the transmitted power in dBm.
- $OEtx$ is the transmitter optical efficiency in dB.
- $OErx$ is the receiver optical efficiency in dB.
- Gtx is the transmitter gain in dB.
- Grx is the receiver gain in dB.
- $LP\text{tx}$ is the transmitter pointing loss in dB.
- $LP\text{rx}$ is the receiver pointing loss in dB.
- LPS is the free-space path loss between the two satellites in dB.

Transmitter and receiver pointing loss, as defined in paper above :

$$LPtx = 4.3429 \times gtx \times (Petx)^2$$

$$LPrx = 4.3429 \times grx \times (Perx)^2$$

where:

- $Petx$ is the transmitter pointing error in radians.
- gtx is the transmitter linear gain.
- $Perx$ is the transmitter pointing error in radians.
- grx is the receiver linear gain.

Transmitter and receiver gain in dB, is

$Gtx = 10 \times log10(gtx)$,

$Grx = 10 \times log10\ (grx)$,

To calculate grx and gtx we can use the following equations, as defined also in ITU-R S.1590,

$gtx = (\pi dtx / \lambda)^2$

$grx = (\pi drx / \lambda)^2$

where:

- λ is the wavelength in m.
- dtx is the diameter of the primary aperture of the transmitter antenna in m.
- drx is the diameter of the primary aperture of the receiver antenna in m.

```
% Calculate transmitter and receiver gain

txGain = (pi*tx.ApertureDiameter/link.Wavelength)^2;

Gtx = 10*log10(txGain); % in dB

rxGain = (pi*rx.ApertureDiameter/link.Wavelength)^2;

Grx = 10*log10(rxGain); % in dB


% Calculate transmitter and receiver pointing loss in dB

txPointingLoss = 4.3429*(txGain*(tx.PointingError)^2);

rxPointingLoss = 4.3429*(rxGain*(rx.PointingError)^2);


% Calculate link margin for inter-satellite link in dB

if link.Type=="inter-satellite"
```

```
  % Free-space path loss between satellites in dB

    pathLoss = fspl(link.SatDistance*1e3,link.Wavelength);

    linkMargin = Ptx + 10*log10(tx.OpticsEfficiency) +
10*log10(rx.OpticsEfficiency) + ...

        Gtx + Grx - txPointingLoss - rxPointingLoss - pathLoss
- Preq;

    disp("Link margin for inter-satellite link is
"+num2str(linkMargin)+" dB")

end
```

Link Budget for Uplink and Downlink

For an optical uplink and downlink, the optical beams go through the atmosphere causing attenuation due to absorption and scattering. To compute the received power for an optical uplink or downlink in dB, use this equation:

$$Pr = Ptx + OEtx + OErx + Gtx + Grx - LPtx - LPrx - LPG - Labs - Lsca,$$

where:

- LPG is the free-space path loss between the ground station and satellite in dB.
- $Labs$ is the atmospheric attenuation loss due to absorption in dB.
- $Lsca$ is the atmospheric attenuation loss due to scattering in dB.

Free-space path loss, as defined in ITU-R S.1590

$$LPG = 20 \times log10(\lambda / 4\pi d_{GS}),$$

where $d\mathrm{GS}$ is the distance between the ground station and satellite.

To compute the distance between the ground station and satellite, use these equations:

$$dGS = -R\,sin(\theta E) + \sqrt{(R\,sin(\theta E))^2 + H^2 + 2RH}$$

$$R = RE + hG$$

$$H = hS - hGS$$

where:

- RE is the radius of the Earth in km.
- hS is the height of the satellite in km.
- $h\mathrm{GS}$ is the height of the ground station in km.
- θE is the elevation angle in degrees.

Atmospheric Attenuation for Uplink and Downlink

The presence of atmospheric molecules and aerosols impacts the propagation of free-space optics due to absorption and scattering. The atmosphere's absorptive properties above 10 THz are conducive for transmission. In this instance, a 1550 nm wavelength, known for its minimal absorption features as outlined in ITU-R P.1621-2 , is taken into account. An absorption loss of 0.01 dB is factored into this example

Get

```
absorptionLoss = 0.01; % Absorption loss in dB
```

Atmospheric scattering is brought about by the presence of aerosol particles and water droplets in the transmission route. Such scattering diverts the transmitted energy off its intended course. This deviation leads to a perceived decline in the signal's strength when it reaches the receiver. The overall loss from scattering is measured in dB.

$$Lsca = Lgeo + Lmie$$

where:

- $L\mathrm{geo}$ is the attenuation due to geometrical scattering in dB.
- $L\mathrm{mie}$ is the attenuation due to Mie scattering in dB.

Geometrical scattering is triggered by phenomena like fog or thick clouds. It happens when particles in the transmission path are considerably larger than the wavelength of the signal. The decrease in signal strength because of this type of scattering, measured in dB, is determined using the Beers-Lambert law, as outlined in the paper.

$$Lgeo = 4.3429 \times Ageo \times dT$$

where:

- $Ageo$ is the attenuation coefficient due to geometrical scattering.
- dT is the distance of the optical beam that propagates through the troposphere layer of the atmosphere.

To compute the attenuation coefficient due to geometrical scattering, use this equation:

$$Ageo=3.91/V\times(\lambda/550)^{-\delta}$$

where:

- V is the visibility in km.
- δ is the particle size coefficient.

Mie scattering results from light dispersion by aerosols. This type of scattering is evident when the size of the particles in the transmission path matches the signal wavelength and is predominantly observed in the lower atmospheric layers. The reduction in signal strength due to Mie scattering, measured in dB, is detailed in ITU-R P.1622-1 Section 3.1.

$$L\text{mie} = 4.3429\times\text{ERmie} / \sin(\theta E)$$

where ERmie is the extinction ratio for Mie scattering.

To calculate the Mie scattering extinction ratio, use this equation:

$$\text{ERmie} = a\,h\text{GS}^3 + b\,h\text{GS}^2 + c\,h\text{GS} + d,$$

where:

- $a = 0.000487\lambda^3 - 0.002237\lambda^2 + 0.003864\lambda - 0.004442$
- $b = -0.00573\lambda^3 + 0.02639\lambda^2 - 0.04552\lambda + 0.05164$
- $c = 0.02565\lambda^3 - 0.1191\lambda^2 + 0.20385\lambda - 0.216$
- $d = -0.0638\lambda^3 + 0.3034\lambda^2 - 0.5083\lambda + 0.425$

- This technique is suitable for ground stations situated at altitudes ranging from 0 to 5 km above sea level and for wavelengths between 800 and 2000 nm. The accuracy of this method is roughly 0.1 dB when the elevation angle exceeds 45º.

```
% Calculate link margin for uplink or downlink

if (link.Type=="uplink") || (link.Type=="downlink")


    % Calculate the distance of the optical beam that propagates through

  % the troposphere layer of the atmosphere in km

                    dT     =     (link.TroposphereHeight     -
gs.Height).*cscd(link.ElevationAngle);


    % Calculate the slant distance for uplink and downlink between

  % satellite A and the ground station for circular orbit in km

    re = physconst('EarthRadius')/1e3; % Radius of Earth in km

    r = re + gs.Height;

    h = satA.Height - gs.Height;

    dGS = -r*sind(link.ElevationAngle) + ...

        sqrt((r*sind(link.ElevationAngle)).^2 + h*h + 2*r*h);
```

% Calculate free-space path loss between the ground station and

% satellite in dB

```
    pathLoss = fspl(dGS*1e3,link.Wavelength);
```

% Calculate loss due to geometrical scattering

% cnc - cloud number concentration in cm-3

% lwc - Liquid water content in g/m-3

```
    [cnc,lwc] = getCloudParameters(link.CloudType);

    visibility = 1.002/((lwc*cnc)^0.6473);                    %
Calculate visibility in km
```

% Get particle size related coefficient

```
    if visibility<=0.5

        delta = 0;

    elseif visibility>0.5 && visibility<=1

        delta = visibility - 0.5;

    elseif visibility>1 && visibility<=6

        delta = 0.16*visibility + 0.34;

    elseif visibility>=6 && visibility<=50

        delta = 1.3;
```

```
    else                                                    %
visibility>50
        delta = 1.6;
    end
    geoCoeff = (3.91/visibility)* ...
         ((link.Wavelength*1e9/550)^-delta);                %
Extinction coefficient
    geoScaLoss = 4.3429*geoCoeff*dT;                        %
Geometrical scattering loss in dB
```

% Calculate loss due to Mie scattering

```
    lambda_mu = link.Wavelength*1e6;                        %
Wavelength in microns
```

% Calculate empirical coefficients

```
     a = (0.000487*(lambda_mu^3)) - (0.002237*(lambda_mu^2)) +
...
        (0.003864*lambda_mu) - 0.004442;
     b = (-0.00573*(lambda_mu^3)) + (0.02639*(lambda_mu^2)) -
...
        (0.04552*lambda_mu) + 0.05164;
    c = (0.02565*(lambda_mu^3)) - (0.1191*(lambda_mu^2)) + ...
        (0.20385*lambda_mu) - 0.216;
    d = (-0.0638*(lambda_mu^3)) + (0.3034*(lambda_mu^2)) - ...
```

```
        (0.5083*lambda_mu) + 0.425;

    mieER = a*(gs.Height^3) + b*(gs.Height^2) + ...

    c*(gs.Height) + d;                                          %
Extinction ratio

    mieScaLoss = (4.3429*mieER)./sind(link.ElevationAngle);   %
Mie scattering loss in dB
```

% Calculate link margin for uplink or downlink in dB

```
    linkMargin = Ptx + 10*log10(tx.OpticsEfficiency) + ...

        10*log10(rx.OpticsEfficiency) + Gtx + Grx - ...

        txPointingLoss - rxPointingLoss - pathLoss - ...

        absorptionLoss - geoScaLoss - mieScaLoss - Preq;

          disp("Link  margin  for  "+num2str(link.Type)+"  is
"+num2str(linkMargin)+" dB")

end
```

This figure will be plotted will give the elevation angle versus and the link margin for this example with `Ptx` = 11 dBm, and the `ElevationAngle` field of the `link` structure varying from 45 to 90 degrees. The link margin increases with the increase in the elevation angle.

<u>It is interest to run this with the following variations:</u>

- link margin for uplink and inter-satellite link.

- link margin and geometrical scattering loss for different cloud types.
- link margin by varying any property of the ground station, satellite, or link.

The same process can be used for e.g a Mars or Venus case hypothetically scenario.

D. Orbit Mean-Elements Message (OMM) File (with the use of Satellite Communications Toolbox)

Assuming we work with satellite communications, need to input data into the Satellite Communications Software.

The Matlab software is compatible with the Orbit Mean-Elements Message (OMM) format. OMM is a subset of the Orbit Data Messages (ODM) standard, formulated by the esteemed Consultative Committee for Space Data Systems (CCSDS). Through OMM, we can easily extract general perturbation (GP) information using standard search methods.

To obtain these OMM files, we should visit the Space Track and CelesTrak websites.

The software accepts OMM files in both XML and JSON formats, however, only specific fields of the OMM file are utilized by the software, while the others are overlooked. Let's first understand the file format and check out additional details on Orbit Data Messages provided by CelesTrak®.

This is how it seems a format of data:

Predicate	Description	Examples
OBJECT_NAME	Satellite names.	Satellite1
MEAN_ELEMENT_THEORY	Mean element theory. This value must be SGP4.	SGP4
EPOCH	Mean Keplerian elements epoch.	2021-10-05T11:17:33
MEAN_MOTION	Mean motion (rev/day).	365
ECCENTRICITY	Eccentricity.	0007976
INCLINATION	Inclination, in degrees.	51.6335
RA_OF_ASC_NODE	Right ascension of ascending node, in degrees.	344.7760
ARG_OF_PERICENTER	Pericenter argument, in degrees.	283.067
MEAN_ANOMALY	Mean anomaly, in degrees.	325.9359
NORAD_CAT_ID	NORAD catalog number (satellite number).	Integer
BSTAR	SGP/SGP4 drag-like coefficient in 1/Earth radii.	16538-3

The Satellite Communications Toolbox can simulate and visually represent satellites as they orbit Earth or any other celestial body, calculate their interaction with ground-based stations, and scrutinize the communication connections they form.

Understanding Coordinate Systems in the exercise scenario:

1. Geodetic Coordinate Basics

Geodetic systems utilize coordinates, namely latitude (lat), longitude (lon), and height (h), to pinpoint a location with respect to an ellipsoid reference. Within satellite scenarios, the World Geodetic System from 1984 (WGS 84) is the go-to ellipsoid.

The starting point of WGS 84 aligns with Earth's gravitational center. Latitude starts from the equator, ranging between -90° to 90°, with positive values indicating northern locations. Longitude begins at the central meridian, and its values can range between -180° to 180° or 0° to 360°. Height in this system is gauged using the standard spheroid's normal.

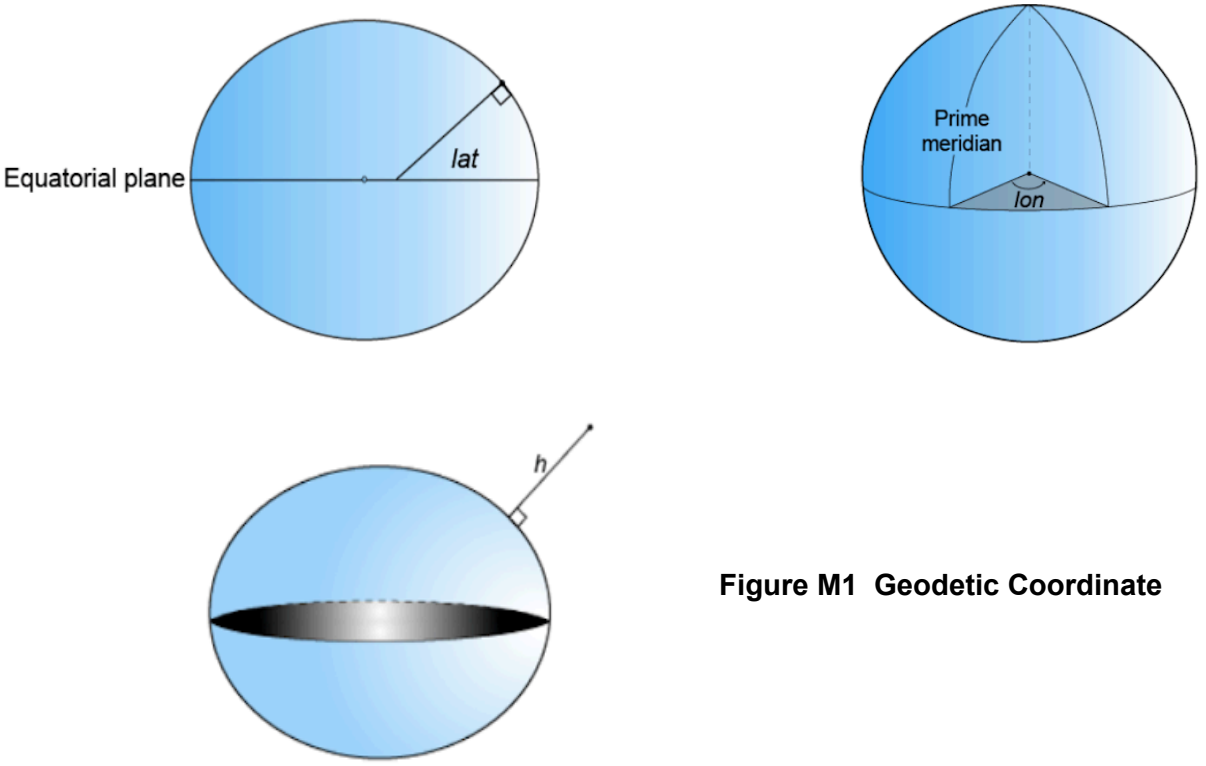

Figure M1 Geodetic Coordinate

2. Earth-Centered Coordinates (or any celestial body's coordinates)

The Earth-Centered Earth-Fixed (ECEF) approach employs Cartesian coordinates:
X, Y, and Z, signifying positions with respect to the ellipsoid's core. This scenario employs the WGS 84 ellipsoid, whose core aligns with Earth's gravitational center. The X, Y, and Z axes intersect the ellipsoid surface at specific latitudes and longitudes.

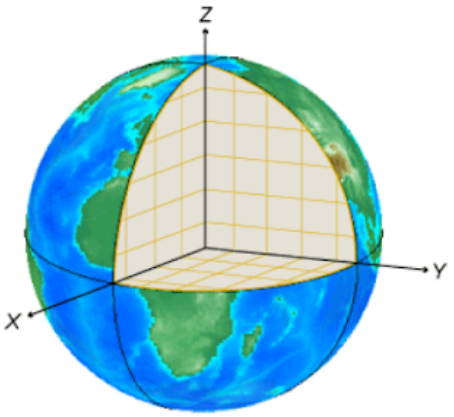

Figure M2 celestial body's coordinates

3. Referring Frames & NED System

A non-rotational frame concerning the stars is crucial for pinpointing space objects. The Geocentric Celestial Reference Frame (GCRF) is a popular choice for satellite scenarios. Besides global systems like GCRF, local systems like North East Down (NED) and Azimuth Elevation Range (AER) are used. NED employs coordinates relative to a local point above the Earth's surface. The axes are oriented towards cardinal directions and follow Earth's surface norms.

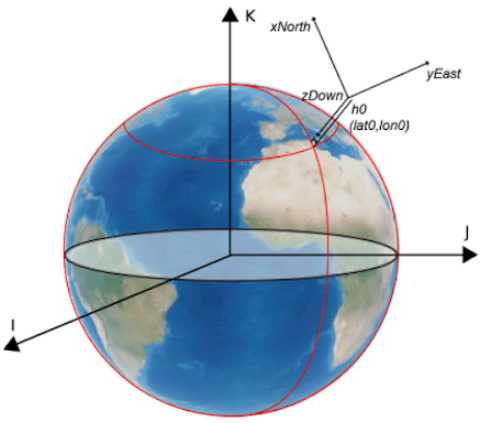

Figure M3 NED System

4. Satellite Orientation: Roll, Pitch, and Yaw

To determine a satellite's orientation, it's common to use three axes intersecting at the satellite's center of mass. The alignment of the satellite concerning the NED frame is described by sequential rotations about these axes. These rotational angles (yaw, pitch, and roll) have a default rotation sequence in many satellite communication tools.

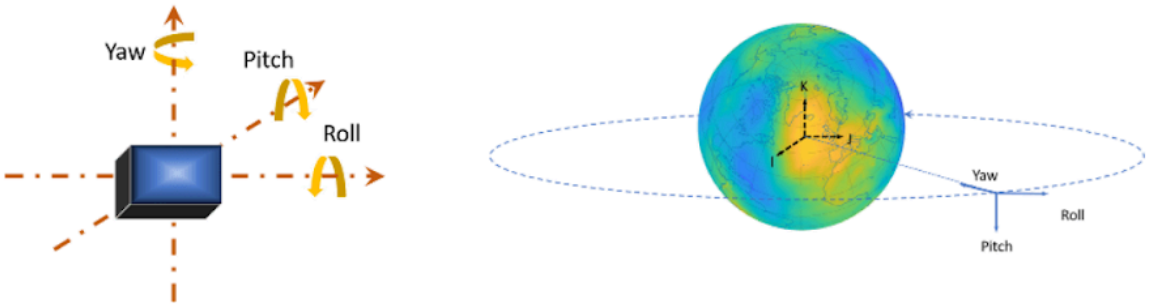

Figure M4 Satellite Orientation

5. AER Coordinate System

The AER system employs spherical coordinates to establish a position using azimuth (az), elevation (elev), and range. The origin here is defined in geodetic coordinates. The angles and distances in this system relate to a local Cartesian system, often centered on a satellite. The azimuth is the angle from the positive eastern direction, elevation is the angle above the horizon, and range refers to the straight-line distance from the object to the reference point.

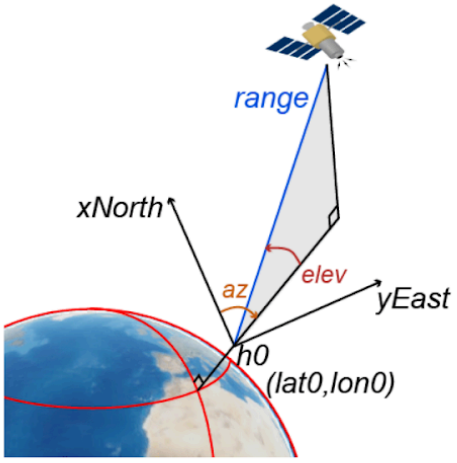

Figure M5 Understanding AER System

1. Introduction to Orbital Elements in Matlab toolbox

To distinctively determine a particular orbit, a set of specific parameters is necessary. Six distinct parameters are vital to precisely define an orbit and the satellite's position within it. Half of these parameters showcase the orientation and position of the satellite on its elliptical path, while the remaining describe the alignment of this orbital plane concerning the celestial frame. Often termed as Keplerian elements, these six are crucial. A visual would typically depict the orbital plane intersecting a reference plane; for satellites around Earth, the GCRF's IJ-plane is the common reference.

2. Defining the Ellipse's Size and Shape:

- Eccentricity (e): This parameter highlights the extent to which the ellipse deviates from a perfect circle.
- Semimajor axis (a): Represented as the average of the closest (periapsis) and furthest (apoapsis) distances of the orbiting body from the central mass it circles around. In simple orbital scenarios, this distance is between the centers of the two bodies.

3. Determining the Orbital Plane's Orientation:

- Inclination (i): Signifies the angular difference between the ellipse and the reference plane, recorded at the point called the ascending node. This point is where the orbiting object moves upward, crossing the reference plane. The inclination angle varies between 0° and 180°, with the Earth's center always residing within this plane. The ascending node is the point where the satellite moves north, crossing the equator, while the descending node is the opposite. The line connecting these two equatorial points is known as the line of nodes.
- Right ascension of ascending node (Ω): Indicates the horizontal alignment of the ascending node concerning the reference frame's primary axis. This alignment, also known as RAAN, can vary between 0° and 360°.

4. The Additional Two Components:

- Argument of periapsis (ω): Represents the ellipse's orientation within the orbital plane, measured from the ascending node to the closest point or periapsis. The angle can range from 0° to 360°.
- True Anomaly (v): Pinpoints the satellite's exact location on the elliptical path at a given instance. It's gauged in a counterclockwise direction starting from the periapsis, varying between 0° and 360°.

Understanding Two Line Element (TLE) Files

The Satellite Communications Toolbox has a satellite function that can utilize a TLE (Two Line Element) file to set up the satellite. For obtaining TLE files, you might want to check out the Space track website.

TLE sets are structured data representations that detail the orbital elements for Earth-orbiting entities at a specified moment, referred to as the epoch. There are different textual configurations to represent these orbital parameters. Among them, the most prevalent is the TLE format endorsed by organizations like NASA and NORAD. Here, every satellite is depicted through three lines: the inaugural line states the satellite's designation, followed by two lines encapsulating the standard TLE.

Consider this illustrative example for a satellite:

Satellite 1
1 25544U 98067A 04236.56031392 .00020137 00000-0 16538-3 0 9993
2 25544 51.6335 344.7760 0007976 126.2523 325.9359 15.70406856328906

Table MATLAB 1 : describes the columns in row 2 (standard TLE set format identical to that used by NORAD and NASA)

Column	Description	Example

1	Line number	1
3–7	Satellite number	25544
8	Elset classification	U
10–17	International designator	98067A
19–32	Element set epoch (UTC)	04236.56031392
34–43	First derivative of the mean motion with respect to time	.00020137
45–52	Second derivative of the mean motion with respect to time (decimal point assumed)	00000-0
54–61	BSTAR drag term	16538-3
63	Element set type	0
65–68	Element number	999
69	Check sum (modulo 10)	3

Table MATLAB 2: *describes the columns in row 3 (standard TLE set format identical to that used by NORAD and NASA)*

Column	Description	Example
1	Line number of element data	2
3–7	Satellite number	25544
9–16	Inclination (in degrees)	51.6335

18–25	Right ascension of the ascending node (in degrees)	`344.7760`
27–33	Eccentricity (leading decimal point assumed)	`0007976`
35–42	Argument of perigee (in degrees)	`126.2523`
44–51	Mean anomaly (in degrees)	`325.9359`
53–63	Mean motion (in revs per day)	`15.70406856`
64–68	Revolution number at epoch (in revs)	`32890`
69	Check sum (modulo 10)	`6`

A TLE (Two Line Element) file provides data in a specific format that describes the orbit of an Earth-orbiting object, such as a satellite. The TLE is commonly used to predict the position of satellites in the sky at a given time. The name "Two Line Element" stems from the fact that the data format consists of two lines, with each line containing specific details about the satellite's orbit. These details include parameters like inclination, right ascension of the ascending node, eccentricity, and mean motion, among others. Combined, these elements allow for the prediction of the satellite's position and velocity at a given epoch (a reference point in time).

A typical TLE file starts with a title line, which provides the name of the satellite, followed by the two lines of orbital data. This format has been widely used by NORAD (North American Aerospace Defense Command) and NASA to distribute satellite tracking information.

For example:

ISS (ZARYA)
1 25544U 98067A   04236.56031392 .00020137 00000-0 16538-3 0 9993
2 25544 51.6335 344.7760 0007976 126.2523 325.9359 15.70406856328906

In this sample:

- "ISS (ZARYA)" is the satellite's name.
- The next two lines are the standard TLE data.

Various software and tools can process TLE files to predict and visualize satellite trajectories and positions.

TLEs (Two Line Elements) are specifically designed for Earth-orbiting objects. This includes satellites, the International Space Station, debris, and other objects in orbit around the Earth. The parameters and the specific format of TLEs are tailored to represent orbits in relation to Earth, taking into account factors like Earth's gravitational constants.
For objects orbiting other celestial bodies or those in interplanetary space, different sets of orbital elements and data formats would be required.
For objects orbiting celestial bodies other than Earth or those moving in interplanetary space, different parameters and data formats would be considered based on the unique characteristics and requirements of the situation. Here are some scenarios and the associated orbital elements or data formats:

1. Objects orbiting other celestial bodies (e.g., moons, planets, asteroids):
    - Different gravitational parameters for the specific body.
    - Size, shape, and rotation rate of the celestial body.
    - Local reference systems for each celestial body, rather than Earth's equatorial system.
    - Perturbations due to other nearby celestial bodies might be considered.

2. Interplanetary spacecraft:
    - Heliocentric or sun-centered elements might be more appropriate.
    - Perturbations from other planets, particularly large ones like Jupiter.
    - Solar radiation pressure and other non-gravitational forces.

3. Data Formats:
    - SPICE kernels: This is a system used by NASA's Navigation and Ancillary Information Facility (NAIF) to handle a wide variety of spacecraft navigation data, including interplanetary missions.
    - State vectors: Direct specification of position and velocity vectors at a certain epoch, which can be more universal than Keplerian elements for non-circular, non-equatorial orbits or for interplanetary trajectories.

- Proprietary formats: Space agencies or companies may have in-house data formats tailored to their specific mission needs.

4. Generalized orbital elements:
For non-Earth-centric orbits or orbits not centered on a celestial body, it might be necessary to use a more generalized set of orbital parameters or state representation.

5. Influence of non-gravitational forces:
For certain missions, especially interplanetary ones, non-gravitational forces such as solar radiation pressure, outgassing, or thrust from propulsion systems play a significant role. These might require additional parameters or modeling considerations.

Different orbital mechanics software or analysis tools might have their preferred formats or element sets, especially if they're designed for specific mission profiles or celestial bodies. It's essential to understand the context and purpose of the mission or analysis to choose the appropriate orbital elements and data representation.

[1] “Basics of Space Flight” https://solarsystem.nasa.gov/basics/chapter5-1/.

[2] “CelesTrak. Frequently Asked Questions: Two-Line Element Set Format.” Accessed March 26, 2016. https://celestrak.com/columns/v04n03/.

E. TMTC inconvenient times in far space communications

The following code implements a Solar Conjunction model and consecutive telecom outage verification. It helps verify TMTC inconvenient times in far space communications.

The TMTC Front-End is a telemetry (TM) and telecommand (TC) tool that gives direct control of spacecraft using baseband interfaces during spacecraft development, assembly, integration, test (AIT), and launch phases. Most of the time, the TMTC links to the spacecraft's On-Board Computer (OBC) or Central Data Management Unit (CDMU) through direct bypass interfaces or an RF SCOE.

Before a launch, the TMTC Front-End is used to test the computers on board the spacecraft, check the flight transponder, or talk to the spacecraft.

Luigi De Maria (2023). Deep Space Telecommunications Blackout (https://www.mathworks.com/matlabcentral/fileexchange/93020-deep-space-telecommunications-blackout), MATLAB Central File Exchange. Retrieved September 20, 2023.

```
function [ck] = TeleBlackout(r_p_E, r_p_S, r_E, R_S, R_E, a_p_sc)
%
% Solar Conjuction Checker - Earth Downlink Blackouts
%
%DESCRIPTION:
%The following code implements the check over telecomm blackouts of a
s/c
%orbiting a planet with respect to Earth.
%
%PROTOTYPE
% [ck] = TeleBlackout(r_p_E, r_p_S, r_S_E, R_S, R_E)
% [ck] = TeleBlackout(r_p_E, r_p_S, r_S_E, R_S, R_E, a_p_sc)
%
%-------------------------------------------------------------------
----
% INPUTS:
% r_p_E [3x1] Earth Pos. Vec. wrt Planet [km]
% r_p_S [3x1] Sun Pos. Vec. wrt Planet [km]
% r_E [3x1] Earth Pos. Vec. wrt Sun [km]
% R_S [1x1] Sun Corona Radius [km]
% R_E [1x1] Earth Radius [km]
% a_p_sc [3x1] S/C Pos. Vec. wrt Planet [km]
%-------------------------------------------------------------------
----
% OUTPUTS:
% ck [1x1] Blackout Checker [-]
%-------------------------------------------------------------------
----
%
%NOTES:
% - the output 'ck' can assume the following results:
% o ck = 2 --> Total Blackout
% o ck = 1 --> Partial Blackout
% o ck = 0 --> No-Blackout
% - If the s/c altitude doesnpt have to be considered or the s/c is on
an
% standalone orbit, then omit the last input
%
```

```
%CALLED FUNCTIONS:
% (none)
%
%UPDATES:
% (non)
%
%REFERENCES:
%  [1]  "Mars  solar  conjunction  prediction  modeling",  Vineet  K.
Srivastava,
% Jai Kumar, Shivali Kulshrestha, Badam Singh Kushvah.
%
%AUTHOR(s):
%Luigi De Maria, 2021
%
%% Connecting Lines: Earth-edges - S/C
%Pos. Vec. of S/C wrt Planet
if nargin == 5
a_p_sc = zeros(3,1);
end
%Pos. Vec. of S/C wrt Sun
a_S_sc = a_p_sc - r_p_S;
%Pos. Vec. of Earth wrt Sun
r_S_E = r_p_E - r_p_S;
%Unit Vec. Orthogonal to Pos. Vec. of Earth wrt Sun
S_S_p          =          (cross(r_S_E,cross(r_S_E,a_S_sc)))          /
norm(cross(r_S_E,cross(r_S_E,a_S_sc)));
%Earth-Edge1 Pos. Vec.
r_S_e1 = r_S_E + R_E * S_S_p;
%Earth-Edge2 Pos. Vec.
r_S_e2 = r_S_E - R_E * S_S_p;
%Earth-Edge1 - S/C Vec.
b = a_S_sc - r_S_e1;
%Earth-Edge2 - S/C Vec.
c = a_S_sc - r_S_e2;
%% Line Equations Coefficients
%Line 1 Intersection with Sun Coefficients
A_S_line1 = (b(1)^2 + b(2)^2)*R_S^2 + b(3)^2*R_S^2;
B_S_line1 = 2*R_S^2 * (-b(2)^2 * a_S_sc(1) + b(2)*b(1)*a_S_sc(2))...
+ 2*R_S^2 * (-b(3)^2 * a_S_sc(1) + b(3)*b(1)*a_S_sc(3));
C_S_line1     =     (b(1)^2*a_S_sc(2)^2     +     b(2)^2*a_S_sc(1)^2     -
2*b(2)*b(1)*a_S_sc(2)*a_S_sc(1)) * R_S^2 ...
+        (b(1)^2*a_S_sc(3)^2        +        b(3)^2*a_S_sc(1)^2        -
2*b(3)*b(1)*a_S_sc(3)*a_S_sc(1)) * R_S^2 ...
- b(1)^2 * R_S^4;
%Line 1 Intersection with Sun Coefficients
```

```
A_S_line2 = (c(1)^2 + c(2)^2)*R_S^2 + c(3)^2*R_S^2;
B_S_line2 = 2*R_S^2 * (-c(2)^2 * a_S_sc(1) + c(2)*c(1)*a_S_sc(2))...
+ 2*R_S^2 * (-c(3)^2 * a_S_sc(1) + c(3)*c(1)*a_S_sc(3));
C_S_line2    =    (c(1)^2*a_S_sc(2)^2    +    c(2)^2*a_S_sc(1)^2    -
2*c(2)*c(1)*a_S_sc(2)*a_S_sc(1)) * R_S^2 ...
+       (c(1)^2*a_S_sc(3)^2       +       c(3)^2*a_S_sc(1)^2       -
2*c(3)*c(1)*a_S_sc(3)*a_S_sc(1)) * R_S^2 ...
- c(1)^2 * R_S^4;
%% Blackout Check
%Line 1 Value
Line1 = (B_S_line1)^2 - 4*A_S_line1*C_S_line1;
%Line 2 Value
Line2 = (B_S_line2)^2 - 4*A_S_line2*C_S_line2;
%Blackout Checker
if (Line1>=0) && (Line2>=0)
if (norm(r_p_E) < norm(r_E))
ck = 0; %No-Blackout (Planet in front of Sun)
else
ck = 2; %Total Blackout
end
elseif (Line1<0) && (Line2>=0)
ck = 1; %Partial Blackout (Line 2)
elseif (Line1>=0) && (Line2<0)
ck = 1; %Partial Blackout (Line 1)
elseif (Line1<0) && (Line2<0)
ck = 0; %No-Blackout
end
end
```


Enhanced Control System for Positioning Deep Space Antennas

by Salawudeen, A.T., Muazu, B.M., Sha Aban, Y.A., Chan, C.J., 2017.University of Jos and Department of Math and Computer Science, Lawrence Technological University, Southfield Michigan, USA, members of Matlab community

Here is the paper:
Salawudeen, A.T., Muazu, B.M., Sha Aban, Y.A., Chan, C.J., 2017. Optimal Design of PID Controller for Deep Space Antenna Positioning Using Weighted Cultural Artificial Fish Swarm Algorithm. J Electr Electron Syst 06. https://doi.org/10.4172/2332-0796.1000243
The Artificial Fish Swarm Algorithm (AFSA) is inspired by how real fish behave in water. Just like fish look for areas with lots of food, either by searching themselves or by following other

fish, AFSA looks for the best solutions to problems. But, while it has a lot of good features, like fast results and being very adaptable, it can sometimes get stuck on a local solution instead of finding the best overall solution. This happens because individual "fish" in the algorithm often find small, local solutions and might miss the bigger picture.

To tackle this, many researchers tried to tweak and modify the algorithm. They found out that certain settings, like how far the "fish" can see (visual distance) and how big their steps are, play a crucial role in how well the algorithm works. For instance, if the visual distance is large, the algorithm searches broadly; if it's small, it searches narrowly. However, finding the right settings for each specific problem remains a challenge.

In this study, the authors introduced a new version of the AFSA by combining it with some "cultural" techniques, which involve using both normative and situational knowledge. They hoped this would stop the algorithm from getting stuck on local solutions. They created four versions of this new approach, called the weighted Cultural Artificial Fish Swarm Algorithm (wCAFSA), and tested them on several problems. One of the main tests was to find the best settings for controlling the movement of a deep-space antenna.

This study introduced four versions of the AFSA, termed as the weighted Cultural Artificial Fish Swarm Algorithm (wCAFSA). These variations were employed to fine-tune a PID controller for controlling the positioning of a deep space antenna. The simulation outcomes showcased the efficacy of these algorithms in refining the PID controller settings. Inside, you'll find the implementation code for wAFSA and a comparison of the results. Corresponding to the research paper, it is given the code:

```
%% Defined the Antenna System Transfer function
clc
clear all
close all
s=tf('s'); %Make 's' a tansfer function symbol
K=input('Please Provide the value of the gain parameter (K):= ');
G=6.63*K/(s^3+101.71*s^2+171*s+6.63*K);%input('Please     Define     the
Transfer   Function   of   the   Plant:=   ');%   %please   defined   the   plant
transfer function
objfunc=@(x) pid_obj(x,G); % Objective Function Handle for the GA
% Defind Algorithm Paramaters
N=80;
D=3;
Lb=0;
```

```
Ub=2;
visual=5;Step=0.75;zig=0.25;try_num=100;
[Kp,Ki,Kd]=wAFSA(N,D,visual,Step,zig,try_num,Lb,Ub,objfunc);
Tf=0.1;
MM=pid(Kp,Ki,Kd,Tf);
DL=feedback(MM*G,1);
step(G)
hold on
step(DL);
legend('Uncontrolled','wAFSA based Controlled ')
xlabel('Time (seconds)')
ylabel('Amplitude')

function [z out]=pid_obj(x,G)
%Note: G is the Plant transfer function
% Z is the cost function output
% K: PID Controller Transfer Function sormulated based on the pid
% command
% lamda=input('Please Provide your Fractional Performance Index OR Zero
to Contue:= ');
% if lamda==0
% lamda=1;
% else
% lamda=lamda;
% end
kp=100*x(1);
ki=100*x(2);
kd=10*x(3);
Tf=0.1;
K=pid(kp,ki,kd,Tf);
T=feedback(K*G,1);%the Closed loop transfer function [T = G*K/(1+G*K)]
info=stepinfo(T);
MP=info.Overshoot;
Ts=info.SettlingTime;
MaxRealPole=-min(max(real(pole(T))),0);
SI=1/MaxRealPole;
w1=0.3;
w2=0.3;
w3=0.4;
% Evaluate the cost function
z=w1*MP+w2*Ts+w3*SI;
out.kp=kp;
out.ki=ki;
out.kd=kd;
out.Tf=Tf;
```

```
out.G=G;
out.K=K;
out.T=T;
out.ClosedLoopStepInfo=info;
out.ClosedLoopPoles=pole(T);
out.MaxRealPole=MaxRealPole;
out.SI=SI;
out.MP=MP;
out.Ts=Ts;
out.z=z;
end
```

compile results:

```
clc
close all
s=tf('s'); %Make 's' a tansfer function symbol
K=50;%input('Please Provide the value of the gain parameter (K):= ');
G=6.63*K/(s^3+101.71*s^2+171*s+6.63*K);
%Gain for wCAFSA_Ns
kp=0.2862;
ki=1.01000;
kd=0.2063;
%Gain for wCAFSA_Sd
Kp=0.2382;
Ki=1.109060000;
Kd=0.235;
%Gain for wAFSA
P=0.2674;
I=1.10500;
D=0.2273;
Tf=0.1;
T=pid(kp,ki,kd,Tf);
CL=feedback(T*G,1);
K=pid(Kp,Ki,Kd,Tf);
DL=feedback(K*G,1);
L=pid(P,I,D,Tf);
EL=feedback(L*G,1);
figure(1)
step(G)
hold on
step(CL,'m')
hold on
step(DL,'k')
hold on
step(EL,'g')
```

```
legend('Close loop response','wCAFSA\_{Ns PID}',...
'wCAFSA\_{Sd PID}','wAFSA PID')
grid on
hold off
clear K
K=100;%input('Please Provide the value of the gain parameter (K):= ');
G=6.63*K/(s^3+101.71*s^2+171*s+6.63*K);
figure(2)
%Ns
Kpp=0.0374;
Kii= 1.0000;
Kdd=0.2073;
%Sd
kpp=0.0399;
kii= 1.140000;
kdd=0.18073;
%wAF
Ppp=0.0474;
Iii= 1.13990000;
Ddd=0.3021;
B=pid(Kpp,Kii,Kdd,Tf);
BB=feedback(B*G,1);
C=pid(kpp,kii,kdd,Tf);
CC=feedback(C*G,1);
A=pid(Ppp,Iii,Ddd,Tf);
AA=feedback(A*G,1);
step(G)
hold on
step(BB)
hold on
step(CC)
hold on
step(AA)
grid on
legend('Close loop response','wCAFSA\_{Ns PID}',...
'wCAFSA\_{Sd PID}','wAFSA PID')
wCAFSA_Ns1=stepinfo(CL)
wCAFSA_Ns2=stepinfo(BB)
wCAFSA_Sd1=stepinfo(DL)
wCAFSA_Sd2=stepinfo(CC)
wAFSA1=stepinfo(EL)
wAFSA2=stepinfo(AA)

function [Kp,Ki,Kd]=wAFSA(N,D,visual,step,zig,try_num,Lb,Ub,objfunc)
```

```
FISHS=0;%input('PLEASE ENTER THE INITIAL FISH MATRIX OR \nPRESS ZERO
(0)FOR MATLAB TO CREATE THEM\nFISH:= ');
global Xmin Xcentre population
% Generate the artificial fishes which is the same as the Food
% concenteration
tic
if FISHS==0
pop=Lb+rand(N,D)*(Ub-Lb);
% pop=rand(N,D);
else
pop=FISHS;
end
popi=pop;%Initial positions of the AF and start with preying conditions
for i=1:N
for j=1:D
fitpopi(j)=objfunc(popi(i,(1:D)));
popj(i,(1:D))=popi(i,(1:D))+rand*visual;%randomly selected position
end
for b=1:D
fitpopj(b)=objfunc(popj(i,(1:D)));
end
if fitpopj<fitpopi
%Execute preying
popi(i,(1:D))=popi(i,(1:D))+rand*step*0.4*(popj(i,(1:D))-popi(i,(1:D)))
/sum((abs(popj(i,(1:D)).^2-popi(i,(1:D)).^2)).^0.5);
Try=try_num;
end
end
if fitpopj>fitpopi
popi(i,(1:D))=popi(i,(1:D))+rand*step;%Execute if preying fails
end
%start Swarming
popii=popi;
fitpopii(i,(1:D))=objfunc(popii(i,(1:D)));
popk=popii+rand*visual;% represent next positions of AF.
for hh=1:N
for h=1:N
Xcentre=zeros(1,D);
nf=1;
if  sum(abs(popk(h,:).^2-popii(h,:).^2).^0.5)<=visual  %Conditions  for
number of fellows btw visual distance
nf=nf+1;
if nf~=0
B=popk(1,D);
end
```

```
Xcentre=Xcentre+B;
end
end
Xcentre=Xcentre/nf;
Ycentre=objfunc(Xcentre);
if nf*Ycentre<zig*fitpopii(hh)
if Ycentre<fitpopii(hh)
popii(hh,:)=popii(hh,:)+rand*step*0.4*(Xcentre-popii(hh,:))/sum((abs(Xc
entre.^2-popii(hh,:).^2)).^0.5);%Uncrowded area
else
clear i;
for i=1:N
popk(i,(1:D))=popii(i,(1:D))+rand*visual;
fitpopk(i,1)=objfunc(popk(i,(1:D)));
if fitpopk(i,1)<fitpopii(i,1)
popii(i,(1:D))=popii(i,(1:D))+rand*step*0.4*(popk(i,(1:D))-popii(i,(1:D
)))/sum((abs(popk(i,(1:D)).^2-popii(i,(1:D)).^2)).^0.5);%Execute
Swarming
else
popi(i,(1:D))=popi(i,(1:D))+rand*step*0.4*(popj(i,(1:D))-popi(i,(1:D)))
/sum((abs(popj(i,(1:D)).^2-popi(i,(1:D)).^2)).^0.5);
end
end
end
end
end
%Start Chasing
popiii=popi;
fitpopiii=objfunc(popii);
popl=popiii+rand*visual;
clear hh h
for hh=1:N
for h=1:N
Xmin=zeros(1,D);
nf=0;
if sum(abs(popl(h,:).^2-popiii(hh,:).^2).^0.5)<=visual
nf=nf+1;
Xmin=[Xmin;popl(h,:)];
end
end
clear h;
for h=1:nf-1
if
sum(abs(popl(h+1,:).^2-popiii(h+1,:).^2).^0.5)<sum((abs(popl(h,:).^2-po
piii(h,:).^2)).^0.5)
```

```
Xmin=Xmin(h+1,:);
else
Xmin=Xmin(h,:);%represent the best artificial fish individual withing
visual distance.
end
end
Ymin=objfunc(Xmin);
if nf*Ymin<zig*fitpopiii(h)
if Ymin(h)<fitpopiii(h)
popiii(hh,:)=popiii(hh,:)+rand*step*0.4*(Xmin-popiii(hh,:))/sum((abs(Xm
in.^2-popiii(hh,:).^2)).^0.5);
else
clear i;
for i=1:N
popl(i,(1:D))=popiii(i,(1:D))+rand*visual;
fitpopl(i,1)=objfunc(fitness,popl(i,(1:D)));
if fitpopl(i,1)<fitpopiii(i,1)
popiii(i,(1:D))=popiii(i,(1:D))+rand*step*0.4*(popl(i,(1:D))-popiii(i,(
1:D)))/sum((abs(popl(i,(1:D)).^2-popiii(i,(1:D)).^2)).^0.5);
end
end
if fitpopl(i,1)>fitpopiii(i,1)
popiii(i,(1:D))=popiii(i,(1:D))+rand*step;
end
end
end
end
%Determing which behavior yield the best solution
population=[];
for Fish=1:N
for property=1:3
if property==1
Best=popi(Fish,:);
end
if property==2
if objfunc(Best)>objfunc(popii(Fish,:))
Best=popii(Fish,:);
end
end
if property==3
if objfunc(Best)>objfunc(popiii(Fish,:))
Best=popiii(Fish,:);
end
end
end
```

```
population=[population;Best];
end
Kp=population(1)
Ki=population(2)
Kd=population(3)
toc
```

REFERENCES

[1] Einstein, A. (1916), Die Grundlage der allgemeinen Relativitätstheorie. Ann. Phys., 354: 769-822. https://doi.org/10.1002/andp.19163540702

[2]Aspect, A., Dalibard, J., Roger, G., 1982. Experimental Test of Bell's Inequalities Using Time-Varying Analyzers. Phys. Rev. Lett. 49, 1804–1807. https://doi.org/10.1103/PhysRevLett.49.1804

[3] Simultaneous observation of the quantization and the interference pattern of a plasmonic near-field." Nature Communications 02 March 2015. DOI: 10.1038/ncomms7407

[4] Georgi, H. (1993). The Physics of Waves. Prentice Hall.

[5] MacDonald, F. (2006). The Electromagnetic Spectrum: Key to the Universe. Chelsea House.

[6] Melia, F. (2007). Observations of the Electromagnetic Spectrum: A Philosophical Exploration of the Unity of the Universe. Philosophical Transactions of the Royal Society A: Mathematical, Physical and Engineering Sciences, 365(1854), 1131-1144.

[7] Merritt, D.; et al. (May 2004). "Consequences of Gravitational Wave Recoil". *The Astrophysical Journal Letters*. 607 (1): L9–L12. arXiv:astro-ph/0402057. Bibcode:2004ApJ...607L...9M. doi:10.1086/421551. S2CID 15404149

[8] Gualandris A, Merritt D, et al. (May 2008). "Ejection of Supermassive Black Holes from Galaxy Cores". *The Astrophysical Journal*. 678 (2): 780–797. arXiv:0708.0771. Bibcode:2008ApJ...678..780G. doi:10.1086/586877. S2CID 14314439

[9] Will, C.M. The Confrontation between General Relativity and Experiment. Living Rev. Relativ. 17, 4 (2014). https://doi.org/10.12942/lrr-2014-4

[10] McWilliams, S.T., Ostriker, J.P., Pretorius, F., 2012. The imminent detection of gravitational waves from massive black-hole binaries with pulsar timing arrays.

[11] Bond, C., Brown, D., Freise, A., Strain, K.A., 2016. Interferometer techniques for gravitational-wave detection. Living Rev Relativ 19, 3. https://doi.org/10.1007/s41114-016-0002-8

[12] Observation of Gravitational Waves from a Binary Black Hole Merger (open access)
Published in Phys. Rev. Lett. 116, 061102 (2016)

[13] Misra, P. and Enge, P. (2006) Global Positioning System: Signals, Measurements, and Performance. 2nd Edition, Ganga-Jamuna Press, Lincoln.

[14] Zumdahl, S.S., and Zumdahl S.A. (2003). Atomic Structure and Periodicity. In Chemistry (6th ed., pp. 290-94), Boston, MA: Houghton Mifflin Company.

[15] NASA (2021). The Electromagnetic Spectrum.

[16] D. Halliday, R. Resnick, and J. Walker. H*alliday & Resnick Fundamentals of Physics John Wiley & Sons Canada, Limited,* (*2010*)

[17]Butters, Alan (December 2006). "Radio Frequency Identification: An Introduction for Library Professionals

[18] Wadham, Rachel (2003). "Radio Frequency Identification". *Library Mosaics*. 14 (5): 22.

[19] Jessica Scarpati. "What is radio frequency (RF, rf)?". *SearchNetworking*. Retrieved 29 January 2021.

[20] IEEE Std 521-2002 *Standard Letter Designations for Radar-Frequency Bands* Archived 2013-12-21 at the Wayback Machine, Institute of Electrical and Electronics Engineers, 2002. (Convenience copy at National Academies Press.)

[21] Massaro, Maria. (2017). Thesis for the Degree of Licentiate of Philosophy. Radio Spectrum Regulation in the European Union: A three-level context.

[22] Golio, M.. (2007). RF and microwave applications and systems.

[23] Hitchcock, R. Timothy (2004). Radio-frequency and Microwave Radiation. American Industrial Hygiene Assn. p. 1. ISBN 978-1931504553.

[24] Kumar, Sanjay; Shukla, Saurabh (2014). *Concepts and Applications of Microwave Engineering*. PHI Learning Pvt. Ltd. p. 3. ISBN 978-8120349353.

[25] Jones, Graham A.; Layer, David H.; Osenkowsky, Thomas G. (2013). *National Association of Broadcasters Engineering Handbook, 10th Ed*. Taylor & Francis. p. 6. ISBN 978-1136034107.

[26] Pozar, David M. (1993). *Microwave Engineering* Addison–Wesley Publishing Company. ISBN 0-201-50418-9.

[27] Sorrentino, R. and Bianchi, Giovanni (2010) *Microwave and RF Engineering*, John Wiley & Sons, p. 4, ISBN 047066021X.

[28] Karmel, Paul R.; Colef, Gabriel D.; Camisa, Raymond L. (1998). *Introduction to Electromagnetic and Microwave Engineering*. John Wiley and Sons. p. 1. ISBN 9780471177814.

[29]Camilo, F., Ray, P.S., Ransom, S.M., Burgay, M., Johnson, T.J., Kerr, M., Gotthelf, E.V., Halpern, J.P., Reynolds, J., Romani, R.W., Demorest, P., Johnston, S., Van Straten, W., Parkinson, P.M.S., Ziegler, M., Dormody, M., Thompson, D.J., Smith, D.A., Harding, A.K., Abdo, A.A., Crawford, F., Freire, P.C.C., Keith, M., Kramer, M., Roberts, M.S.E., Weltevrede, P., Wood, K.S., 2009. RADIO DETECTION OF LAT PSRs J1741-2054 AND J2032+4127: NO LONGER JUST GAMMA-RAY PULSARS. ApJ 705, 1–13. https://doi.org/10.1088/0004-637X/705/1/1

[30] National Aeronautics and Space Administration, Science Mission Directorate. (2010). X-Rays. Retrieved [insert date - e.g. August 10, 2016], from NASA Science website: http://science.nasa.gov/ems/11_xrays

[31] What Is a Gravitational Wave? NASA https://spaceplace.nasa.gov/gravitational-waves/en/

[32]Introduction to the Electromagnetic Spectrum https://science.nasa.gov/ems/01_intro

[33]Gama Ray Astronomy https://imagine.gsfc.nasa.gov/science/toolbox/gamma_ray_astronomy1.html

[34] Gamma Rayshttps://youtu.be/TA5SLDilUWs?feature=shared

[35] XRAYS https://youtu.be/CCAYcuCWOnM?feature=shared

National Aeronautics and Space Administration, Science Mission Directorate. (2010).

[36] Hitchcock, R. Timothy (2004). Radio-frequency and Microwave Radiation. American Industrial Hygiene Assn. p. 1. ISBN 978-1931504553.

[37] Ishigaki, K.; Shiraishi, M.; Suzuki, S.; Asada, M.; Nishiyama, N.; Arai, S. (2012). "Direct intensity modulation and wireless data transmission characteristics of terahertz-oscillating resonant tunnelling diodes". *Electronics Letters*. 48 (10): 582. Bibcode:2012ElL....48..582I. doi:10.1049/el.2012.0849.

[38] Chacksfield, Marc (16 May 2012). "Scientists show off the future of Wi-Fi – smash through 3Gbps barrier". *Tech Radar*. Retrieved 16 May 2012.

[39] "New chip enables record-breaking wireless data transmission speed". *techcrunch.com*. 22 November 2011. Retrieved 30 November 2011.

[40] *Article 2.1: Frequency and wavelength bands"*. *Radio Regulations* (zipped PDF) (2016 ed.). International Telecommunication Union. 2017. Retrieved 9 November 2019

[41] Denny, S.P., J.Y. Suen, and P.M. Lubin, Fundamental limits of detection in the far infrared. New Astronomy, 2013. 25 p. 114–129.

[42] Suen, Jonathan. (2016). Terabit-per-Second Satellite Links: a Path Toward Ubiquitous Terahertz Communication. Journal of Infrared, Millimeter, and Terahertz Waves. 37, 615–639. https://doi.org/10.1007/s10762-016-0257-x

[43] Ma, J., L. Moeller, and J. Federici, Experimental Comparison of Terahertz and Infrared Signaling in Controlled Atmospheric Turbulence. Journal of Infrared, Millimeter, and Terahertz Waves, 2014. 36(2): p. 130–143.

[44] Emrick, R., et al., The Sky's the Limit: Key Technology and Market Trends in Satellite Communications. Microwave Magazine, IEEE, 2014. 15(2): p. 65–78.

[45] Cisco Systems, Cisco Visual Networking Index: Forecast and Methodology, 2014–2019. 2014: San Jose, CA, USA.

[46] Suen, J.Y., et al., Modeling of Terabit Geostationary Terahertz Satellite Links From Globally Dry Locations. Terahertz Science and Technology, IEEE Transactions on, 2015. 5(2): p. 299–313.

[47] National Aeronautics and Space Administration, Science Mission Directorate. (2010). Infrared Waves. Retrieved [insert date - e.g. August 10, 2016], from NASA Science website: http://science.nasa.gov/ems/07_infraredwaves

[48] National Aeronautics and Space Administration, Science Mission Directorate. (2010). Visible Light. Retrieved [insert date - e.g. August 10, 2016], from NASA Science website: http://science.nasa.gov/ems/09_visiblelight

[49] Nave, R. "Spectral Colors". *Hyperphysics*. Retrieved 2022-05-11

[50] D. H. Sliney (February 2016). "What is light? The visible spectrum and beyond". *Eye*. 30 (2): 222–229. doi:10.1038/eye.2015.252. ISSN 1476-5454

[51] Reference Solar Spectral Irradiance: Air Mass 1.5". Archived from the original on 27 January 2011. Retrieved 12 November 2009.

[52] Haigh, Joanna D. (2007). "The Sun and the Earth's Climate: Absorption of solar spectral radiation by the atmosphere". *Living Reviews in Solar Physics*. 4 (2): 2. Bibcode:2007LRSP....4....2H. doi:10.12942/lrsp-2007-2

[53] Wacker, Matthias; Holick, Michael F. (1 January 2013). "Sunlight and Vitamin D". ***Dermato-endocrinology*****. 5 (1): 51–108. doi:10.4161/derm.24494. ISSN 1938-1972. PMC 3897598. PMID 24494042**

[54] Lynch, David K.; Livingston, William Charles (2001). ***Color and Light in Nature*** **(2nd ed.). Cambridge: Cambridge University Press. p. 231. ISBN 978-0-521-77504-5. Archived from the original on 31 December 2013. Retrieved 12 October 2013. Limits of the eye's overall range of sensitivity extends from about 310 to 1050 nanometers**

[55] Dash, Madhab Chandra; Dash, Satya Prakash (2009). ***Fundamentals of Ecology 3E*****. Tata McGraw-Hill Education. p. 213. ISBN 978-1-259-08109-5. Archived from the original on 31 December 2013. Retrieved 18 October 2013. Normally the human eye responds to light rays from 390 to 760 nm. This can be extended to a range of 310 to 1,050 nm under artificial conditions.**

[56] Cronin, Thomas W.; Bok, Michael J. (15 September 2016). "Photoreception and vision in the ultraviolet". ***Journal of Experimental Biology*****. 219 (18): 2790–2801. doi:10.1242/jeb.128769. hdl:11603/13303. ISSN 1477-9145. PMID 27655820. S2CID 22365933. Archived from the original on 24 June 2022. Retrieved 23 June 2022.**

[57] Beeson, Steven; Mayer, James W (23 October 2007). "12.2.2 Discoveries beyond the visible". ***Patterns of light: chasing the spectrum from Aristotle to LEDs*****. New York: Springer. p. 149. ISBN 978-0-387-75107-8.**

[58] Hockberger, Philip E. (2002). "A history of ultraviolet photobiology for humans, animals and microorganisms". ***Photochem. Photobiol.*** **76 (6): 561–79. doi:10.1562/0031-8655(2002)0760561AHOUPF2.0.CO2. PMID 12511035. S2CID 222100404**

[59]The ozone layer also protects living beings from this. Lyman, T. (1914). "Victor Schumann". ***The Astrophysical Journal*****. 38: 1–4. Bibcode:1914ApJ....39....1L. doi:10.1086/142050.**

[60]"ISO 21348 Definitions of Solar Irradiance Spectral Categories" (PDF). ***Space Weather (spacewx.com)*****. Archived from the original (PDF) on 29 October 2013. Retrieved 25 August 2013.**

[61] Bally, John; Reipurth, Bo (2006). ***The Birth of Stars and Planets*****. Cambridge University Press. p. 177.**

[62] Bark, Yu B.; Barkhudarov, E.M.; Kozlov, Yu N.; Kossyi, I.A.; Silakov, V.P.; Taktakishvili, M.I.; Temchin, S.M. (2000). "Slipping surface discharge as a source of hard UV radiation". ***Journal of Physics D: Applied Physics*****. 33 (7): 859. Bibcode:2000JPhD...33..859B. doi:10.1088/0022-3727/33/7/317. S2CID 250819933**

[63] (Batool et al., 2019) Batool, S., Bibi, A., Frezza, F., Mangini, F., 2019. Benefits and hazards of electromagnetic waves, telecommunication, physical and biomedical: a review. European Review for Medical and Pharmacological Sciences 23, 3121–3128. https://doi.org/10.26355/eurrev_201904_17596

[64] Cambridge Core - Plasma Physics and Fusion Physics - Introduction to Space Physics - edited by Margaret G. Kivelson DOI: 10.1017/9781139878296

[65] Boudjemai, A., Hocine, R., Guerionne, S., 2015. Space environment effect on earth observation satellite instruments, in: 2015 7th International Conference on Recent Advances in Space Technologies (RAST). Presented at the 2015 7th International Conference on Recent Advances in Space Technologies (RAST), IEEE, Istanbul, Turkey, pp. 627–634. https://doi.org/10.1109/RAST.2015.7208419

[66] Kessler, D. J., & Cour-Palais, B. G. (1978). Collision frequency of artificial satellites: The creation of a debris belt. Journal of Geophysical Research, 83(A6), 2637-2646.

[67] Baumjohann, W., & Treumann, R. A. (2009). Basic space plasma physics. Imperial College Press.

[68] Eastwood, J. P., et al. (2015). The science of space weather. Philosophical Transactions of the Royal Society A, 373(2042).

[69] Gonzalez, W. D., et al. (1994). What is a geomagnetic storm? Journal of Geophysical Research, 99(A4), 5771-5792.

[70] Akasofu, S. I. (2017). Exploring the secrets of the aurora. Springer.

[71] Bruno, R., & Carbone, V. (2013). The Solar Wind and Magnetosphere System. Reviews of Modern Physics, 85(2), 767.

[72]McComas, D. J., Dayeh, M. A., Funsten, H. O., Schwadron, N. A., & Zirnstein, E. J. (2019). The Heliopause's Location, Structure, and Shape. Nature Astronomy, 3(2), 224-229.

[73] Hedin, A. E. (1991). Extension of the MSIS thermosphere model into the middle and lower atmosphere. Journal of Geophysical Research, 96(A2), 1159-1172.

[74] Garrett, H. B., & Whittlesey, A. C. (2011). Guide to mitigating spacecraft charging effects. John Wiley & Sons.

[75] Gilmore, D. G. (Ed.). (2002). Spacecraft thermal control handbook: Fundamental technologies. Aerospace Press.

[76] Tribble, A. C. (2003). The space environment: Implications for spacecraft design. Princeton University Press.

[77] Molina, J. M., & Nosei, L. (2016). Space environmental effects on spacecraft: LEO atomic oxygen. Aerospace Lab Journal, 12, 1-12.

[78] Fortescue, P., Swinerd, G., & Stark, J. (2011). Spacecraft systems engineering. John Wiley & Sons.

[79]Z.J. Yu, Spacecraft magnetic field observations as a probe of planetary interiors—Methodology and application to Jupiter and Saturn. Thesis submitted in partial fulfillment of requirements for the Ph.D. Degree, UCLA, 2004

[80] Russell, C.T., Dougherty, M.K., 2010. Magnetic Fields of the Outer Planets. Space Sci Rev 152, 251–269. https://doi.org/10.1007/s11214-009-9621-7 (Russell and Dougherty, 2010)

[81] Bamufleh, Dalal & Almohammadi, Randa & Alharbi, Esraa & Almalki, Maram. (2020). User Acceptance of Enterprise Resource Planning (ERP) Systems in Higher Education Institutions: A Conceptual Model. International Journal of Enterprise Information Systems. 17. 144- 163. 10.4018/IJEIS.20210101.oa1.

[81] D. Hengeveld, J. Braun, E. Groll, and A. Williams. "Review of Modern Spacecraft Thermal Control Technologies and Their Application to Next-Generation Buildings." 2010. International High Performance Buildings Conference. Paper 40.

[82] Thermal Management Technologies. "Products, Thermal Components: Flexible Thermal Straps." [Online] Accessed 2018. Available at: https://www.tmt-ipe.com/thermal-components

[83] Cassé, M. & Maslov, V.I.. (2023). COSMIC RAY SOURCE AND SOLAR ENERGETIC PARTICLES. Problems of Atomic Science and Technology. 109-112. 10.46813/2023-146-109.

[84] Beckman, John. (2021). Cosmic Rays? Cosmic Particles. 10.1007/978-3-030-68372-6_9.

[85] De la Torre Luque, Pedro. (2022). Cosmic-ray propagation and production of secondary particles in the Galaxy.

[86] Bate, R. R., Mueller, D. D., & White, J. E. (1971). Fundamentals of Astrodynamics. Dover Publications.

[87]Curtis, H. D. (2013). Orbital Mechanics for Engineering Students. Elsevier.

[88] Pisacane, V. L. (2005). Fundamentals of Space Systems. Oxford University Press.

[89] Asmar, S. W., Firre, D., Accomazzo, A., Bhanji, A. M., Ferri, P., Hudiburg, J. J., … & Mann, G. (2018). Nasa's deep space network and esa's tracking network strategic partnership to enable solar system exploration. 2018 SpaceOps Conference. https://doi.org/10.2514/6.2018-2430

[90] Bhamidipati, S., Mina, T., & Gao, G. X. (2022). Time transfer from gps for designing a smallsat-based lunar navigation satellite system. NAVIGATION: Journal of the Institute of Navigation, 69(3), navi.535. https://doi.org/10.33012/navi.535

[91] Danzmann, K. and Rüdiger, A. (2003). Lisa technology concept, status, prospects. Classical and Quantum Gravity, 20(10), S1-S9. https://doi.org/10.1088/0264-9381/20/10/301

[92] Banerjee, A. and Bhattacharya, R. (2022). On the solar dynamics from radio signal communication by recent solar probes. Journal of Physics: Conference Series, 2161(1), 012037. https://doi.org/10.1088/1742-6596/2161/1/012037

[93] Williamson, M. (1998). Deep space communications. Iee Review, 44(3), 119-122. https://doi.org/10.1049/ir:19980303

[94] Andrews, L., Phillips, R., Bagley, Z., Plasson, N., & Stotts, L. (2014). Hybrid optical/radio frequency (rf) communications., 295-342. https://doi.org/10.1007/978-1-4939-0918-6_9

[95] Bondyopadhyay, P. (1995). Guglielmo marconi - the father of long distance radio communication - an engineer's tribute. https://doi.org/10.1109/euma.1995.337090

[96] Akyildiz, I. F., Akan, Ö. B., Chen, C., Fang, J., & Su, W. (2004). The state of the art in interplanetary internet. IEEE Communications Magazine, 42(7), 108-118. https://doi.org/10.1109/mcom.2004.1316541

[97] Mukherjee, J. and Ramamurthy, B. (2013). Communication technologies and architectures for space network and interplanetary internet. IEEE Communications Surveys &Amp; Tutorials, 15(2), 881-897. https://doi.org/10.1109/surv.2012.062612.00134

[98] Forney, G. D. and Costello, D. J. (2007). Channel coding: the road to channel capacity. Proceedings of the IEEE, 95(6), 1150-1177. https://doi.org/10.1109/jproc.2007.895188

[99] Chou, Hsi-Tseng. "An Effective Design Procedure of Multibeam Phased Array Antennas for the Applications of Multisatellite/Coverage Communications." IEEE Transactions on Antennas and Propagation 64 (2016): 4218-4227.

[100] Vijay K. Garg, CHAPTER 6 - Multiple Access Techniques, Editor(s): Vijay K. Garg, In The Morgan Kaufmann Series in Networking, Wireless Communications & Networking, Morgan Kaufmann, 2007, Pages 149-191, https://doi.org/10.1016/B978-012373580-5/50040-5.

[101] J.N Pelton. "The Basics of Satellite Communications." s.l.: Professional Education International, Inc., 2006.

[102]JPL. Mars Cube One (MarCO). Jet Propulsion Laboratory California Institute of Technology | CubeSat. [Online] Available at: https://www.jpl.nasa.gov/cubesat/missions/marco.php

[103]S. Xie et al. "Wireless Sensor Network for Satellite Applications: A Survey and Case Study." Unmanned Systems, Vol. 2, pp. 261-277, 2014.

[104] Kilic, Ozlem & Zaghloul, Amir. (2010). Interference in Cellular Satellite Systems. 10.5772/9997.

[105] Palacin, Baptiste & Fonseca, Nelson & Romier, Maxime & Contreres, Romain & Angevain, Jean-Christophe & Toso, Giovanni & Mangenot, Cyril. (2017). Multibeam Antennas for Very High Throughput Satellites in Europe: Technologies and Trends. 10.23919/EuCAP.2017.7928493.

[106] Hideki Takenaka et al. Satellite-to-ground quantum-limited communication using a 50-kg-class microsatellite, Nature Photonics (2017). DOI: 10.1038/nphoton.2017.107

[107]Ortiz, F.; Monzon Baeza, V.; Garces-Socarras, L.M.; Vásquez-Peralvo, J.A.; Gonzalez, J.L.; Fontanesi, G.; Lagunas, E.; Querol, J.; Chatzinotas, S. Onboard Processing in Satellite Communications Using AI Accelerators. *Aerospace*, *10*, 101. https://doi.org/10.3390/aerospace10020101

[108] Biswas, Abhijit et al. "Status of NASA's deep space optical communication technology demonstration." 2017 IEEE International Conference on Space Optical Systems and Applications (ICSOS) (2017): 23-27.

During this thesis period, I perused several journals related to this topic.

The articles can be found in various journals such as IEEE Transactions on Aerospace and Electronic Systems, IEEE Journal on Selected Areas in Communications, Optics Express, IEEE Photonics Technology Letters, Google Scholar, and open platforms.